PNAS

www.pnas.org

Supplementary Information for

Discovery of a dual-action small molecule that improves neuropathological features of Alzheimer's disease mice

Min Hee Park,[a,b,1] Kang Ho Park,[a,b,1] Byung Jo Choi,[a,c] Wan Hui Han,[a,b] Hee Ji Yoon,[a,b] Hye Yoon Jung,[a,b] Jihoon Lee,[d] Im-Sook Song,[d] Dong Yu Lim,[e] Min-Koo Choi,[e] Yang-Ha Lee,[f] Cheol-Min Park,[f] Ming Wang,[g] Jihoon Jo,[h] Hee-Jin Kim,[i] Seung Hyun Kim,[i] Edward H. Schuchman,[j] Hee Kyung Jin,[a,c,2] Jae-sung Bae[a,c,2]

Correspondence to Jae-sung Bae, and Hee Kyung Jin
Email: jsbae@knu.ac.kr, and hkjin@knu.ac.kr

This PDF file includes:

       Supplementary Materials and Methods
       Figs. S1 to S23
       Tables S1 to S2
   References for SI reference citations

Materials and Methods

Chemical compounds screening

Chemical compounds (1,273) from a sphingolipid-targeted library and a functional inhibitor of ASM (FIASMA) derivative-targeted library were tested in triplicate assays at 10 µM of compound (stock con. 50 mM diluted in DMSO) for 30 min in PS1 fibroblasts with an abundance ASM activity. After 30 min cells were lysed in homogenization buffer containing 50 mM HEPES (Sigma-Aldrich, H3375), 150 mM NaCl (Sigma-Aldrich, S3014), 0.2% Igepal CA-630 (Sigma-Aldrich, I8896), and protease inhibitor (Calbiochem, 539131) (1, 2). Three microliters of cells lysate were mixed with 3 µl of 200 µM Bodipy-C12-sphingomyelin (Invitrogen, D7711) assay buffer (0.2 M of sodium acetate buffer, pH5.0, 0.2 mM $ZnCl_2$, and 0.2% Igepal CA-630) and incubated at 37 °C for 20 min. The hydrolysis reactions were stopped by adding 114 µl or 54 µl of ethanol, and centrifuged at 13,000 rpm for 5 min. Thirty microliters of the supernatant was then transferred to a sampling glass vial and 5 µl was applied onto a UPLC (ultra performance liquid chromatography, Waters) system for analysis. Quantification was achieved by comparison to Bodipy-C12-ceramide (Avanti Polar Lipids, 860512P) standards using the Waters Millennium software. Data for each compound was normalized to percent inhibition based on control cells with DMSO only within each test plate. The common backbone of compounds with a percent inhibition > 30% was identified and further optimization was performed based on lipophilicity. Hits were further qualified through direct binding to ASM by SPR, confirmation of direct and selective ASM inhibition in biochemical and cellular assays, pharmacokinetics, drug ability, and in vivo efficacy.

General chemical synthesis for KARI 501, KARI 401, KARI 301, and KARI 201

All the reactions were carried out in oven-dried glassware under nitrogen atmosphere with freshly distilled dry solvents prepared under anhydrous conditions unless otherwise indicated. Flash column chromatography was performed with Silica Flash P60 silica gel (230 – 400 mesh). All reagents were obtained from commercial sources and were used without further purification. Proton (^{1}H) and carbon (^{13}C) NMR spectra were recorded on a 400/100 MHz Agilent 400M FT-NMR spectrometer or 400/100 MHz Bruker Advance

III HD FT-NMR spectrometer. NMR solvents were obtained from Cambridge Isotope Laboratories and the residual solvent signals were taken as the reference (7.26 ppm for ^{1}H NMR spectra and 77.0 ppm for ^{13}C NMR spectra in CDCl$_3$). Mass analysis was carried out using an Agilent 6130 mass spectrometer. High-resolution mass analysis was performed with Bruker HCT Basic System.
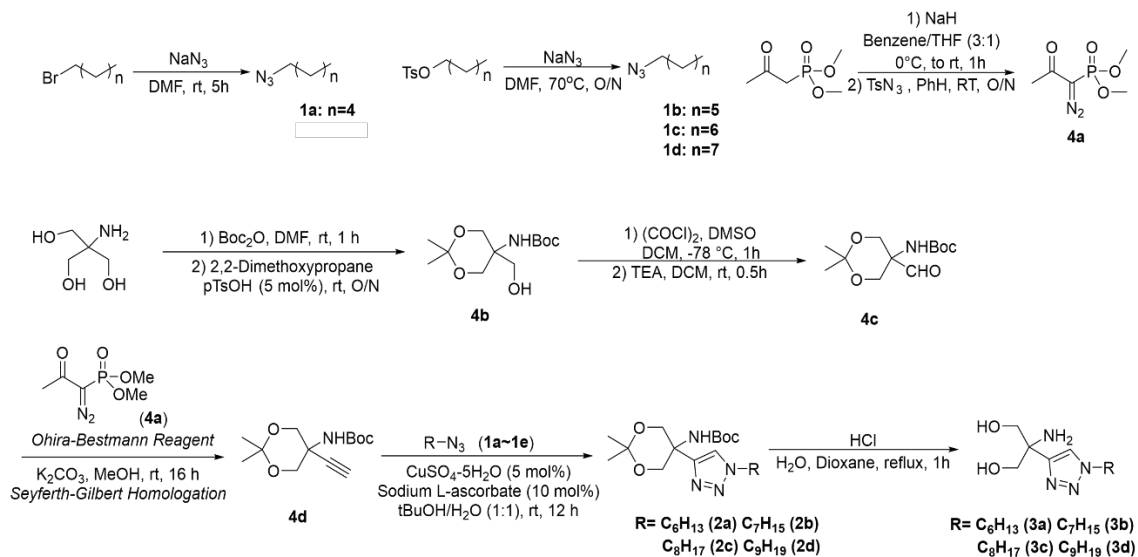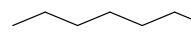

Synthetic procedures for azido alkanes

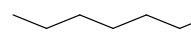### General Procedure A (for 1a azido-alkane)

To a solution of bromoalkane (1 eq) in DMF (0.2 M) was added sodium azide (3 eq) in proportions while stirring at r.t. The reaction was stirred for 5 h at r.t., and the mixture was poured into ice-cold water, extracted with diethyl ether 3 times. The combined organic layers were washed three times with water, dried over NaSO$_4$, and filtered. The solution was concentrated under reduced pressure to yield desired azido-alkane product as clear oil.
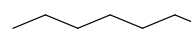
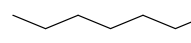### General Procedure B (for 1b, 1c, 1d azido-alkane)

To a solution of alkyl 4-methylbenzenesulfonate (1 eq) in DMF (0.2 M) was added sodium azide (5 eq) in proportions while stirring at r.t. The reaction mixture was heated at 70 $^{\circ}$C and stirred overnight, and the mixture was poured into ice-cold water, extracted with diethyl ether 3 times. The combined organic layers were washed three times with water,

dried over NaSO$_4$, and filtered. The solution was concentrated under reduced pressure to yield desired azido-alkane product as clear oil.

 1-azidohexane (1a) (3) ^{1}H NMR (400 MHz, CDCl$_3$): δ 3.26 (t, J =7.0Hz, 2H), 1.64-1.56 (m, 2H), 1.39-1.29 (m, 6H), 0.90 (t, J =6.9 Hz, 3H). Yield: 71% (270 mg, 2.12 mmol)

 1-azidoheptane (1b) (4) ^{1}H NMR (400 MHz, CDCl$_3$): δ 3.26 (t, J = 7.0 Hz, 2H), 1.60 (dt, J = 14.5, 7.0 Hz, 2H), 1.41 – 1.24 (m, 8H), 0.88 (t, J = 7.1 Hz, 1H). Yield: 66% (220 mg, 1.56 mmol)

 **1-azidooctane (1c)** (5) ^{1}H NMR (400 MHz, CDCl$_3$): δ 3.25 (t, J = 7.0 Hz, 2H), 1.63-1.56 (m, 2H), 1.40 – 1.23 (m, 10H), 0.88 (t, J = 7.0 Hz, 3H). Yield: 85% (230 mg, 1.48 mmol)

 1-azidononane (1d) (6) ^{1}H NMR (400 MHz, CDCl$_3$): δ 3.25 (t, J = 7.0 Hz, 2H), 1.65 – 1.53 (m, 2H), 1.40 – 1.20 (m, 12H), 0.88 (t, J = 7.0 Hz, 3H)

Synthetic procedures for triazole derivatives

**General Procedure C (for triazole derivatives 2a~2d)**

1-azidoalkane (**1a**, 1 eq), alkyne (**4d**, 1 eq) and copper(II) sulfate pentahydrate (0.05 eq) was dissolved in 1:1 mixture of butanol/H$_2$O (0.2 M). To the reaction mixture was added sodium ascorbate (0.1 eq) and the mixture was stirred for 12 h at r.t. Upon completion of the reaction, the mixture was concentrated under reduced pressure and diluted ethyl acetate, washed with water three times. The organic layer was dried over Na$_2$SO$_4$, filtered and concentrated. The crude material was purified by flash chromatography using ethyl acetate and hexane (3:7) to yield triazole derivative **2a~2d** as white solid.
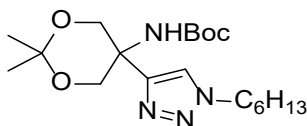
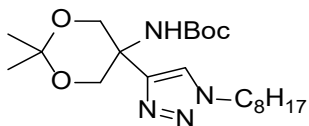**tert-butyl (5-(1-hexyl-1H-1,2,3-triazol-4-yl)-2,2-dimethyl-1,3-dioxan-5-yl)carbamate (2a)**

^{1}H NMR (400 MHz, CDCl$_3$): δ 7.64 (s, 1H), 5.64 (br s, 1H), 4.38 (br s, 2H), 4.32 (t, J =7.3, 2H), 4.12 (d, J = 11.5 Hz, 2H), 1.93-1.86 (m, 2H), 1.60 (s, 3H), 1.51 (s, 3H), 1.42 (s, 9H),

1.34-1.27 (m, 6H), 0.88 (t, J =7.0 Hz, 3H). ^{13}C NMR (100 MHz, CDCl$_3$): δ 154.84, 147.45, 122.28, 98.41, 79.75, 65.31, 50.38, 31.10, 30.17, 28.31, 26.14, 22.37, 13.90. MS (APCI, M+H$^+$): m/z found 383.3; Yield: 79% (95.0 mg, 0.248 mmol)
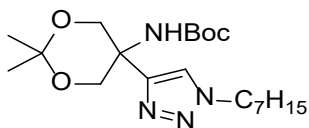
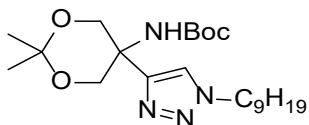**tert-butyl (5-(1-heptyl-1H-1,2,3-triazol-4-yl)-2,2-dimethyl-1,3-dioxan-5-yl)carbamate (2b)**

^{1}H NMR (400 MHz, CDCl3): δ 7.63 (s, 1H), 5.64 (br s, 1H), 4.37 (br s, 2H), 4.31 (t, J =7.3, 2H), 4.10 (d, J = 11.6 Hz, 2H), 1.90-1.86 (m, 2H), 1.53 (s, 3H), 1.50 (s, 3H), 1.41 (s, 9H), 1.33-1.24 (m, 8H), 0.86 (t, J =7.0 Hz, 3H). ^{13}C NMR (100 MHz, CDCl$_3$): δ 154.00, 121.48, 97.57, 78.89, 64.47, 49.54, 30.70, 29.39, 27.79, 27.49, 25.60, 21.66, 13.15. MS (ESI, M+H$^+$): m/z found 397.2; Yield: 74% (94.0 mg, 0.237 mmol)

tert-butyl (2,2-dimethyl-5-(1-octyl-1H-1,2,3-triazol-4-yl)-1,3-dioxan-5-yl)carbamate (2c)

^{1}H NMR (400 MHz, CDCl$_3$): δ 7.64 (s, 1H), 5.64 (br s, 1H), 4.40 (br s, 2H), 4.31 (t, J =7.3, 2H), 4.11 (d, J = 11.6 Hz, 2H), 1.93-1.85 (m, 2H), 1.54 (s, 3H), 1.51 (s, 3H), 1.42 (s, 9H), 1.31-1.24 (m, 10H), 0.87 (t, J =7.1 Hz, 3H). ^{13}C NMR (100 MHz, CDCl$_3$): δ 154.93, 147.53, 122.37, 98.48, 79.79, 50.46, 31.77, 30.32, 29.10, 29.01, 28.41, 26.57, 22.66, 14.12. MS (APCI, M+H$^+$): m/z found 411.3; Yield: 85% (71.0 mg, 0.173 mmol)

tert-butyl (2,2-dimethyl-5-(1-nonyl-1H-1,2,3-triazol-4-yl)-1,3-dioxan-5-yl)carbamate (2d)

^{1}H NMR (400 MHz, CDCl$_3$): δ 7.63 (s, 1H), 5.64 (br s, 1H), 4.38 (br s, 2H), 4.31 (t, J =7.3, 2H), 4.10 (d, J = 11.6 Hz, 2H), 1.90-1.86 (m, 2H), 1.53 (s, 3H), 1.50 (s, 3H), 1.41 (s, 9H), 1.31-1.24 (m, 12H), 0.86 (t, J =7.1 Hz, 3H). ^{13}C NMR (100 MHz, CDCl$_3$): δ 154.93, 147.53, 122.37, 98.48, 79.79, 50.46, 31.77, 30.32, 29.10, 29.01, 28.41, 26.57, 22.66, 14.12. MS (APCI, M+H$^+$): m/z found 425.3; Yield: 86% (115.0 mg, 0.271 mmol)
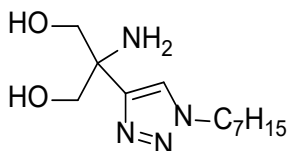
General Procedure D (for triazole derivatives 3a~3d)

The triazole derivative (**2a~2d**, 1 eq) was dissolved in mixed (2:3) solution of 4N HCl(aq)/Dioxane and refluxed for 1 h. After the completion of the reaction, solvent including water was removed under reduced pressure. Dried crude mixture was then purified by column chromatography using aqueous ammonia, methanol, dichloromethane (2:10:88) to yield desired product **3a~3d** as white solid.
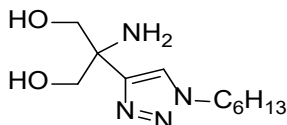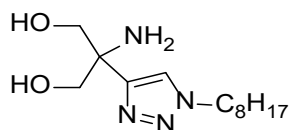

2-amino-2-(1-hexyl-1H-1,2,3-triazol-4-yl)propane-1,3-diol (3a)
^{1}H NMR (400 MHz, CDCl$_3$): δ 7.69 (s, 1H), 4.30 (t, J = 8.0 Hz, 2H), 3.84-3.62 (m, 6H), 1.87-1.86 (m, 2H), 1.32-1.27 (m, 6H), 0.87 (t, J =6.8 Hz, 3H). ^{13}C NMR (100 MHz, CDCl$_3$): δ 121.82, 67.09, 50.8, 31.66, 31.27, 30.29, 26.35, 22.54, 14.07. HRMS (ESI, M+H$^+$): m/z calcd. for C$_{11}$H$_{23}$N$_4$O$_2$$^+$ 243.1816, found 243.1815; Yield: 84% (38.0 mg, 0.157 mmol)

2-amino-2-(1-heptyl-1H-1,2,3-triazol-4-yl)propane-1,3-diol (3b)
^{1}H NMR (400 MHz, CDCl$_3$): δ 7.70 (s, 1H), 4.31 (t, J = 7.4 Hz, 2H), 3.80 (br s, 4H), 3.35 (br s, 2H), 1.90-1.87 (m, 2H), 1.32-1.25 (m, 8H), 0.86 (t, J =7.0 Hz, 3H). ^{13}C NMR (100 MHz, CDCl$_3$): δ 149.54, 122.04, 66.31, 57.10, 50.62, 31.66, 30.30, 28.76, 26.62, 22.63, 14.12. HRMS (ESI, M+H$^+$): m/z calcd. for C$_{12}$H$_{25}$N$_4$O$_2$$^+$ 257.1972, found 257.1972; Yield: 78% (38.0 mg, 0.148 mmol)

2-amino-2-(1-octyl-1H-1,2,3-triazol-4-yl)propane-1,3-diol (3c)

^{1}H NMR (400 MHz, CDCl$_3$): δ 7.62 (s, 1H), 4.24 (t, J = 7.3 Hz, 2H), 3.77 (br s, 3H), 3.47 (br s, 3H), 1.84-1.80 (m, 2H), 1.33-1.19 (m, 10H), 0.81 (t, J =7.0 Hz, 3H). ^{13}C NMR (100 MHz, CDCl$_3$): δ 121.79, 66.87, 50.65, 31.83, 30.32, 29.81, 29.36, 29.07, 26.68, 22.80, 22.76, 14.18. HRMS (ESI, M+H$^+$): m/z calcd. for C$_{13}$H$_{27}$N$_4$O$_2$$^+$ 271.2129, found 271.2128; Yield: 58% (18.0 mg, 0.066 mmol)
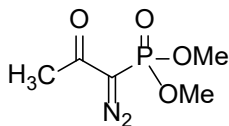

2-amino-2-(1-nonyl-1H-1,2,3-triazol-4-yl)propane-1,3-diol (3d)

^{1}H NMR (400 MHz, CDCl$_3$): δ 7.61 (s, 1H), 4.30 (t, J = 7.4 Hz, 2H), 3.79 (br s, 4H), 2.93 (br s, 2H), 1.90-1.87 (m, 2H), 1.33-1.25 (m, 12H), 0.87 (t, J =7.1 Hz, 3H). ^{13}C NMR (100 MHz, CDCl$_3$): δ 150.94, 121.56, 67.23, 56.42, 50.59, 31.89, 30.32, 29.43, 29.27, 29.09, 26.65, 22.73, 14.18. HRMS (ESI, M+H$^+$): m/z calcd. for C$_{14}$H$_{28}$N$_4$O$_2$$^+$ 285.2285, found 285.2285; Yield: 87% (40.0 mg, 0.141 mmol)
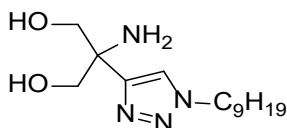
Synthesis of alkyne derivative (4a~4d)

dimethyl (1-diazo-2-oxopropyl)phosphonate (4a) (7)

Sodium hydride (60% in mineral oil) (500 mg, 3.0 mmol) was suspended in dry benzene (7.8 ml) and dry THF (2.66 ml) under nitrogen. This mixture was cooled on ice, then the solution of dimethyl (2-oxopropyl)-phosphonate (500 mg, 3.0 mmol) in dry benzene (7.8 ml) was added. A white solid was formed. The reaction mixture was stirred for 1 h at r.t. A solution of 4-methylbenzene-1-sulfonyl azide (621 mg, 0.525 mmol) in dry benzene (1.5 ml) was added. The mixture was stirred over night at r.t., then flitered through a celite pad

and washed with toluene (20 ml, x 3) and EtOAC (50 ml, x 4) and concentrated in vacuo. A dark orange oil was obtained. The crude material was purified by column chromatography using EtOAc obtained as a pale yellow oil (350 mg, 61%).

^{1}H NMR (400 MHz, CDCl$_3$): δ 3.87 (s, 3H), 3.84 (s, 3H), 2.27 (s, 3H).
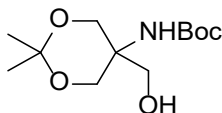
Tert-Butyl 5-(Hydroxymethyl)-2,2-dimethyl-1,3-dioxan5-ylcarbamate (4b) (8)

To a suspension of tris(hydroxymethyl)aminomethane (3.0 g, 24.76 mmol) in DM (22.5 ml) was added Boc$_2$O (5.94 g, 27.23 mmol), and the mixture was stirred at r.t. for 1 h. 2,2-Dimethoxypropane (3.64 ml, 29.71 mmol) and p-toluenesulfonic acid monohydrate (236 mg, 1.23 mmol) were added, an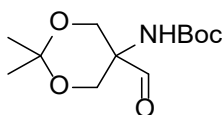d stirred overnight. The reaction mixture was diluted with Et$_2$O, washed with saturated NaHCO$_3$ and brine, dried, and concentrated in vacuo. The crude material was purified by recrystallization from Et$_2$O-hexane afforded **4b** (5.50 g, 85%) as colorless crystals.

^{1}H NMR (400 MHz, CDCl$_3$): δ 5.32 (br s, 1H), 4.26 (br s, 1H), 3.86-3.78 (dd, J =5.0 Hz, 11.3 Hz, 4H), 3.72 (d, J =6.4 Hz, 2H), 1.45 (S, 12H), 1.43 (s, 3H).

Tert-butyl (5-formyl-2,2-dimethyl-1,3-dioxan-5-yl)carbamate (4c) (8)

To a solution of oxalyl chloride (1.969 ml, 22.96 mmol) in CH$_2$Cl$_2$ (60 ml) at -78 °C was added DMSO (2.4 ml, 34.44 mmol). The mixture was stirred for 30 min at -78 °C, and a solution of **4b** (3.0 g, 11.48 mmol) in CH$_2$Cl$_2$ (8 ml) was added, and stirred at -78 °C for 30 min. The mixture was treated with triethylamine (9.6 ml, 68.89 mmol), and allowed to warm to r.t. After 30 min the reaction mixture was diluted with 1 M HCl (14 ml), washed with saturated NaHCO$_3$ and brine, dried, and concentrated in vacuo. The crude material was purified by flash chromatography using EtOAc: Hexane (1:3) as an eluent furnished tert-butyl(5-formyl-2,2-dimethyl-1,3-dioxan-5-yl)carbamate (2.40 g, 82%) as a white solid.

^{1}H NMR (400 MHz, CDCl$_3$): δ 9.63 (s, 1H), 5.55 (br s, 1H), 4.06 (d, J =11.9 Hz, 2H), 3.95 (d, J =11.7 Hz, 2H), 1.46 (s, 15H).
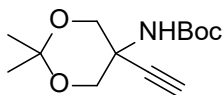
tert-Butyl 5-Ethynyl-2,2-dimethyl-1,3-dioxan-5-ylcarbamate (4d) (9)

A solution of aldehyde **4c** (1.2 g, 4.6 mmol) and dimethyl-1-diazo-2-oxopropylphosphonate **4a** (1.78 g, 9.266 mmol) in MeOH (12 ml) was treated with anhydrous K$_2$CO$_3$ (1.28 g, 9.266 mmol) at r.t. and stirred for 16 h. The mixture was diluted with diethyl ether (150 ml) and washed successively with saturated NaHCO$_3$ (50 ml), water (30 ml), brine (30 ml) and dried over Na$_2$SO$_4$. The solution was concentrated in vacuo and the crude material was purified by flash chromatography (10 % ethyl acetate in hexanes) to give alkyne **4d** as a white solid (2.40 g, 82%).

^{1}H NMR (400 MHz, CDCl$_3$): δ 5.15 (br s, 1H), 4.03 (d, J = 11.6 Hz, 2 H), 3.97 (d, J = 11.7 Hz, 2 H), 2.42 (s, 1 H), 1.47 (s, 12 H), 1.42 (s, 3 H).

General chemical synthesis for KARI 101
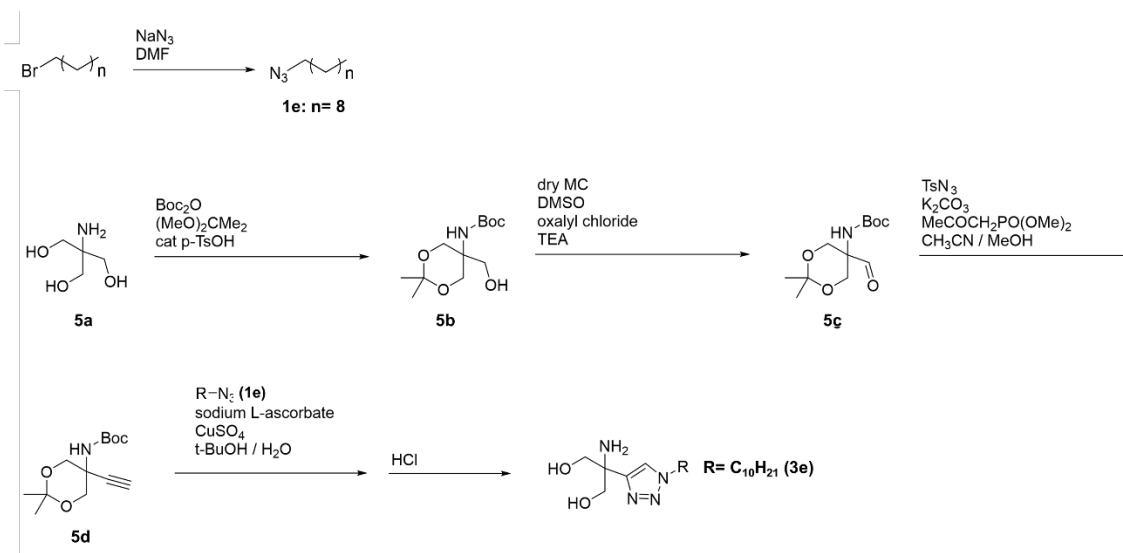
General Procedure A (for 1e azido-alkane)

To a solution of 1-bromodecane (9.9 g, 37 mmol) in DMF (50 ml) was added sodium azide (4.9 g, 75 mmol, 2 eq). The mixture was stirred at r.t. for 2 days and poured into ice water

(200 ml) and was extracted with ether. The organic layer was washed with H_2O, brine, dried over $MgSO_4$ and concentrated to give 1-azidodecane.

3.28

(t, 2H), 1.62 (m, 2H,), 1.40-1.29 (m, 14H), 0.91 (t, 3H); Yield: 91% (6.2 g)

Synthesis of alkyne derivative (5a~5d)

Tert-Butyl 5-(Hydroxymethyl)-2,2-dimethyl-1,3-dioxan5-ylcarbamate (5b)

To a suspension of tris(hydroxymethyl)amino-methane, **5a** (25.0 g, 0.206 mol) in DMF (500 ml) was added Boc_2O (49.5 g, 1.1 eq). After stirring the mixture at r.t. for 2 h, 2,2-dimethoxypropane (30.4 ml, 1.2 eq) and p-TsOH.H_2O (2.0 g, 0.05 eq) was added. The mixture was stirred at r.t. for 18 h and diluted with Et_2O (500 ml). The organic layer was washed saturated $NaHCO_3$ solution (300 ml) and brine (200 ml). The organic layer was dried over $MgSO_4$ and concentrated. The residue was crystallized with n-hexane to give *tert*-butyl 5-(hydroxymethyl)-2,2-dimethyl-1,3-dioxan-5-ylcarbamate, **5b** as a white solid (32.0 g, 59.4%).

^{1}H NMR (600 MHz, $CDCl_3$): δ 5.32 (s, 1H), 3.86–3.80 (m, 4H), 3.73 (s, 2H), 3.68 (s, 1H), 1.46–1.44 (m, 15H)
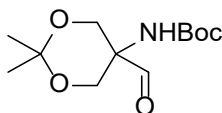
Tert-butyl (5-formyl-2,2-dimethyl-1,3-dioxan-5-yl)carbamate (5c)

DMSO (43.7 ml, 5 eq) was added dropwise to a solution of oxalyl chloride (33.4 ml, 3.17 eq) in dry MC (340 ml) at -78 °C. The mixture was stirred for 15 min and then a solution of *tert*-butyl 5-(hydroxymethyl)-2,2-dimethyl-1,3-dioxan-5-ylcarbamate, **5b** (32.0 g, 0.123 mol) in dry MC (340 ml) was added dropwise. The mixture was stirred for 2 h and then Et_3N (171 ml, 10 eq) was added. The mixture was stirred for 10 min, then cooling bath was removed and the mixture was allowed to r.t. The pale brown suspension was then diluted with EA (300 ml) and washed with 10% NH_4OH (1,500 ml). The organic layer was

concentrated and the residue was subjected to SiO_2 column chromatography by eluting with EA / n-hexane = 1 / 10 to give *tert*-butyl(5-formyl-2,2-dimethyl-1,3-dioxan-5-yl)carbamate, **5c** as a white solid (15.0 g, 47.2%).

^{1}H NMR (400 MHz, CDCl$_3$): δ 9.64 (s, 1H), 5.56 (s, 1H), 4.07 (d, 2H, J=12.0 Hz), 3.95 (d, 2H, J=12.0 Hz), 1.47 (s, 15H)
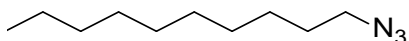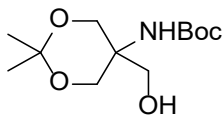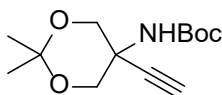

tert-Butyl 5-Ethynyl-2,2-dimethyl-1,3-dioxan-5-ylcarbamate (5d)

Dimethyl-2-oxopropyl-phosphonate (1.6 g, 1.02 eq) was added to a suspension of K_2CO_3 (3.0 g, 2.25 eq) and p-toluenesulfonyl azide (14% solution in toluene, 15.8 ml, 1.05 eq) in acetonitrile (50 ml) and the mixture was stirred vigorously at r.t. for 2.5 h. A solution of *tert*-butyl 5-formyl-2,2-dimethyl-1,3-dioxan-5-ylcarbamate, **5c** (2.5 g, 9.64 mmol) in methanol (40 ml) was added to the first reaction mixture. After the addition of K_2CO_3 (2.7 g, 2.06 eq), the mixture was stirred for 1.5 h, concentrated at reduced pressure and the residue was diluted MC (200 ml) and H_2O (200 ml). The organic layer was washed with H_2O (200 ml), dried over $MgSO_4$ and concentrated at reduced pressure. The residue was subjected to SiO_2 column chromatography by eluting with EA / n-hexane = 1 / 9 to give *tert*-butyl 5-ethynyl-2,2-dimethyl-1,3-dioxan-5-ylcarbamate, **5d** as a white solid (2.3 g, 93.4%).

^{1}H NMR (400 MHz, CDCl$_3$): δ 5.15 (s, 1H), 4.05-3.95 (m, 4H), 2.43 (s, 1H), 1.48-1.38 (m, 15H)

General Procedure B (for triazole derivatives 3e)

To a mixture of *tert*-butyl 5-ethynyl-2,2-dimethyl-1,3-dioxan-5-ylcarbamate, **5d** (4.0 g, 15 mmol), 1-azidohexane (3.16 g, 17 mmol), sodium *L*-ascorbate (4.03 g, 20 mmol), *t*-BuOH (60 ml), H_2O (128 ml) and MC (104ml) was added $CuSO_4.5H_2O$ (1.56 g, 6 mmol). The two phase solution was stirred under air at r.t. for 18 h. The aqueous layer was extracted with MC. The combined organic layer was dried over $MgSO_4$ and concentrated under reduced pressure. The residue was subjected to SiO_2 column chromatography by eluting with EA / n-Hexane = 1 / 6 to give a solid (6.5 g). The obtained solid was treated with c-

HCl (21 ml) and ethanol (210 ml) and it was vigorously stirred at room temperature for 6 h. The reaction mixture was concentrated under reduced pressure and was recrystallized in acetone to give 2-amino-2-(1-decyl-1H-1,2,3-triazol-4-yl)propane-1,3-diol, **3e** as a white solid (2.6 g, 52.4%).
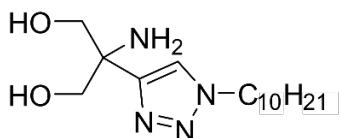
2-amino-2-(1-decyl-1H-1,2,3-triazol-4-yl)propane-1,3-diol (3e)

^{1}H NMR (500 MHz, methanol-d_4): δ 8.06 (s, 1H), 4.41 (t, 2H), 3.95 (dd, *J*= 20Hz, 15Hz, 4H), 1.91 (t, 2H), 1.29-1.33 (m, 14H), 0.89 (t, 3H). ^{13}C NMR (500 MHz, methanol-d_4): δ 144.9, 124.3, 63.7(2C), 60.8, 51.5, 33.0, 31.3, 30.6, 30.5, 30.4, 30.1, 27.5, 23.7, 14.4. found 298.4243; Yield: 52.4% (2.6 g, 8.715 mmol)

Molecular docking

Molecular modeling studies were performed using Discovery Studio Programs (2018, Accelrys) and figures were generated using PyMOL programs. The 3D coordinates of human ASM were obtained from the protein data bank for docking studies (PDB entry 5I81). 5I81 represents a crystal structure of ASM with two zine ions. Preparation of the protein was performed with the Prepare Protein protocol and a binding site was created using the Define and Edit Binding Site protocol (default parameters were used). Compounds were drawn in ChemDraw. Phosphocholine was selected as ligand template (27). Energy minimization of ligands was performed by the Clean Geometry module in Discovery Studio, and conformations were generated using the Generate Conformations protocol and the Best method (other parameters were kept at the default values). Top ten conformations with the highest degree of similarity to phosphocholine were chosen for docking simulation. Docking of the small molecule was performed using the CDOCKER protocol, and analysis of ligand interactions at the binding site was performed using the Ligand Interactions tool followed by visual inspection.

Surface plasmon resonance (SPR) spectroscopy

SPR binding experiments were performed using a Biacore® T200 instrument (Biacore, now GE Healthcare). Recombinant ASM was kindly provided by Prof. Edward H. Schuchman (Icahn School of Medicine at Mount Sinai, New York, New York, USA) (10). ASM was immobilized on the surface of a CM5 sensor chip (GE Healthcare) utilising standard amine coupling chemistry. The CM5 sensor chip surface was activated by an injection of 0.4 M EDC and 0.1 M NHS at 10 µl min^{-1} for 420 s. HBS-EP buffer containing was used as the running buffer with pH7.4 (0.01 M HEPES, 0.15 M NaCl, 3 mM EDTA, and 0.005% v/v surfactant P20). ASM (theoretical pI = 6.8) at 25 µg ml^{-1} in 10 mM sodium acetate, pH4.5, injected over the activated surface at 10 µl min^{-1} for 600 s. The amount of ASM immobilized on the activated surface was typically 5500 response units (RU). The excess hydroxysuccinimidyl groups on the surface were deactivated with 1 M ethanolamine hydrochloride, pH8.5 for 420 s at a flow rate of 10 µl min^{-1}. The surface of a reference flow cell was activated with 0.4 M EDC/0.1 M NHS for 420 s with a flow rate of 10 µl min^{-1}, and then deactivated with a 420 s exposure of 1 M ethanolamine at a flow rate of 10 µl min^{-1}. With no ligand bound to the flow path, the control flow cell was used to detect nonspecific binding of the small molecules to the sensor chip surface during screening affinity assays. For compound sample preparation, compounds were dissolved in an appropriate amount of DMSO to give a 25 mM solution. The samples were diluted with the assay buffer (10 mM phosphate buffer, 137 mM NaCl, 2.7 mM KCl, pH7.4, 0.05% v/v surfactant P20, 0.5% DMSO) to yield compound solutions for the assay of concentrations that varied from 0.7 µM to 125 µM. Prior to analyte injection, the series S CM5 chip was conditioned with three 30 s cycles of assay buffer followed by three startup cycles, allowing the response to stabilize before analyte injection. Data were collected at a temperature of 37 °C and individual compound samples were tested from lowest to highest concentrations. During each sample cycle, analyte was injected for 300 s at a flow rate of 10 µl min^{-1}. A dissociation period was monitored for 300 s after analyte injection to wash any remaining analyte from the sensor chip before running the next sample. The Biacore T200 was programmed to run an automated assay with the various small-molecule samples. The responses measured in the blank flow cell (control) were subtracted from the response measured in the flow cell with protein immobilized. Equilibrium constants (KD) were

calculated using the 'affinity' model in Biacore T200 Evaluation Software. All experiments were repeated three times.

Biochemical IC$_{50}$ determinations

The fluorescent ASM assay was performed in a 96 well plate using HNPPC (2-N-Hexadecanoyl-4-nitrophenylphosphorylcholine, Gojira Fine Chemicals, HN1004) as the substrate. ASM and HNPPC were diluted to 2 µg ml^{-1} and 1 mM in assay buffer (50 mM MES, 0.5 µM ZnCl^2, pH6.5) and incubated for 10 min at 37 °C. Small compounds with various concentrations (0.1 µM to 100 µM) were pre-incubated for 60 min at 37 °C together with 2 µg ml^{-1} ASM, and then HNPPC was added. For the standard curve, *p*-nitrophenol was used (Sigma-Aldrich, 241326). After incubation for 6 h at r.t., the reaction was stopped by addition of developing buffer (0.2 M NaOH) and the absorbance of HNPPC was measured at 410 nm. The percent inhibition was then calculated: 100 - [100 x negative control (pmol/min/µg)] / [substrate blank (OD) x conversion factor (pmol/OD, derived using calibration standard *p*-nitrophenol) / incubation time (min) x amount of enzyme (µg)]. The IC$_{50}$ was analyzed using the GraphPad Prism 7.0 software. Each experiment was performed in triplicate.

Enzyme kinetics

To obtain information on the mechanism of KARI 201, ASM activity inhibition kinetic analysis was carried out at various concentrations of Bodipy-C12-sphingomyelin (Invitrogen, D7711) ranging from 0 to 500 µM in the presence and absence of KARI 201. For kinetic measurements, KARI 201 (0, 1, 10 or 100 µM) was pre-incubated with ASM for 1 h at 37 °C before the addition of substrate. After pre-incubation, each concentration of Bodipy-C12-sphingomyelin was added and incubated for 20 min at 37 °C. The reactions were stopped by adding 100% ethanol and centrifuged at 13,000 rpm for 5 min. The supernatant was then transferred to a sampling glass vial and 5 µl was applied onto a UPLC system (Waters) for analysis of ASM activity as described below. Vmax and K$_M$ were analyzed using GraphPad Prism 7.0 software. Each experiment was performed in triplicate.

ASM, NSM, AC, and SphK activity assays

We performed the enzymatic activity measurements as previously described (1) using a UPLC system (Waters). Briefly, the brains or cells were lysed in homogenization buffer containing 50 mM HEPES (Sigma-Aldrich, H3375), 150 mM NaCl (Sigma-Aldrich, S3014), 0.2% Igepal CA-630 (Sigma-Aldrich, I8896), and protease inhibitor (Calbiochem, 539131) (14). Three microliters of the samples (plasma, brain, or cells lysate) were mixed with 3 µl of 200 µM Bodipy-C12-sphingomyelin (Invitrogen, D7711) diluted in 0.2 M of sodium acetate buffer, pH5.0, 0.2 mM $ZnCl_2$, and 0.2% Igepal CA-630 or 200 µM C12 NBD-ceramide (Cayman chemical, 202850-01-9) diluted in 0.2 M of citrate/phosphate, pH4.5, 10% FBS assay buffer and incubated at 37 °C for 1 h. The hydrolysis reactions were stopped by adding 114 µl or 54 µl of ethanol, and centrifuged at 13,000 rpm for 5 min. Thirty microliters of the supernatant was then transferred to a sampling glass vial and 5 µl was applied onto a UPLC system for analysis. SphK activity was followed as phosphorylation of (7-nitro-2-1,3-benzoxadiazol-4-yl)-derythro (NBD)-sphingosine (Avanti Polar Lipids, 860490P) to NBD-S1P (Avanti Polar Lipids, 860492P) as described previously (11). Quantification was achieved by comparison to Bodipy-C12-ceramide, NBD-sphingosine and NBD-S1P standards using the Waters Millennium software. NSM activity was analyzed using a nSMase activity assay kit (Echelon Biosciences, K-1800) according to the manufacturer's protocol.

Lipid extraction and ceramide/sphingomyelin/sphingosine/S1P quantification
We prepared samples for lipid extraction as previously described (2, 11). Samples were lysed in homogenization buffer containing 50 mM HEPES (Sigma-Aldrich, H3375), 150 mM NaCl (Sigma-Aldrich, S3014), 0.2% Igepal CA-630 (Sigma-Aldrich, I8896), and protease inhibitor (Calbiochem, 539131). To quantify the ceramide, sphingomyelin, sphingosine and S1P levels, the dried lipid extract was resuspended in 0.2% Igepal CA-630. To quantify ceramide, sphingomyelin, and sphingosine, 2 µl of the lipid extracts in 0.2% Igepal CA-630 was mixed with 2 µl of a lipid assay solution (0.2 M citrate-phosphate buffer, pH4.5, 0.3 M NaCl, 0.2 mM $ZnCl_2$) and incubated at 37 °C for 1 h. Four microliters of the lipid extracts were added into 20 µl of NDA derivatization reaction mixture (25 mM borate buffer, pH9.0, containing 2.5 mM each of NDA and NaCN). The reaction mixture was diluted 1:3 with ethanol, incubated at 50 °C for 10 min and centrifuged (13,000 g for

5 min). An aliquot (30 µl) of the supernatant was then transferred to a sampling glass vial and 5 µl was applied onto an UPLC system for analysis. The fluorescence was monitored using a model 474 scanning fluorescence detector (Waters). Quantification of the ceramide, sphingomyelin, sphingosine and S1P peaks were calculated using the Waters Millennium software.

PK and brain distribution of KARI 501, KARI 201 or KARI 101

C57BL/6 mice were administered KARI 501, KARI 201 or KARI 101 at doses of 1 mg kg^{-1} (i.v.) or 10 mg kg^{-1} (p.o.) (12). Venous blood samples were collected at 5, 15, and 30 min, and 1, 2, 4, 8, and 24 h post-dose. 30 µl of plasma was separated from whole blood by centrifugation and stored at -80 °C until analysis. Brain samples were also collected at 1, 2, 4, and 24 h post-dose, and heart, liver, and kidney samples were collected at 24 h post-dose, thoroughly rinsed with physiological saline, and weighed. 20 % tissue homogenates were prepared by homogenizing the tissue samples with 4 volumes of saline. A 30 µl aliquot of plasma or a 50 µl aliquot of tissue homogenates was deproteinized by addition of 200 µl cold methanol (containing naringenin as internal standard at 20 ng ml^{-1}) and centrifuged at 13,200 rpm for 10 min. A 10 µl aliquot of the supernatant was injected into an Agilent 6470 LC-MS/MS system. Separation was performed on a Synergy Polar RP column (4 µm particle size, 2.0 mm x 150 mm, Phenomenex) using a mobile phase that consisted of methanol and water (85:15, v/v) with 0.1% formic acid at a flow rate of 0.2 ml min^{-1}. Quantification was carried out using multiple reaction monitoring (MRM) at m/z 243→226 for KARI 501, 285→268 for KARI 201, 327→310 for KARI 101 and m/z 271→151 for naringenin (internal standard) in negative ionization mode and collision energy of 20 eV. Oral BA values were calculated as follows: BA%=AUC$_{p.o.}$ normalized by p.o. dose/AUC$_{i.v.}$ normalized by i.v. dose × 100.

Microsomal stability

KARI 501, KARI 201 or KARI 101 stock solutions (10 mM dissolved in methanol) were diluted with potassium phosphate buffer (pH7.4) to make a concentration of 10 µM. A 10 µl aliquot of this solution was then added to an 80 µl aliquot of 100 mM potassium phosphate buffer (pH7.4) containing human or mouse liver microsomes (80 µl of 0.625 mg

protein ml^{-1} phosphate buffer) and incubated at 37 °C for 10 min before adding 10 µl of an NADPH regenerating system to start the reaction (12). Reactions were stopped at 0, 15, 30, 60, and 90 min time-points by the addition of 200 µl cold acetonitrile (containing propranolol as internal standard at 20 ng ml^{-1}) and centrifuged at 13,200 rpm for 10 min. A 2 µl aliquot of the supernatant was injected into the LC-MS/MS system. The ratio of the peak area of the test compound/internal standard was used to determine the % remaining of each compound over time. The half- life ($T_{1/2}$) and % compound remaining after 30 min were then calculated.

Cytochrome P450 inhibition

KARI 501, KARI 201 or KARI 101 stock solutions (10 mM dissolved in methanol) were serially diluted with methanol to make concentrations of 100, 250, 500, 2500, and 10000 µM and then further diluted 5-fold using potassium phosphate buffer (pH7.4) (12). Probe substrate cocktail solutions for seven major cytochrome P450 isozymes (phenacetin (100 µM for 1A2), bupropion (50 µM for 2B6), diclofenac (20 µM for 2C9), mephenytoin (100 µM for 2C19), dextromethorphan (5 µM for 2D6), chlorzoxazone (50 µM for 2E1), and midazolam (5 µM for 3A4) were prepared with phosphate buffer. A 5 µl aliquot of each compound solution and a 5 µl aliquot of each probe substrate cocktail solution was incubated at 37 °C with human liver microsomes (80 µl of 0.625 mg protein ml^{-1} phosphate buffer) for 10 min before the addition of 10 µl of the NADPH regenerating system to start the reaction. Reactions were stopped at 15 min by the addition of 200 µl cold acetonitrile (containing propranolol as internal standard at 20 ng ml^{-1}) and centrifuged at 14,000 rpm for 10 min. A 2 µl aliquot of the supernatant was injected into the LC-MS/MS system. The ratio of the peak area of the test compound/internal standard was used to determine the % metabolic activity of probe substrate according to the concentrations of each compound added.

Kinase profiler, enzyme assay, and GPCR screening

Kinase profiler (430 kinases), enzyme assays (38 enzymes), and GPCR (170 GPCRs) screening of KARI 201 (10 µM) was performed at Eurofins Pharma Discovery (France).

Mice

Transgenic mouse lines over-expressing the hAPP695swe (APP) and presenilin-1M146V (PS1) mutations were originated from GlaxoSmithKline (Harlow, UK) (13) and maintained as described previously (1, 11, 12). We purchased 5xFAD mice from Jackson Labs (Stock number. 34840-JAX). To examine the possible therapeutic effect of KARI 201 in APP/PS1 mice, KARI 201 (1, 5, or 10 mg kg^{-1}) was administrated daily p.o. for 6 weeks to 7.5-mo-old APP/PS1 mice until the age of 9 months, and AMI (100 mg kg^{-1}, Sigma-Aldrich, A8404) was administrated daily p.o. in their drinking water to 6-mo-old APP/PS1 mice for 12 weeks. A control group received water without drug. Mouse survival and body weight were checked every week. Also, to confirm the possible therapeutic efficacy of KARI 201 in 5xFAD, KARI 201 (10 mg kg^{-1}) was injected daily p.o. for 4 weeks to 3-mo-old 5xFAD mice until the age of 4 months. The block randomization method was used to allocate the animals to experimental groups. To eliminate the bias, all investigators were blinded to the experimental groups and analysis such as data collection and data analysis. Mice were housed at a 12 h day/12 h night cycle with free access to water and food pellets. All protocols were approved by the Kyungpook National University Institutional Animal Care and Use Committee.

Plasma collection

Mouse blood was collected into sodium heparin-coated tubes via intracardial bleed at the time of death. Plasma was generated by centrifugation of freshly collected blood and aliquots were stored at -80 °C until use. Human plasma samples were obtained from individuals with AD and age-matched non-AD controls from Hanyang University Hospital (Table S1). Informed consent was obtained from all subjects according to the ethics committee guidelines at the Hanyang University Hospital (IRB no. HYUH 2016-12-029-003).

Histological analysis

For immunofluorescence staining, brain was cut on a vibratome (30 μm). Thioflavin S (Sigma-Aldrich, T1892) staining was carried out according to previously described procedures (30, 31). The following antibodies were used: 6E10 (mouse, 1:100, Signet,

SIG39300), SMA (mouse, 1:400, Sigma-Aldrich, A2547), AT8 (mouse, 1:500, Thermo Fisher Scientific, MN1020), Synaptophysin (rabbit, 1:100, Abcam, ab32127), MAP2 (chicken, 1:100, Abcam, ab5392), Synapsin 1 (rabbit, 1:100, Synaptic systems, 106 103), PSD95 (rabbit, 1:100, Abcam, ab18258), Iba1 (rabbit, 1:500, Wako, 019-19941), GFAP (rabbit, 1:500, Dako, N1506), Lamp1 (mouse, 1:200, Abcam, ab24170), Ki67 (mouse, 1:100, BD Science, 550609), BrdU (rat, 1:100, Abcam, ab6326), Doublecortin (DCX, rabbit, 1:400, Abcam, ab18723), SOX2 (mouse, 1:100, R&D system, MAB2018), S100β (rabbit, 1:100, Dako, Z0311), and c-Fos (mouse, 1:100, Abcam, ab208942). All were visualized using Alexa anti-mouse 488 and 633, Alexa anti-rabbit 488 and 594, or anti-chicken 488 as secondary antibodies. The sections were analyzed with a laser-scanning confocal microscope (FV3000; Olympus) or with a BX51 microscope (Olympus). MetaMorph software (Molecular Devices) was used for quantification. IMARIS software (Bitplane) (14) was used for analysis of three-dimensional reconstruction of microglia. Confocal images were taken through a z-stack (total z-axis length = 10 μm) and were imported into the IMARIS software. Cell body width was measured, and cell dendrites were automatically detected using the analysis tool. Then, the image was converted into a 3D image, and the cell body volume, process length, number of branches, and terminal tips were automatically quantified.

Western blotting

Samples were lysed in RIPA buffer (Cell signaling Technologies, 9806), then subjected to SDS-PAGE and transferred to a nitrocellulose membrane. Membranes were blocked with 5% milk, incubated with primary antibody and then incubated with the appropriate horseradish peroxidase-conjugated secondary antibody (1, 2, 11, 12). Primary antibodies to the following proteins were used: ASM (mouse, 1:500, Abcam, ab74281), S1PR1 (rabbit, 1:500, Abcam, ab11424), 6E10 (mouse, 1:500, Signet, SIG39300), BACE-1 (mouse, 1:1,000, Millipore, MAB5308), Synaptophysin (rabbit, 1:2000, Abcam, ab32127), PSD95 (mouse, 1:1000, Millipore, MAB1596), Synapsin 1 (rabbit, 1:1000, Synaptic systems, 106 103), MAP2 (chicken, 1:10000, Abcam, ab5392), LC3 (rabbit, 1:1,000, Cell Signaling Technology, 4108S), Beclin-1 (rabbit, 1:1,000, Cell Signaling Technology, 3738S), p62 (rabbit, 1:1,000, Cell Signaling Technology, 5114S), cathepsin D (goat, 1:500, R&D

Systems, BAF1029), TFEB (Goat, 1:500, Invitrogen, PA1-9109), Lamp1 (rabbit, 1:1,000; Abcam, ab24170), pAMPK (rabbit, 1:1,000, Cell Signaling Technology, 2535), AMPK (rabbit, 1:1,000, Cell Signaling Technology, 2532), pPI3K (rabbit, 1:1,000, Cell Signaling Technology, 4228), PI3K (rabbit, 1:1000, Cell Signaling Technology, 4257), pERK (rabbit, 1:1000, Cell Signaling Technology, 9105), ERK (rabbit, 1:1,000, Cell Signaling Technology, 4695), and β-actin (1:1,000, Santa Cruz, SC-1615). We performed densitometric quantification using the ImageJ software (National Institutes of Health). Images have been cropped for presentation.

ELISA

For measurement of Aβ40, Aβ42, and ASM, we used commercially available ELISA kits (Invitrogen, KHB3481 for Aβ40; Invitrogen, KHB3441 for Aβ42; and MyBioSource, MBS724194 for ASM). Cortex and hippocampus of mice were homogenized in buffer containing 0.02 M guanidine. ELISA was then performed for Aβ40, Aβ42 and ASM according to the manufacturer's instructions.

BrdU injection

Mice received intraperitoneal injections of BrdU (Sigma, B5002) dissolved in 0.9% NaCl/0.007 M NaOH solution 4 times a day (100 mg kg^{-1}, 2 hours apart). After 1 month, mice were sacrificed and brain was isolated for immunofluorescence staining.

Electrophysiology

For extracellular recordings of field excitatory postsynaptic potentials (fEPSP), animals were sacrificed by cervical dislocation. The brain was quickly removed and hemispheres were separated and cooled in ice-cold aCSF containing 124 mM NaCl, 3 mM KCl, 26 mM NaHCO$_3$, 1.25 mM NaH$_2$PO$_4$, 2 mM CaCl$_2$, 1 mM MgSO$_4$ and 10 mM glucose. Transverse hippocampal slices (400 μm) were prepared using a McIlwain tissue chopper (Mickle Laboratory Engineering Co. Ltd.) and incubated in aCSF with carbogen gas (95% O$_2$/5% CO$_2$) at room temperature for 1 h before recording. Extracellular recordings were conducted in a submerged chamber perfused with aCSF at (28-29 °C) at 2ml min^{-1}. To record field excitatory postsynaptic potentials (fEPSPs), a stimulating bipolar electrode (66

μm twisted nichrome wire) was placed on the hippocampal Schafer collateral pathway. Assessment of fEPSPs in the CA1 region by glass microelectrodes prepared on a micropipette puller (P-1000; Sutter Instrument, Novato, CA, USA) and filled with 3M NaCl (3-5 MΩ). The signals were digitized with a Multiclamp 700B amplifier (Axon Instruments). Before baseline acquisition, the stimulation intensity was adjusted to 30-50% of the maximum fEPSP slope. Single pulses delivered at 0.03Hz to obtain 30 min stable baseline recordings, LTP was induced by delivering $2 \times$ tetanus stimuli (100 Hz bursts for 1 s with a 30 s interval). All stored slopes of the responses were an average of four successive recordings. For LTP analysis, the individual slopes were normalized to the average of baseline recordings. The slope of the evoked field potential responses was assessed and expressed relative to the normalized preconditioning baseline. Randomization procedures are not applicable to these experiments. Data were collected and analyzed in a double-blind fashion.

Behavioral studies

We performed behavioral studies to assess spatial learning and memory in the Morris water maze as previously described (1, 2, 11, 12). Animals were given four trials per day for 10 d to learn the task. At day 11, animals were given a probe trial in which the platform was removed. Fear conditioning was conducted by previously described techniques (1, 11, 12). On the conditioning day, mice were individually placed into the conditioning chamber. After a 60 s exploratory period, a tone (10 kHz, 70 dB) was delivered for 10 s; this served as the conditioned stimulus (CS). The CS co-terminated with the unconditioned stimulus (US), a scrambled electrical footshock (0.3 mA, 1 s). The CS-US pairing was delivered twice at a 20 s intertrial interval. On day 2, each mouse was placed in the fear-conditioning chamber containing the same exact context, but with no administration of a CS or foot shock. Freezing was analyzed for 5 min. On day 3, a mouse was placed in a test chamber that was different from the conditioning chamber. After a 60 s exploratory period, the tone was presented for 60 s without the foot shock. The rate of freezing response of mice was used to measure the fear memory. The open field test was used for locomotion and anxious behaviors as previously described (11). The open field box consisted of a square box. Each animal was placed in the box for 10 min. Overall activity in the box was measured, and the

amount of time and distance traveled in the center arena was noted. After each trial, the test chambers were cleaned with a damp towel and distilled water followed by 70% alcohol. The light-dark test was used for assessing the anxiety-like behavior as previously described (2). One chamber was brightly illuminated, whereas the other chamber was dark. Mice were placed into the dark chamber and allowed to move freely between the two chambers with the door open for 10 min. The total number of transitions, latency to first enter the light chamber, distance traveled, and time spent in each chamber were recorded.

Cell culture and treatment

Human fibroblast lines (normal and PS1) acquired from the Coriell Institute were maintained in DMEM with 10% FBS. Cells were treated with small compounds and AMI (10 µM or 0 to 50 µM) for 30 min or 24 h, and then protein or mRNA was extracted from cell lysate for sphingolipid analysis, western blotting and real-time PCR analysis. To investigate the direct effect of the KARI compounds on the lysosomes, LysoTracker^{TM} Red DND-99 (Invitrogen, L7528) at a final concentration 25 nM was added and incubated at 37 °C for 30 min after addition of the KARI compounds or AMI treatment (10 µM). For detection of phospholipidosis, cells were treated for 24 h with LipidTOX Green phospholipidosis detection reagent (Invitrogen, H34351), together with the KARI compounds or AMI (10 µM). The MFI of LysoTracker and LipidTOX was analyzed by flow cytometry (Attune NxT, ThermoFisher). A minimum of 10,000 events per sample was acquired. To confirm the proteolytic degradation of ASM by the KARI compounds, PS1 fibroblast were pre-incubated for 24 h with 25 µM leupeptin (Sigma-Aldrich, L2884) or PBS, and then treated with the KARI compounds or AMI for 30 min and ASM activity was subsequently determined. The PS1-derived supernatant medium (P-sup) and FBS (negative control) were treated with or without $ZnCl_2$ (100 µM) added to the assay buffer (250 mM sodium acetate, 0.1% NP-40 (Igepal), pH5.0) and incubated with compounds (10 µM) for 1 h at 37 °C. After 1 h, Bodipy-C12-sphingomyelin (0.5 µM) was added and incubated for 30 min at 37 °C. The reactions were stopped by adding 100% ethanol and centrifuged at 13,000 rpm for 5 min. The activity of secretory ASM was determined using UPLC system as described above.

Cell viability and apoptosis assay

The effect of small compounds on cell viability and death was assessed using the WST-1 assay (Roche, 5015944001). Briefly, seeded cells were treated with compounds (10 μM) and incubated for 30 min. WST-1 solution was then added to each well, and the cells were further incubated. After 4 h, the absorbance was measured with a plate reader. These experiments were repeated 4–6 times. Cell death was detected by the *In Situ* Cell Death Detection Kit, TMR red (Roche, 12156792910). Analysis was performed according to the manufacturer's protocol.

Preparation of human iPSCs-derived neurons

PS1-iPSCs were established from patient skin fibroblasts (Coriell Institute) as previously described (1, 11). Established PS1-iPSCs were tested to confirm the absence of mycoplasma contamination using MycoAlert PLUS Mycoplasma detection kit (Lonza, LT07). An iPSC cell line (HPS0063) from a healthy individual was obtained from the RIKEN Bioresource Center (1, 11). For neural differentiation of human iPSCs (1, 11), iPSC colonies were detached from feeder layers and cultured in suspension as embryonic bodies for 30 d in bacteriological dishes. Embryonic bodies were then enzymatically dissociated into single cells and the dissociated cells cultured in suspension in serum-free media hormone mix media for 10-14 d to allow the formation of NSs. NSs were passaged repeatedly by dissociation into single cells followed by culture in the same manner. For terminal differentiation, dissociated NSs were allowed to adhere to poly-L-ornithine– and laminin-coated coverslips and cultured for 10 d.

Mouse and human hippocampal neuron culture

To confirm the role of KARI 201 in neurons, cells from E18 C57BL/6 mice were prepared as previously described (11, 15). Hippocampus were dissected and then dissociated followed by incubation in papain (Worthington, LS003120) at 37 °C for 15 min. Neurons were plated on poly-L-lysine-coated coverslips with neuronal culture medium, serum-free Neurobasal medium (Gibco, 21103) containing 2% B27 supplements (Gibco, 17504-044), 1 mM Glutamax supplement (Gibco, 35050-061), and 100 U ml^{-1} streptomycin/ 100 U ml^{-1} penicillin (Gibco, 10378016) at 37 °C in a humidified atmosphere of 5% CO_2. Human

hippocampal neurons acquired from the Innoprot (P10153) were maintained in neuronal media (Innoprot, P60157). Mouse hippocampal neurons were treated with purified, recombinant ASM to measure autophagy regulation. NH_4Cl was used to inhibit the autophagic flux. For some experiments Aβ 1-42 (1 μM, 24 h, Invitrogen, 03112) was added to the neuron cultures and then ghrelin (10 μM, 1 h, TOCRIS, 1463) or KARI 201 (10 μM, 1 h) was added. The cells were analyzed for synaptic density using MAP2 (chicken, 1:100, Abcam, ab92434), PSD95 (rabbit, 1:100, Abcam, ab18258) and vGlut1 (mouse, 1:100, Abcam, ab134283) antibodies.

Mouse hippocampal neural stem cell (NSC) culture

NSCs from the hippocampus were isolated from the mouse brain as previously described (16, 17). In brief, the hippocampus of WT (6 to 8-week-old) was minced in ice-cold Hibernate A/B27/Glutamax medium (HABG) (all from Invitrogen) and dissociated using papain (Worthington, LS003120) solution. After tissue trituration, cells were separated by Optiprep (Sigma-Aldrich, D1556) density gradient centrifugation. Fractionated neural progenitors and microglia were cultured in Neurobasal A (Invitrogen, 10888-022)/B27 medium with glutamax (0.5 mM), gentamycin (10 μg ml^{-1}, Gibco, 15710-060), mouse fibroblast growth factor 2 (mFGF2, 5 ng ml^{-1}, Invitrogen, RP-8626) and mouse platelet-derived growth factor-bb (mPDGFbb, 5 ng ml^{-1}, Invitrogen, PMG0044). Neural progenitors proliferated in suspension and formed aggregates (NSs). Every 2 days, half of the medium was replaced with fresh culture medium.

Neurosphere (NS) formation assay and EdU staining

To detect NSCs in the hippocampus, NSs were cultured as previously described (16). Aβ 1-42 (1 μM, 24 h, Invitrogen, 03112) was exposed to the NSs and then ghrelin or KARI 201 was added (10 μM, 1 h). NSs were then mechanically dissociated and the resulting viable individual cells were counted. These cells were plated 1×10^4 cells per well in uncoated 24-well plates. After 7 days of incubation, formed NSs were counted in each well using a microscope. A minimum cutoff size of 50 μm in diameter was used in defining a NS. All experiments were carried out at least three times, and at least six wells per condition

and per experiment were counted. Cell proliferation was measured using EdU (5-ethynyl-2'-deoxyuridine) assay kit (Thermo Fisher Scientific, C10339)

HEK 293T cell culture and transfection

HEK293 cells (ATCC, CRL-1573) were seeded in poly-D-lysine–coated 24-well plates the day before transfection, at a density of 50,000 cells per well. Transient transfections were performed using Lipofectamine 2000 (Thermo Fisher) according to the manufacturer's instructions. Cells were transfected with 200-300 ng DNA (pCMV-hGHSR, cDNA Resource Center, GHSR0A0000) and 0.6 μl Lipofectamine 2000 per well for 5 h. Ghrelin (10 μM, 1 h, TOCRIS, 1463) or KARI 201 (10 μM, 1 h) was added to the cells 48 h after the transfection was started, and the cells were then analyzed for Ca^{2+} immobilization assays, ghrelin/ghrelin receptor signaling, and ghrelin receptor internalization (rabbit, 1:100, Abcam, ab969250).

Ca^{2+} immobilization assay

HEK293 cells transfected with hGhrR were incubated in loading buffer (HBSS supplemented with 20 mM HEPES, 1 mM $CaCl_2$, 1mM $MgCl_2$, 0.7 mg/mL probenicid, 0.2% Fluo-4) (50 μL per well) containing the Ca^{2+}-sensitive fluorophore (Fluo-4 AM, Life Technologies). The cells were incubated for 1 h at 37 °C and then were washed twice in loading buffer. Cells were stored in the dark at 37 °C until visualization under a laser scanning confocal microscope equipped with a live cell chamber system (FV3000, Olympus). For image acquisition, cells within a single field of view were imaged over 1 min in the absence of compound (line base) with a 10 s shuttered interval between each image. When each compound at various concentrations (0.01 nM to 100 μM) was added the field of view was imaged over a 2 min period, with a 10 s shuttered interval between each image. Fluorescent intensity changes (from t 0) were measured and expressed as the area under the curve and normalized against baseline. EC_{50} values were analyzed using GraphPad Prism 7.0 software. Each experiment was performed in triplicate.

RNA seq

Total RNA was isolated from cortical neurons, cortical microglia, and hippocampus of WT, APP/PS1, and APP/PS1 mice treated with KARI 201 using the Trizol reagent (Invitrogen, 15596026). RNA quality was assessed in an Agilent 2100 bioanalyzer using the RNA 6000 Nano Chip (Agilent Technologies), and RNA quantification was performed using a ND-2000 Spectrophotometer (Thermo Inc). To prepare and sequence libraries, libraries were prepared from 1μg of total RNA using the SMARTer Stranded RNA-Seq Kit (Clontech Laboratories, Inc). rRNA was removed using a RIBO COP rRNA depletion kit (LEXOGEN, Inc). The rRNA depleted RNAs were used for cDNA synthesis and shearing following the manufacture's instruction. Indexing was performed using the Illumina indexes 1-12. The enrichment step was carried out using of PCR. Subsequently, libraries were checked using the Agilent 2100 bioanalyzer (DNA High Sensitivity Kit) to evaluate the mean fragment size. Quantification was performed using the library quantification kit using a StepOne Real-Time PCR System (Life Technologies, Inc). High-throughput sequencing was performed as paired-end 100 sequencing using HiSeq 2500 (Illumina, Inc). Then, total RNA-Seq reads were mapped using TopHat software tool in order to obtain bam file (alignment file). Read counts mapped on transcripts region were extracted from the alignment file using bedtools and Bioconductor that uses R statistical programming language. The alignment file also was used for assembling transcripts, estimating their abundances and detecting differential expression of genes, linc RNAs or isoforms. And we used the FPKM (fragments per kilobase of exon per million fragments) as the method of determining the expression level of the gene regions. Quantile normalization method was used for comparison between samples. Functional gene classification was performed by DAVID (http://david.abcc.ncifcrf.gov/).

RNA isolation and real-time PCR analysis

RNA was extracted from the brain homogenates and cell lysates using the RNeasy Lipid Tissue Mini kit and RNeasy Plus Mini kit (QIAGEN) according to the manufacturer's instructions. cDNA was synthesized from 5 μg of total RNA using a commercially available kit (Takara Bio Inc.). Quantitative real-time PCR was performed using a Corbett research RG-6000 real-time PCR instrument. Used primers are described in SI Appendix, Table. S2.

Statistical analysis

Sample sizes were determined by G-Power software (with $\alpha = 0.05$ and power of 0.8). In general, statistical methods were not used to re-calculate or predetermine sample sizes. Variance was similar within comparable experimental groups. Individuals performing the experiments were blinded to the identity of experimental groups until the end of data collection and analysis for at least one of the independent experiments. Comparisons between two groups were performed with a Student's t-test. In cases where more than two groups were compared to each other, a one way analysis of variance (ANOVA) was used, followed by Tukey's HSD test. All statistical analyses were performed using SPSS statistical software and GraphPad Prism 7.0 software. *$P < 0.05$, **$P < 0.01$, and ***$P < 0.001$ were considered to be significant.
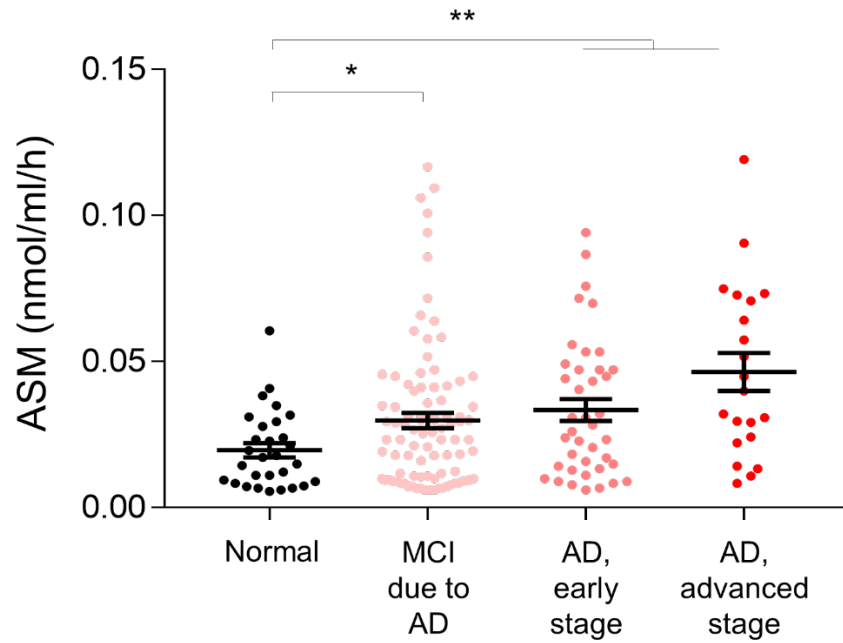
Fig. S1. ASM activity in plasma of AD patients with disease progression (normal n = 29; MCI due to AD n = 93; AD, early stage n = 40; AD, advanced stage n = 36). One-way analysis of variance, Tukey's post hoc test. G, Student's t test. *P < 0.05, **P < 0.01. All error bars indicate s.e.m.
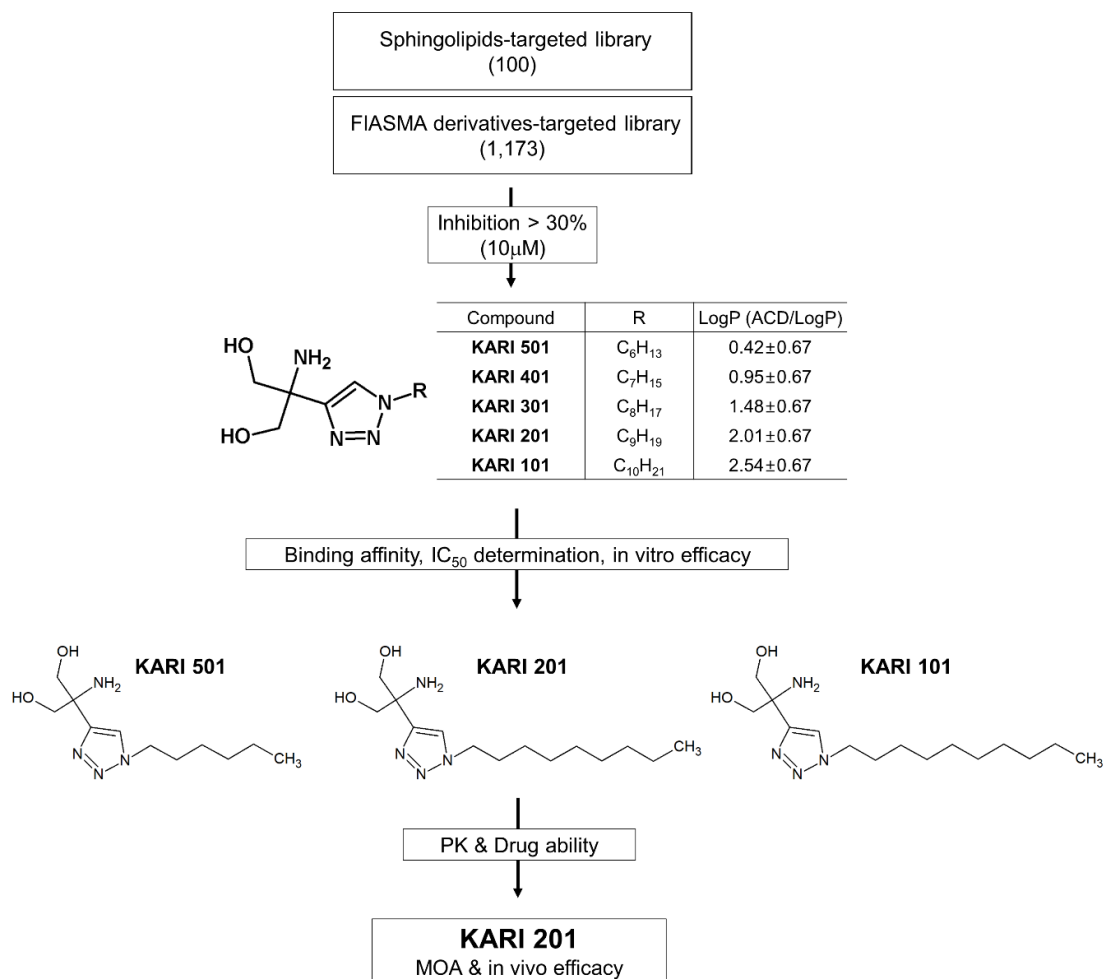
Fig S2. Chemical compound screening. The primary endpoint (% inhibition) was determined from cell-based ASM activity assays. A total of 1,273 chemical compounds from two targeted libraries, a sphingolipid-targeted library and FIASMA derivative-targeted library, were screening in PS1 fibroblasts at 10 µM concentration for 30 min. Data for each compound was normalized to percent inhibition based on control cells. The backbone of compounds with a percent inhibition > 30% was identified as 2-amino-2-(1,2,3-triazol-4-yl)propane-1,3-dio, and R represents modifications to the backbone by the addition of 6 - 10 alkyl groups based on lipophilicity (LogP). Five compounds (KARI 101-KARI 501) were further analyzed by determing direct binding to ASM, IC_{50} determination, and in vitro efficacy. Based on these assays, three compounds were selected and pharmacokinetics and drug ability were performed. Finally, the mechanism of action and in vivo efficacy were performed using KARI 201.
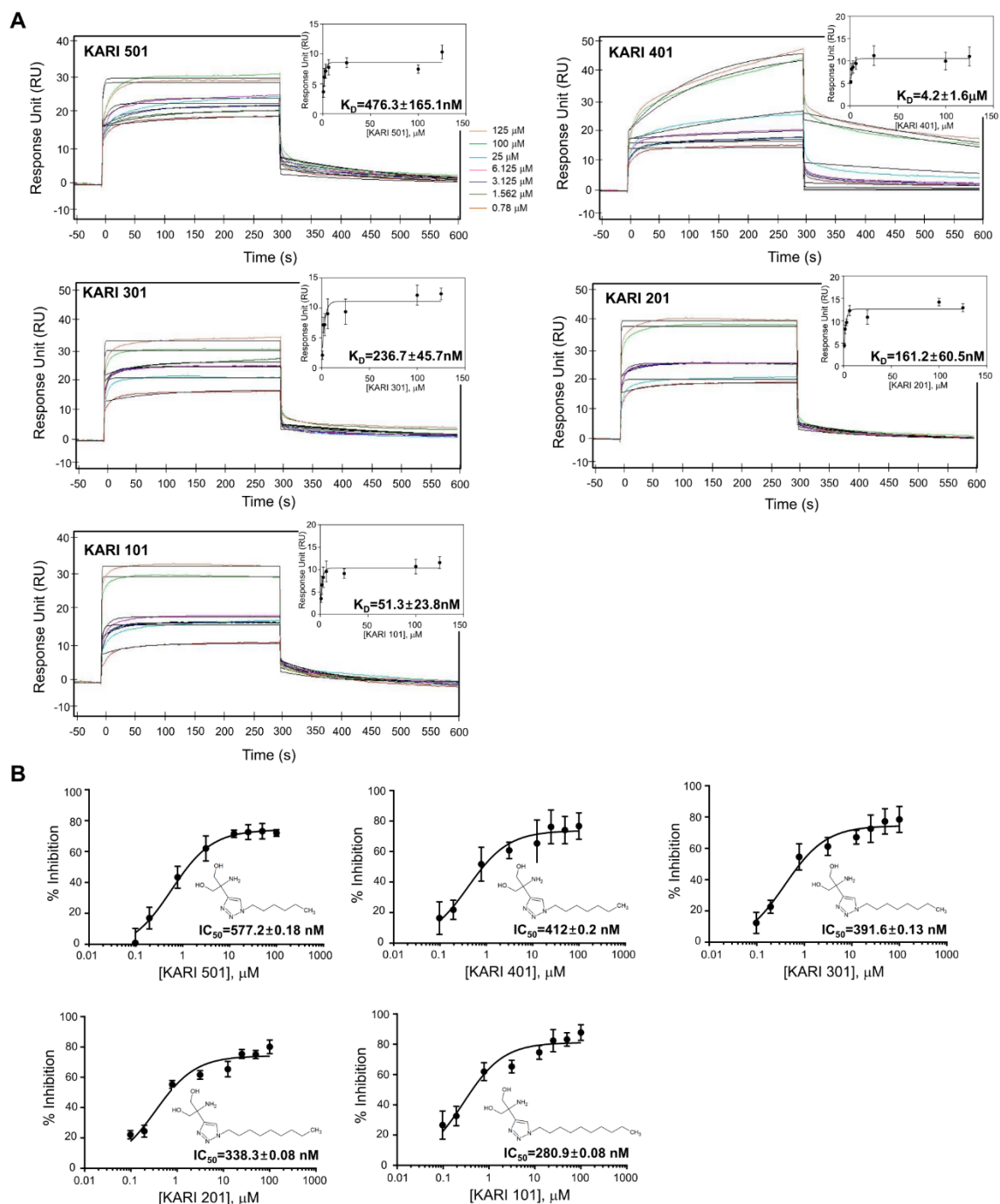
Fig. S3. KARI compounds directly bind to ASM and inhibit its activity. (**A**) Representative binding sensorgrams depicting the interaction of each compounds with ASM assessed by SPR detection. Binding data (dose-dependent lines) were fit (black lines) to a simple affinity model. Mean ± s.e.m. equilibrium binding dissociation constant (K_D) determined from three independent experiments with similar results. (**B**) Effect of various

concentrations of each compound on the direct inhibition of ASM activity (data are mean ± s.e.m.; n = 3 independent experiments).
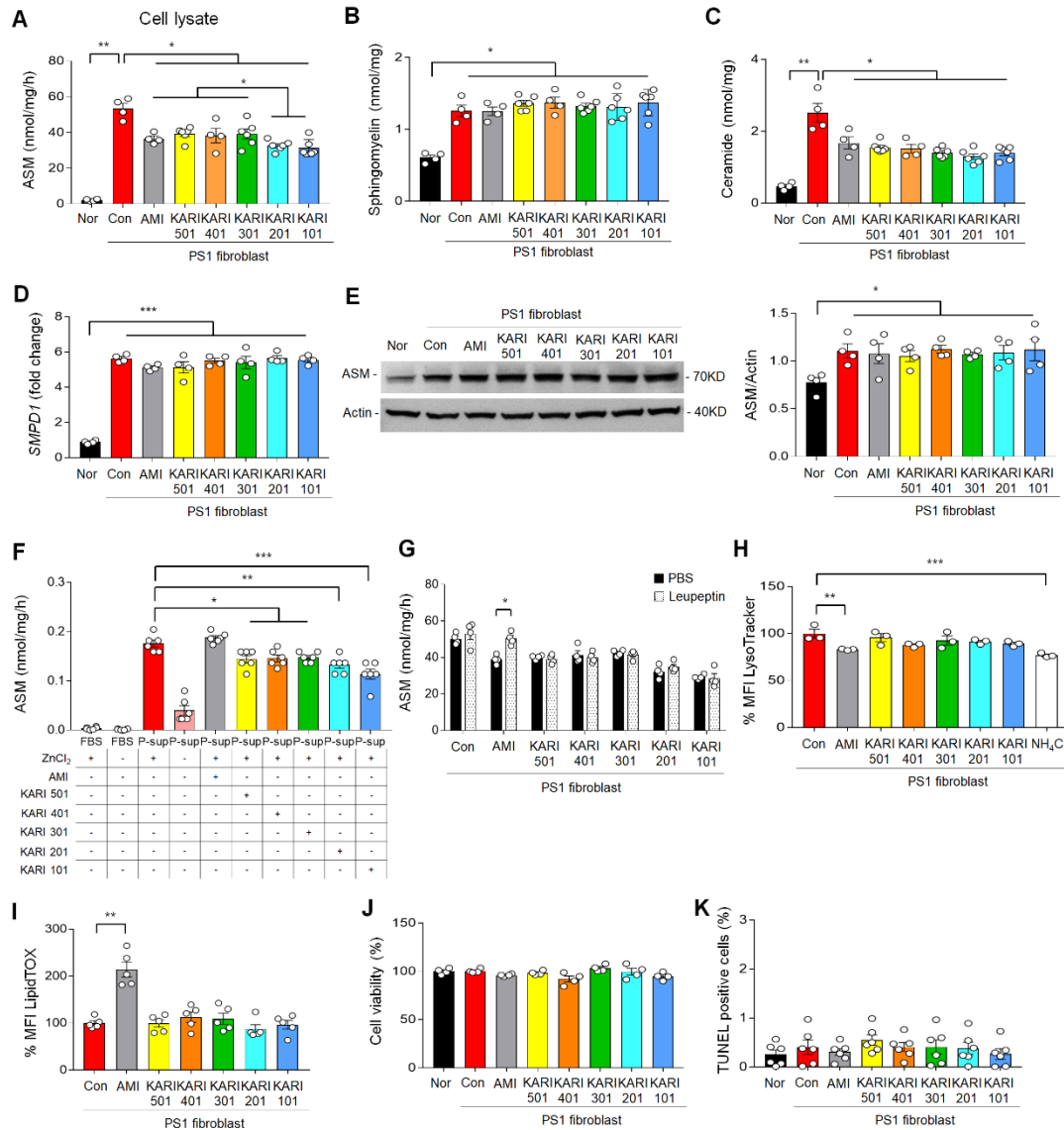
Fig. S4. Direct inhibition of ASM activity by KARI compounds in PS1 fibroblasts. (**A to C**) ASM activity (A), sphingomyelin (B), and ceramide (C) were assessed after 30 min KARI compounds (10 μM) or AMI (10 μM) treatment in the PS1 fibroblasts (n = 4-6 per group). (**D and E**) Fold change of *Smpd1* mRNA (D) or ASM protein level (E) (n = 4 per group). (**F**) PS1-derived supernatant medium (P-sup) and FBS were treated as indicated with or without addition of $ZnCl_2$ to the assay buffer and the activity of secretory ASM was determined (n = 6 per group). (**G**) PS1 fibroblasts were pre-incubated for 24 h 25 μM leupeptin, then treated KARI compounds or AMI for 30 min, and ASM activity was subsequently determined (n = 4 per group). (**H and I**) Effect of KARI compounds or AMI

on lysosomal pH (H, n = 3 per group) and phospholipid accumulation (I, n = 5 per group) through FACS analysis of PS1 fibroblasts stained with LysoTracker red and LipidTOX Green in PS1 fibroblasts. (**J** and **K**) WST1 assay (J, cell viability) and TUNEL assay (K, apoptotic cells) in PS1 fibroblasts after KARI compounds or AMI treatment (n = 4-6 per group). A-F and H-K, One-way analysis of variance, Tukey's post hoc test. G, Student's t test. $*P < 0.05$, $**P < 0.01$, $***P < 0.001$. All error bars indicate s.e.m.
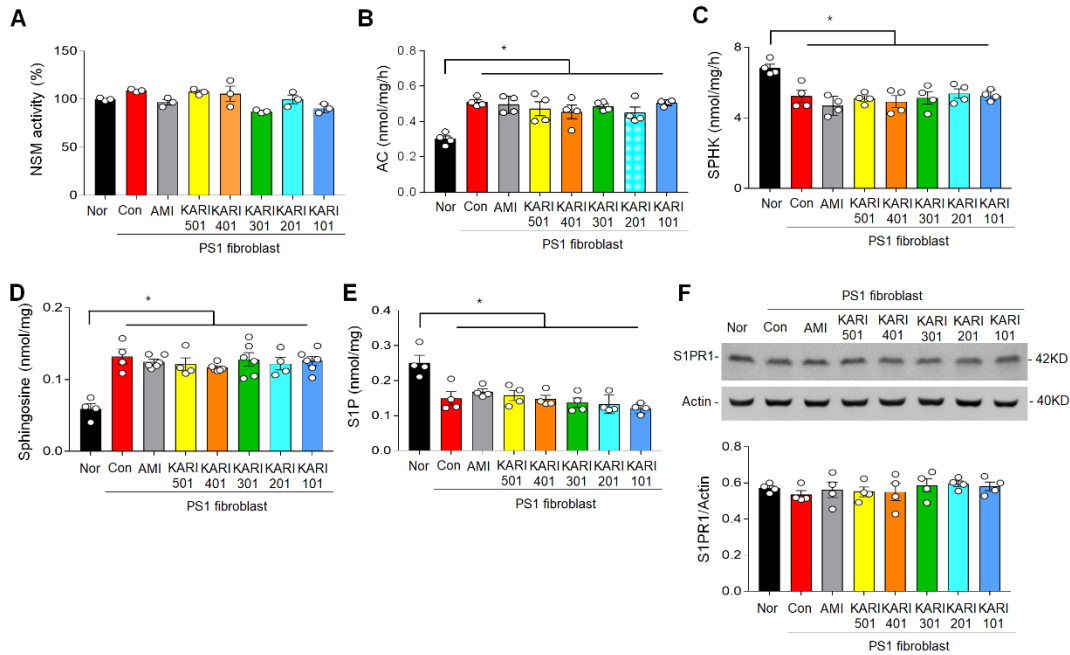
Fig. S5. The effects on other sphingolipids by KARI compounds in PS1 fibroblast. (**A** to **E**) NSM activity (A, n = 3 per group), AC activity (B, n = 4 per group), SPHK activity (C, n = 4 per group), Sphingosine (D, n = 4-6 per group), and S1P (E, n = 4 per group) were assessed after 30 min KARI compounds (10 μM) or AMI (10 μM) treatment in the PS1 fibroblasts. (**F**) Western blot analysis of S1PR1 in PS1 fibroblasts with KARI compounds (10 μM) or AMI treatment (n = 4 per group). A-F, One-way analysis of variance, Tukey's post hoc test. *P < 0.05. All error bars indicate s.e.m.
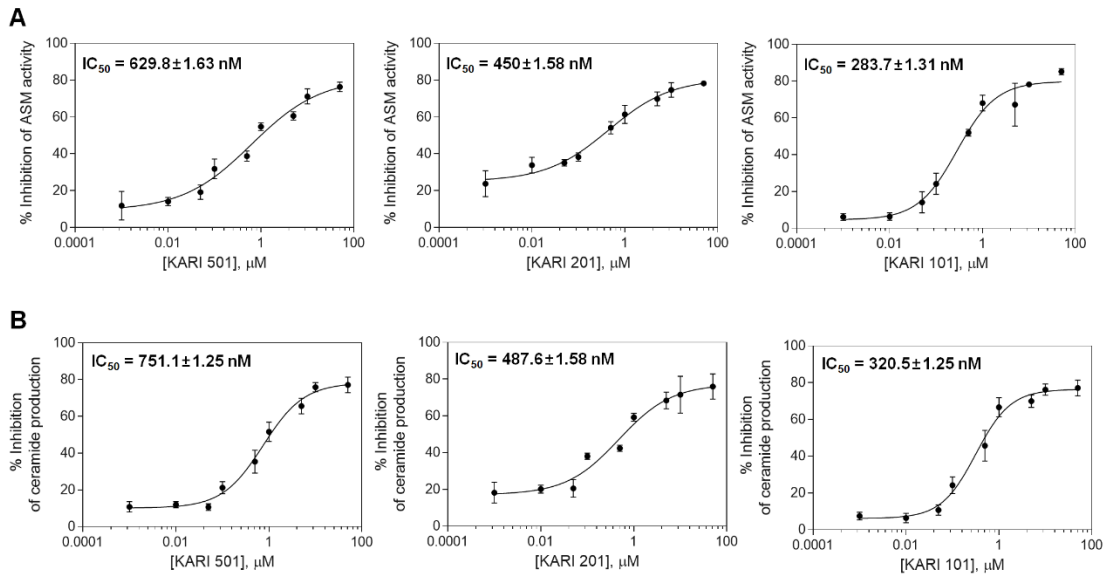
Fig. S6. Cell-based IC$_{50}$ for inhibition of ASM activity and ceramide production by KARI 501, KARI 201, and KARI 101 in PS1 fibroblasts. (**A** and **B**) Concentration-dependent inhibition of ASM activity (A) and ceramide production (B) in PS1 fibroblasts by KARI 501, KARI 201 or KARI 101 (10 µM) (n = 3-4 independent experiments per group). All error bars indicate s.e.m.

A

p.o. 10 mg/kg

i.v. 1 mg/kg

PK parameter (Plasma)	KARI 501		KARI 201		KARI 101	
	p.o.10 mg/kg	i.v.1 mg/kg	p.o.10 mg/kg	i.v.1 mg/kg	p.o.10 mg/kg	i.v.1 mg/kg
AUC_{last} (ng·h/mL)	3128.46 ±1596.36	427.10 ±27.85	4981.59 ±526.29	743.46 ±16.23	4231.82 ±155.04	851.11 ±46.39
AUC_{inf} (ng·h/mL)	3130.75 ±1596.14	433.24 ±29.66	5029.87 ±573.49	751.16 ±16.14	4289.3 ±98.75	852.41 ±47.01
Half-life$_{plasma}$ (h)	2.54±0.31	3.14±1.65	3.44±0.72	3.78±0.54	4.07±0.67	2.59±0.15
MRT (h)	4.2±2.05	2.54±0.80	4.85±0.29	3.36±0.54	6.09±0.73	3.85±0.29
C_{max} (ng/mL)	554.74 ±91.95	/	1293.81 ±148.81	/	658.956 ±27.30	/
Co (ng/mL)	/	631.89 ±106.79	/	123.16 ±92.92	/	365.58 ±169.32
T_{max} (h)	0.50±0.43	/	0.33±0.14	/	0.63±0.15	/
BA (%)	72.26	/	66.96	/	50.12	/

B

p.o. 10 mg/kg

i.v. 1 mg/kg

PK parameter (Brain)	KARI 501		KARI 201		KARI 101	
	p.o.10 mg/kg	i.v.1 mg/kg	p.o.10 mg/kg	i.v.1 mg/kg	p.o.10 mg/kg	i.v.1 mg/kg
AUC_{last} (ng·h/mL)	4424.24 ±750.22	715.77 ±3.399	7414.07 ±632.16	1351.54 ±143.91	16023.5 ±994.33	3370.77 ±219.60
C_{max} (ng/mL)	413.96 ±36.89	/	532.10 ±101.14	/	759.08±24.05	/
Co (ng/mL)	/	100.41 ±85.60	/	42.10 ±11.28	/	201.67 ±75.98
T_{max} (h)	2.33±1.53	/	2.33±1.53	/	8±4.00	/
MRT (h)	3.83±0.12	3.89±0.15	7.23±0.53	4.79±0.02	11.81±0.69	6.68±0.25
Brain distribution	1.41	1.68	1.49	1.82	3.25	3.74

C

Fig. S7. PK studies of KARI 501, KARI 201, and KARI 101. (**A** and **B**) Mean plasma (A) and brain (B) concentration vs. time profiles of KARI 501, KARI 201, and KARI 101 after single dose p.o. and i.v. administration at doses of 10 mg kg⁻¹ and 1 mg kg⁻¹, respectively (n = 3-5 mice per group). PK parameters of each compound in plasma (A) and brain (B) after p.o. or i.v. administration in mouse. (**C**) Tissue concentrations of each compound at 24 h in mouse following p.o. or i.v. delivery (n = 3-5 mice per group). All error bars indicate s.e.m.

A

Compound	Microsome	% remaining after 0.5h		half-life
		mean	SEM	(h)
KARI 501	Human	82.01	1.78	3.12
	Mouse	98.21	1.87	41.71
KARI 201	Human	83.72	4.88	2.01
	Mouse	91.17	4.04	5.67
KARI 101	Human	54.10	0.35	0.87
	Mouse	95.42	0.60	5.16

B
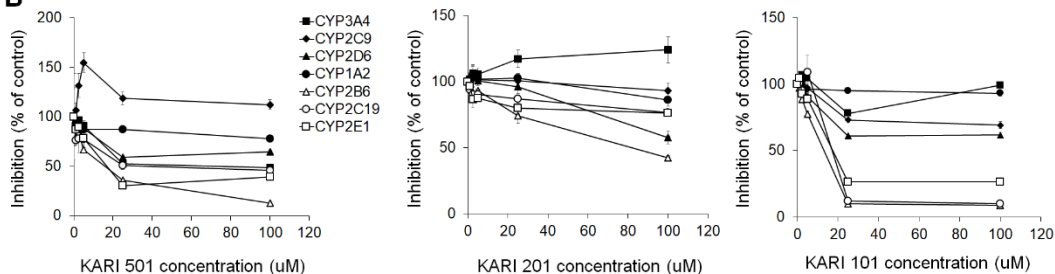
Compound	IC$_{50}$ (µM)						
	CYP3A4	CYP2C9	CYP2D6	CYP1A2	CYP2B6	CYP2C19	CYP2E1
KARI 501	55.5	>100	>100	>100	12.9	53.8	20.7
KARI 201	>100	>100	>100	>100	76.4	>100	>100
KARI 101	>100	>100	>100	>100	9.1	19.3	15.4

Fig. S8. Microsomal stability and CYP inhibition of KARI 501, KARI 201, and KARI 101. (**A**) % compound remaining after 0.5 h and the half-life of KARI 501, KARI 201, and KARI 101 after incubation with human and mouse liver microsomes (n = 3 independent experiments per group). (**B**) The IC$_{50}$ (µM) and % inhibition of 7 major CYP isozymes by each compound at 25 µM (n = 3 independent experiments per group). All error bars indicate s.e.m.
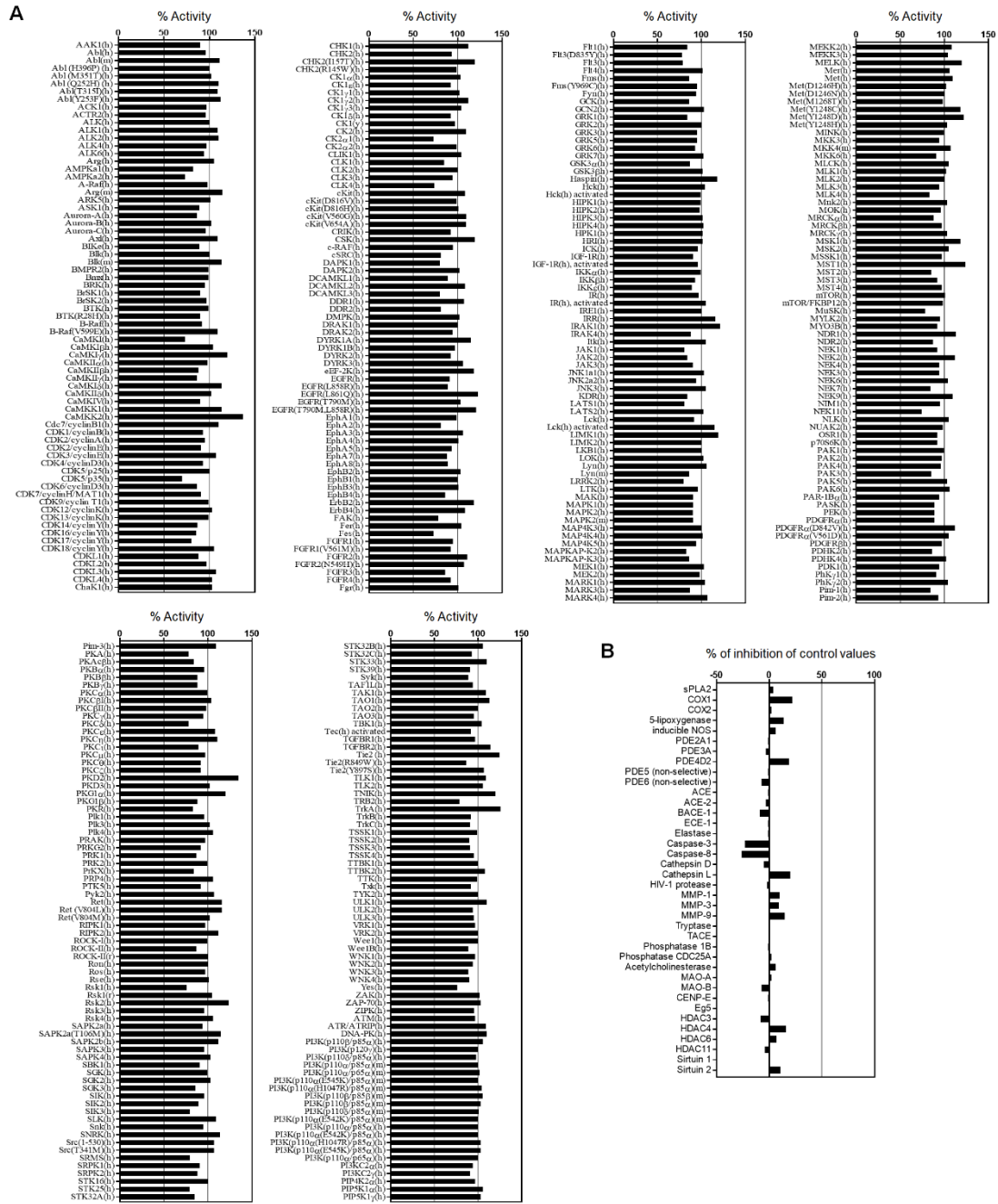
Fig. S9. Off target effects of KARI 201. (**A** and **B**) The inhibitory activity of KARI 201 (10 μM) was assessed against panel of 430 kinases profiler (A) and 38 enzymes (B). The results presented in a indicate the remaining activity of each kinase (average of two duplicate determinations) in the presence of 10 μM of KARI 201 ± standard deviation. Compound enzyme inhibition effect (average of two duplicate determinations) was calculated as a % inhibition of control enzyme activity. All error bars indicate s.e.m.
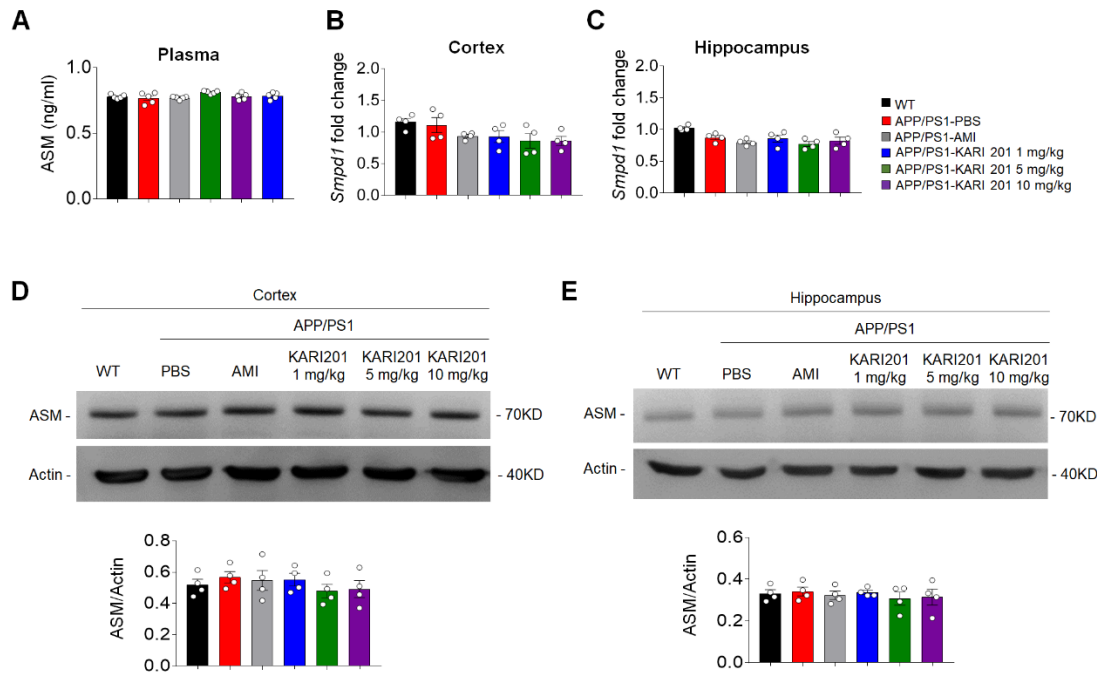
Fig. S10. KARI 201 does not affect mRNA and protein levels of ASM in plasma, cortex, and hippocampus of APP/PS1 mice. (**A**) ASM protein levels in plasma of APP/PS1 mice with AMI or KARI 201 (n = 5 mice per group). (**B** to **E**) ASM mRNA and protein levels in cortex (B, D) or hippocampus (C, E) of APP/PS1 mice treated with AMI or KARI 201 (n = 4 mice per group). A-E, One-way analysis of variance, Tukey's post hoc test. All error bars indicate s.e.m. All data analysis was done at 9-mo-old mice.
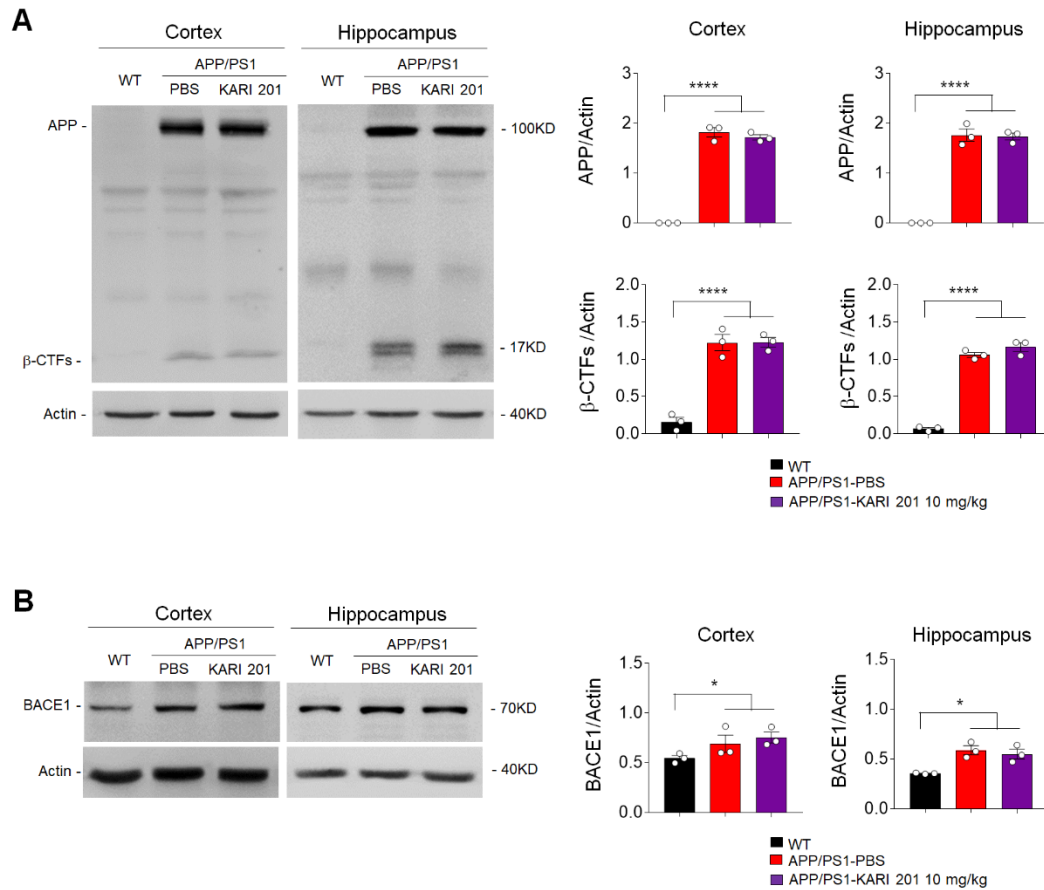
Fig. S11. KARI 201 does not affect processing of APP. (**A** and **B**) Western blot analysis and quantification of APP and β-CTF level (A) and BACE1 level (B) in cortex or hippocampus of WT and APP/PS1 mice treated with PBS or 10mg kg^{-1} of KARI 201 (n = 3 mice per group). A and B, One-way ANOVA, Tukey's post hoc test. *P < 0.05, ****P < 0.0001. All error bars indicate s.e.m. All data analysis was done at 9-mo-old mice.
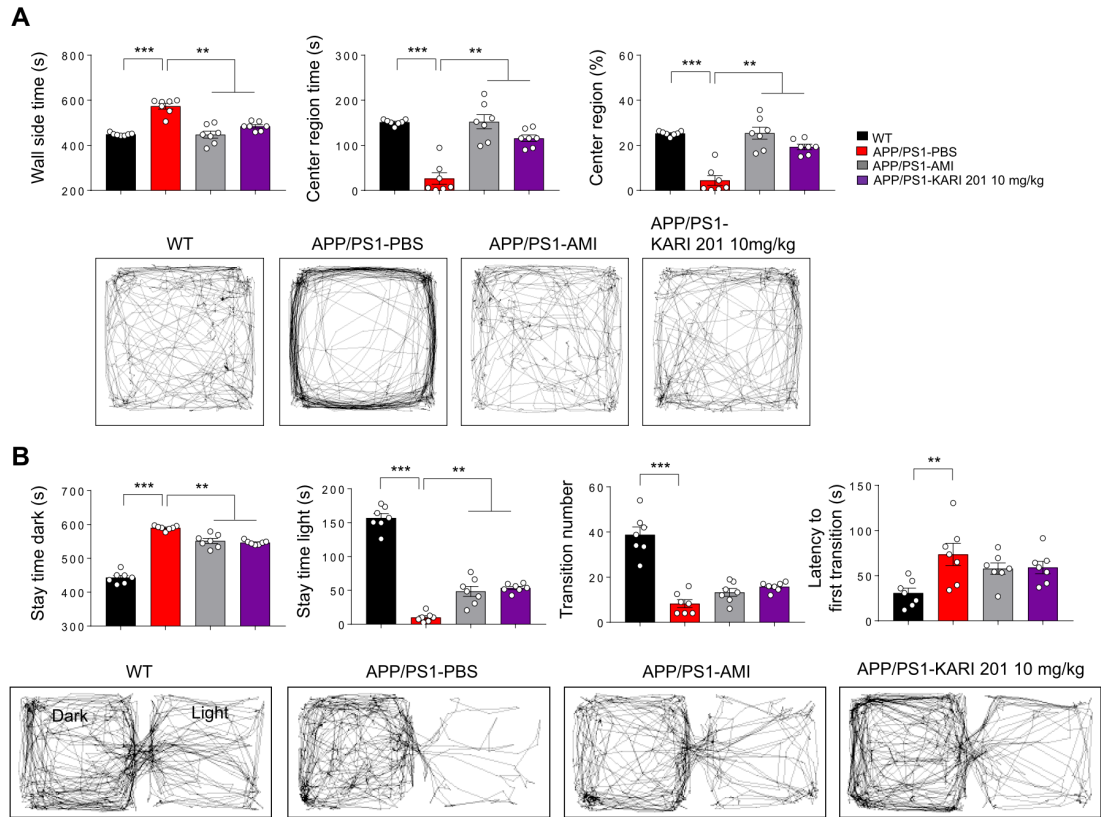
Fig. S12. KARI 201 restores AD-like behavior in APP/PS1 mice. (**A**) Time spent in the wall side and center regions and percent of center region during open field test (top, n = 7 mice per group). Representative traces of mouse movement during open field test (bottom). (**B**) Time spent in the dark and light, the number of light-dark transition, and latency to the first transition during light-dark test (top, n = 7 mice per group). Representative traces of mouse movement during light-dark test (bottom). A and B, One-way ANOVA, Tukey's post hoc test. **P < 0.01, ***P < 0.001. All error bars indicate s.e.m. All data analysis was done at 9-mo-old mice.
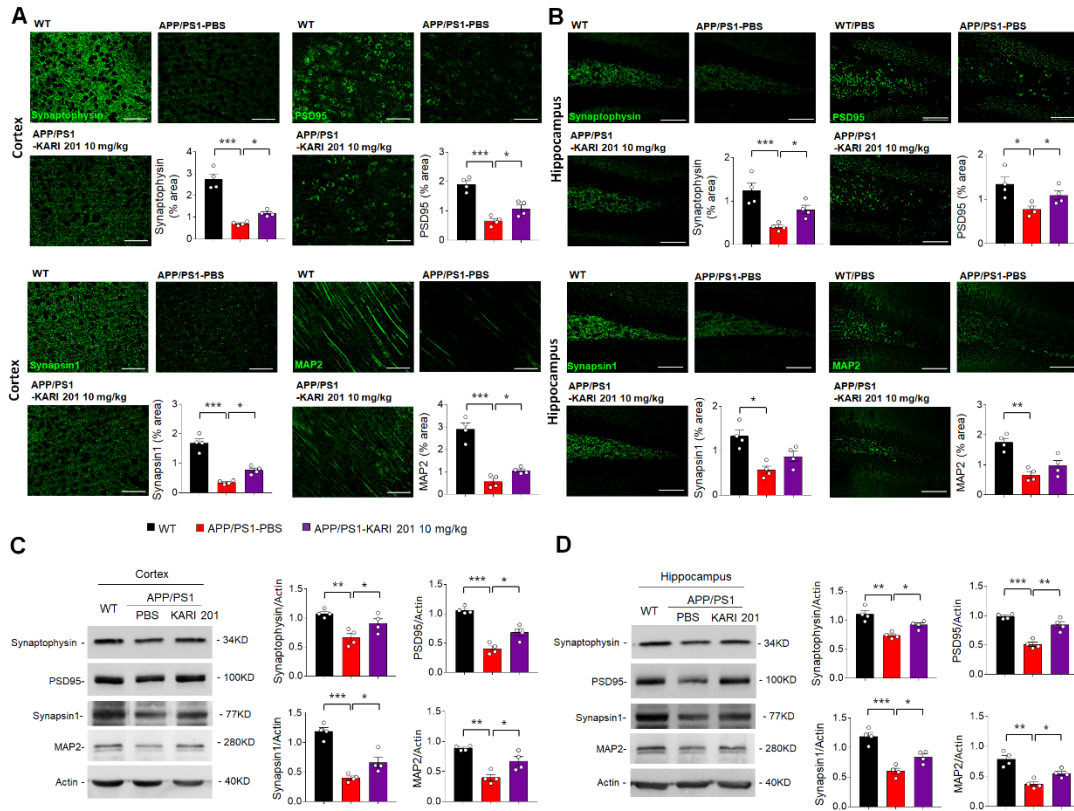
Fig. S13. KARI 201 improves synapse loss in APP/PS1 mice. (**A** and **B**) Representative immunofluorescence images and quantification of synaptophysin, PSD95, synapsin1, and MAP2 in cortex and hippocampus of WT and APP/PS1 mice treated with PBS or KARI 201 (n = 4 mice per group). Scale bars, 100 μm. (**C** and **D**) Western blot analysis for synaptophysin, PSD95, synapsin1, and MAP2 in cortex and hippocampus of each group (n = 4 mice per group). A-D, One-way ANOVA, Tukey's post hoc test. $*P < 0.05$, $**P < 0.01$, $***P < 0.001$. All error bars indicate s.e.m. All data analysis was done at 9-mo-old mice.
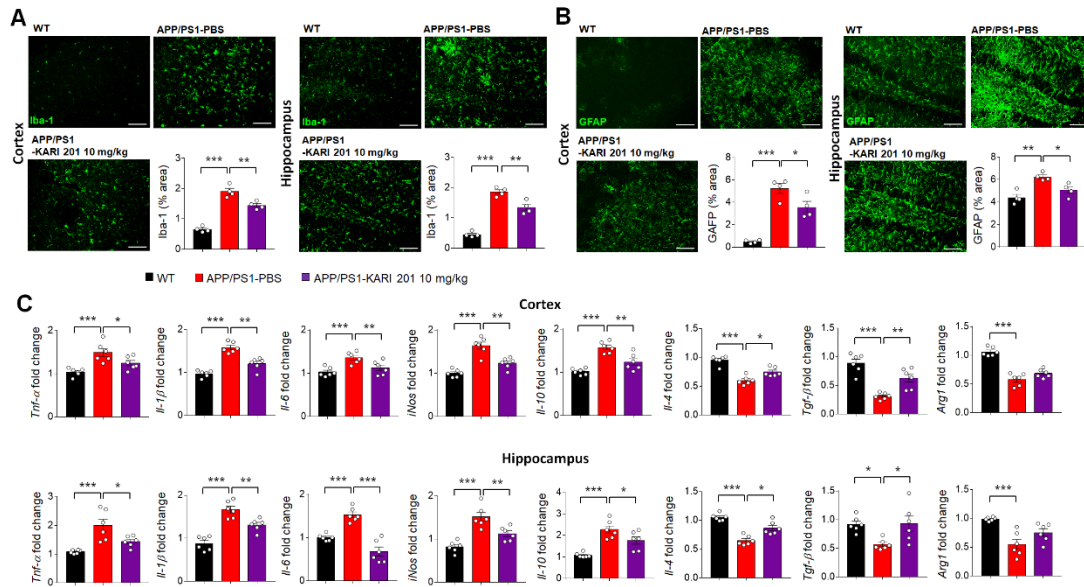
Fig. S14. KARI 201 improves neuroinflammation in APP/PS1 mice. (**A** and **B**) Immunofluorescence images and quantification of microglia (Iba-1) and astrocyte (GFAP) in cortex and hippocampus of WT and APP/PS1 mice treated with PBS or KARI 201 (n = 4 mice per group). Scale bars, 100 μm. (**C**) mRNA levels of inflammatory markers in cortex and hippocampus of each group (n = 6 mice per group). Pro-inflammatory marker: *Tnf-α*, *Il-1β*, *Il-6*, and *iNos*, Immunoregulatory cytokine: *Il-10*, Anti-inflammatory marker: *Il-4*, *Tgf-β*, and *Arg1*. A-D, One-way ANOVA, Tukey's post hoc test. *P < 0.05, **P < 0.01, ***P < 0.001. All error bars indicate s.e.m. All data analysis was done at 9-mo-old mice.
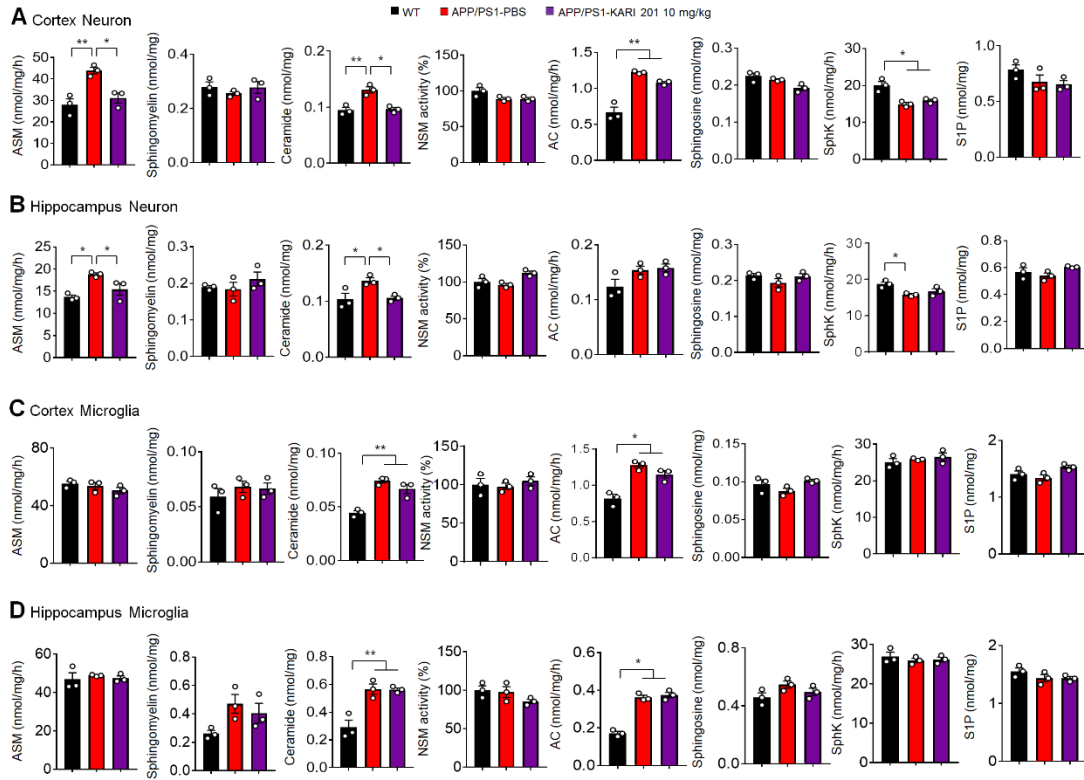
**Fig. S15. KARI 201 reduces ASM activity in neurons of APP/PS1 mice. (A** to **D)** ASM activity, sphingomyelin, ceramide, NSM activity, AC activity, SphK activity, sphingosine, and S1P in neuron (A, B) or microglia (C, D) derived from cortex and hippocampus of WT and APP/PS1 treated with PBS or KARI 201 (n = 3 per group). A-D, One-way ANOVA, Tukey's post hoc test. *P < 0.05, **P < 0.01. All error bars indicate s.e.m. All data analysis was done at 9-mo-old mice.
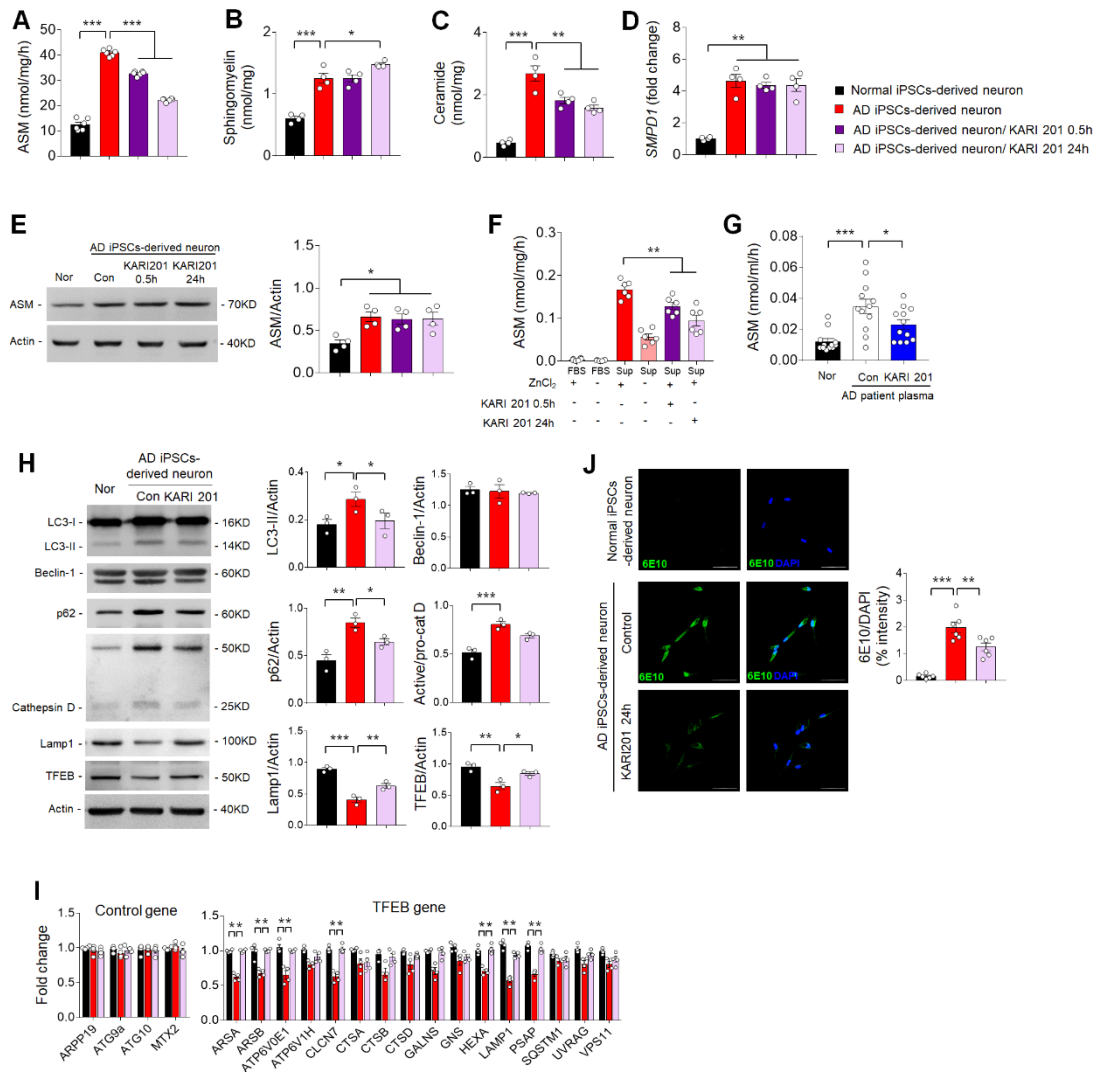
Fig. S16. KARI 201-mediated reduction of ASM activity restores autophagy dysfunction in neurons derived from AD patient iPSCs. (**A** to **C**) ASM activity (A), sphingomyelin (B), and ceramide (C) were assessed after 30 min or 24 h KARI 201 (10 μM) treatment in normal or AD patient iPSCs-derived neuron (n = 4-6 per group). (**D** and **E**) Fold change of *SMPD1* mRNA (D) or ASM protein level (E) in each group (n = 4 per group). (**F**) AD patient iPSCs-derived neuron supernatant medium (Sup) and FBS were treated as indicated with or without addition of $ZnCl_2$ to the assay buffer, and the activity of secretory ASM was determined (n = 6 per group). (**G**) ASM activity in the plasma of AD patients with KARI 201 incubation for 24 h (n = 12 per group). (**H**) Western blot analyses for LC3, beclin-1, p62, Cathepsin D, Lamp1, and TFEB in the normal or AD

patient iPSC–derived neuron after KARI 201 treatment (n = 3 per group). (**I**) Quantitative real-time PCR analysis of control or TFEB-target gene expression (n = 4 per group). (**J**) Immunocytochemistry and quantification for Aβ (6E10) (n = 6 per group). Scale bars, 50 μm. A-J One-way analysis of variance, Tukey's post hoc test. *P < 0.05, **P < 0.01, ***P <0.001. All error bars indicate s.e.m.
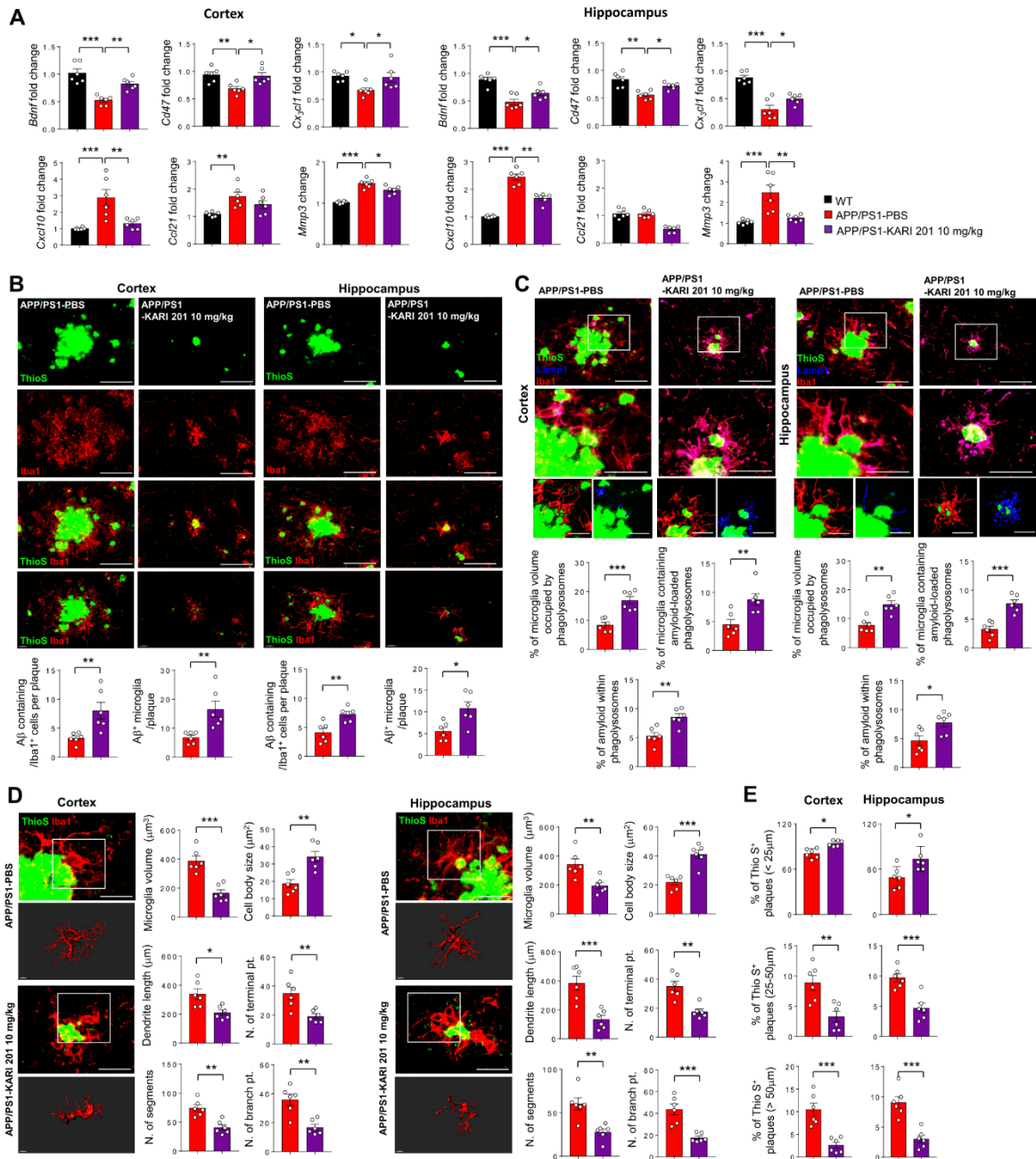
Fig. S17. KARI 201 ameliorates microglial phagocytosis by regulating neuronal off/on signals. (**A**) mRNA levels of Off (*Bdnf, Cd47, and Cx3cl1)* and On signal (*Cxcl10, Ccl21, and Mmp3*) in cortex and hippocampus of WT and APP/PS1 mice treated with PBS or KARI 201 (n = 6 mice per group). (**B**) Immunostaining images of the colocalization of microglia (Iba1, red) with Aβ aggregates (ThioS, green) and quantification of Aβ positive cells and microglia. (n = 6 mice per group). Scale bars = 10 μm. (**C**) Top, immunofluorescence images of ThioS (Aβ plaques, green) encapsulated within Lamp1+

structures (phagolysosomes, blue) in microglia (Iba1, red) present in cortex and hippocampus of each group. Low-magnification scale bars, 30 μm; High-magnification scale bars, 20 μm; 3D reconstruction from confocal image stacks scale bars, 10 μm. Bottom, quantification of microglia volume occupied by Lamp1$^+$ phagolysosomes, percent of microglia containing Aβ-loaded phagolysosomes and Aβ encapsulated in phagolysosomes (n = 6 mice per group). (**D**) Left, morphology of microglia (Iba1, red) surrounding Aβ (ThioS, green) in cortex and hippocampus of each group. High magnification (Scale bars, 20 μm) and imaris-based three-dimensional images (Scale bars, 10 μm) of microglia surrounding Aβ. Right, imaris-based automated quantification of microglial morphology (n = 6 mice per group). (**E**) Morphometric analysis of Aβ plaques in cortex and hippocampus of each group (n = 6 mice per group). Brain sections were labeled with ThioS and plaques were counted and assigned to three mutually exclusive size categories based on maximum diameters: small <25 μm; medium 25-50 μm; or large >50 μm. A, One-way analysis of variance, Tukey's post hoc test. B-E, Student's t test. *P < 0.05, **P < 0.01, ***P <0.001. All error bars indicate s.e.m. All data analysis was done at 9-mo-old mice.
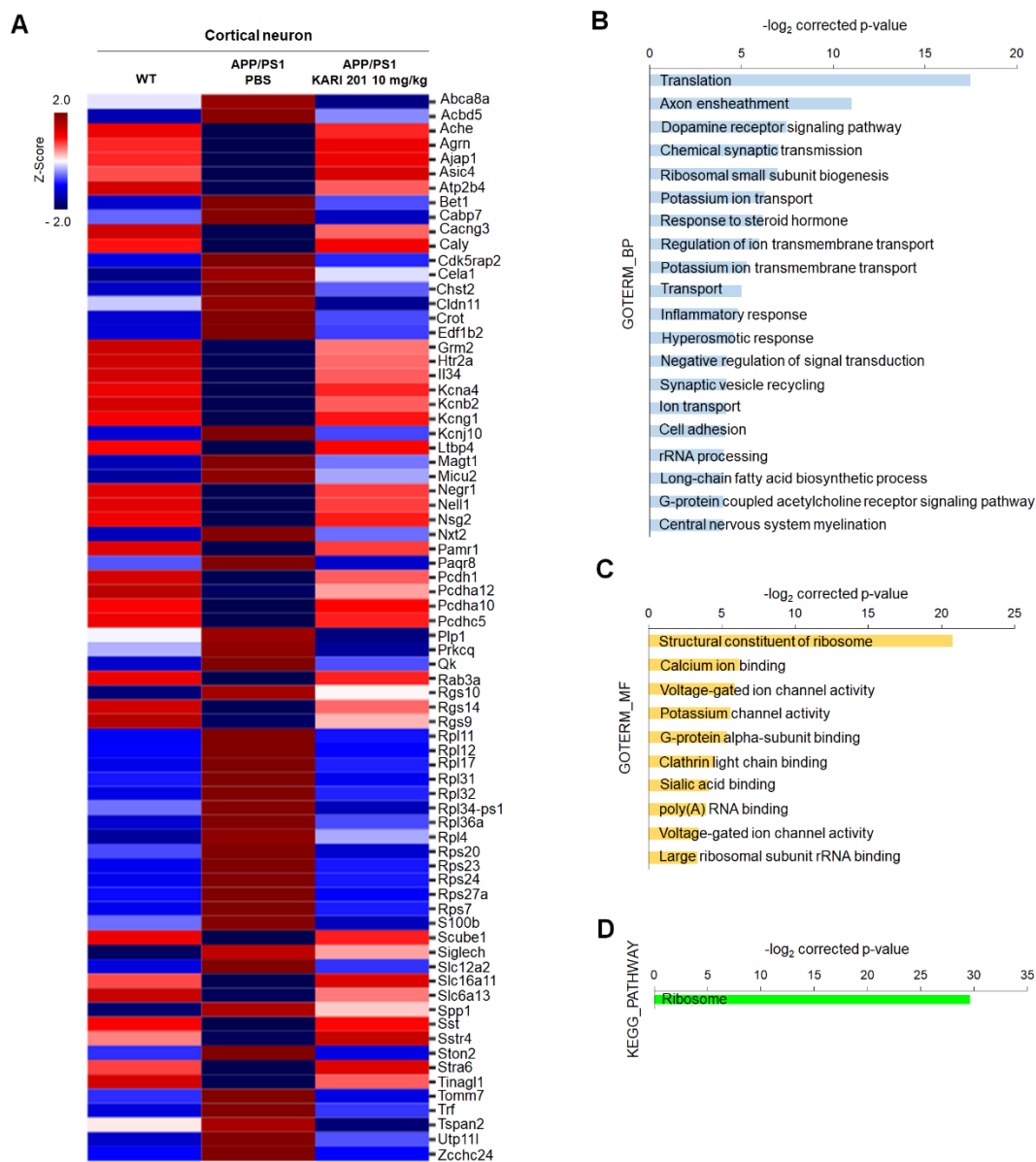
Fig. S18. RNA sequencing in neurons isolated cortex of WT and APP/PS1 mice treated with PBS or KARI 201. (**A**) Heatmap analysis of RNA seq expression data of cortical neurons (n = 3 per group). (**B** to **D**) GO term enrichment analysis of biological process (GOTERM_BP) (B), molecular function (GOTERM_MF) (C), and KEGG pathway enrichment analysis (D) was performed using DAVID Bioinformatics Resources 6.8. All data analysis was done at 9-mo-old mice.
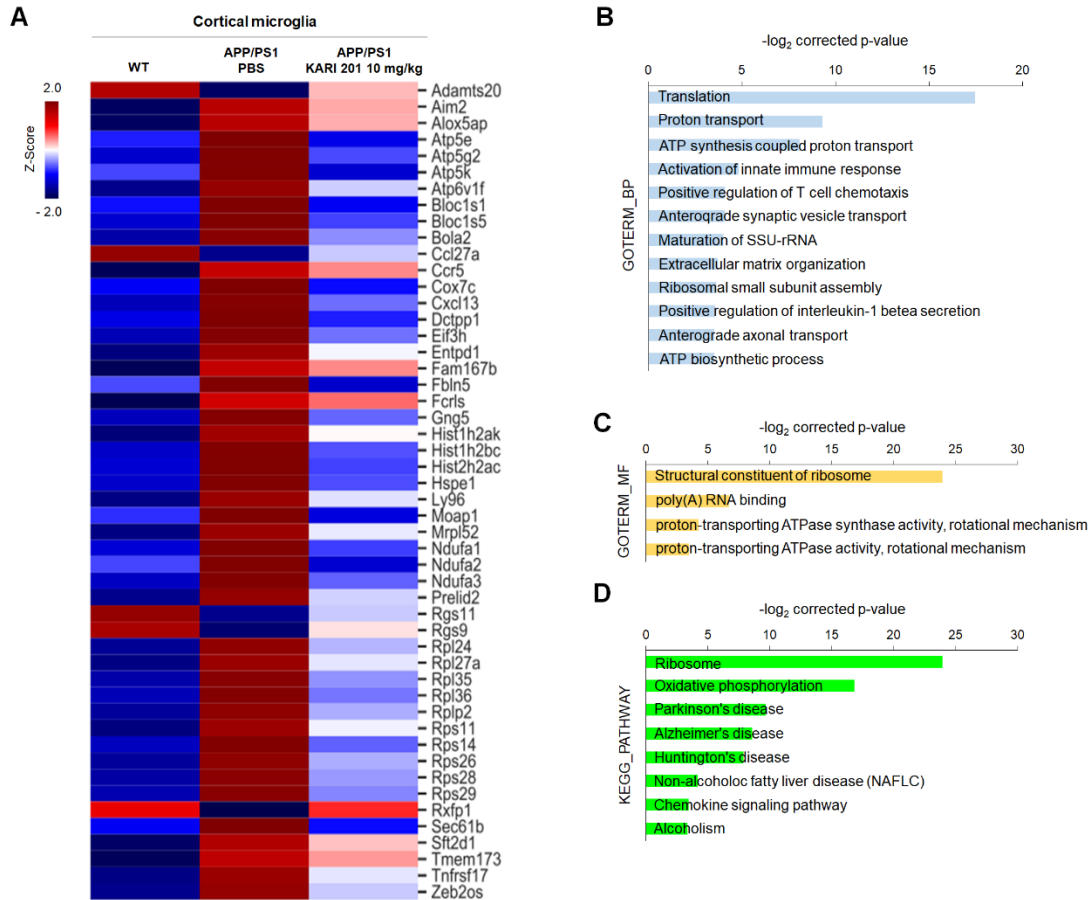
Fig. S19. RNA sequencing in microglia isolated cortex of WT and APP/PS1 mice treated with PBS or KARI 201. (**A**) Heatmap analysis of RNA seq expression data of cortical microglia (n = 3 per group). (**B** to **D**) GO term enrichment analysis of biological process (GOTERM_BP) (B), molecular function (GOTERM_MF) (C), and KEGG pathway enrichment analysis (D) was performed using DAVID Bioinformatics Resources 6.8. All data analysis was done at 9-mo-old mice.
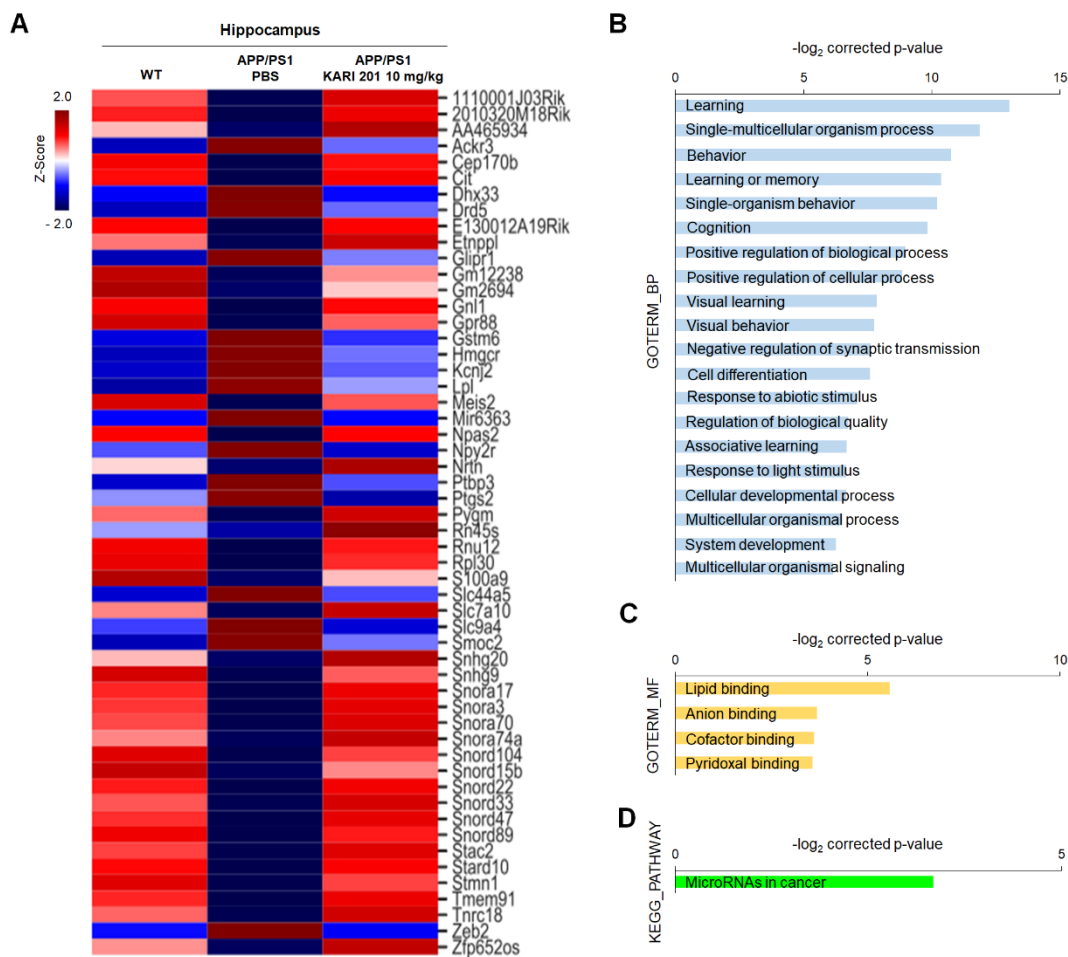
Fig. S20. KARI 201 enhances gene expression related to hippocampal learning and memory in APP/PS1 mice. (**A**) Heatmap analysis of RNA seq expression data of hippocampus isolated from WT and APP/PS1 mice injected with PBS or KARI 201 (n = 3 per group). (**B** to **D**) GO term enrichment analysis of biological process (GOTERM_BP) (B), molecular function (GOTERM_MF) (C), and KEGG pathway enrichment analysis (D) was performed using DAVID Bioinformatics Resources 6.8. All data analysis was done in 9-mo-old mice.
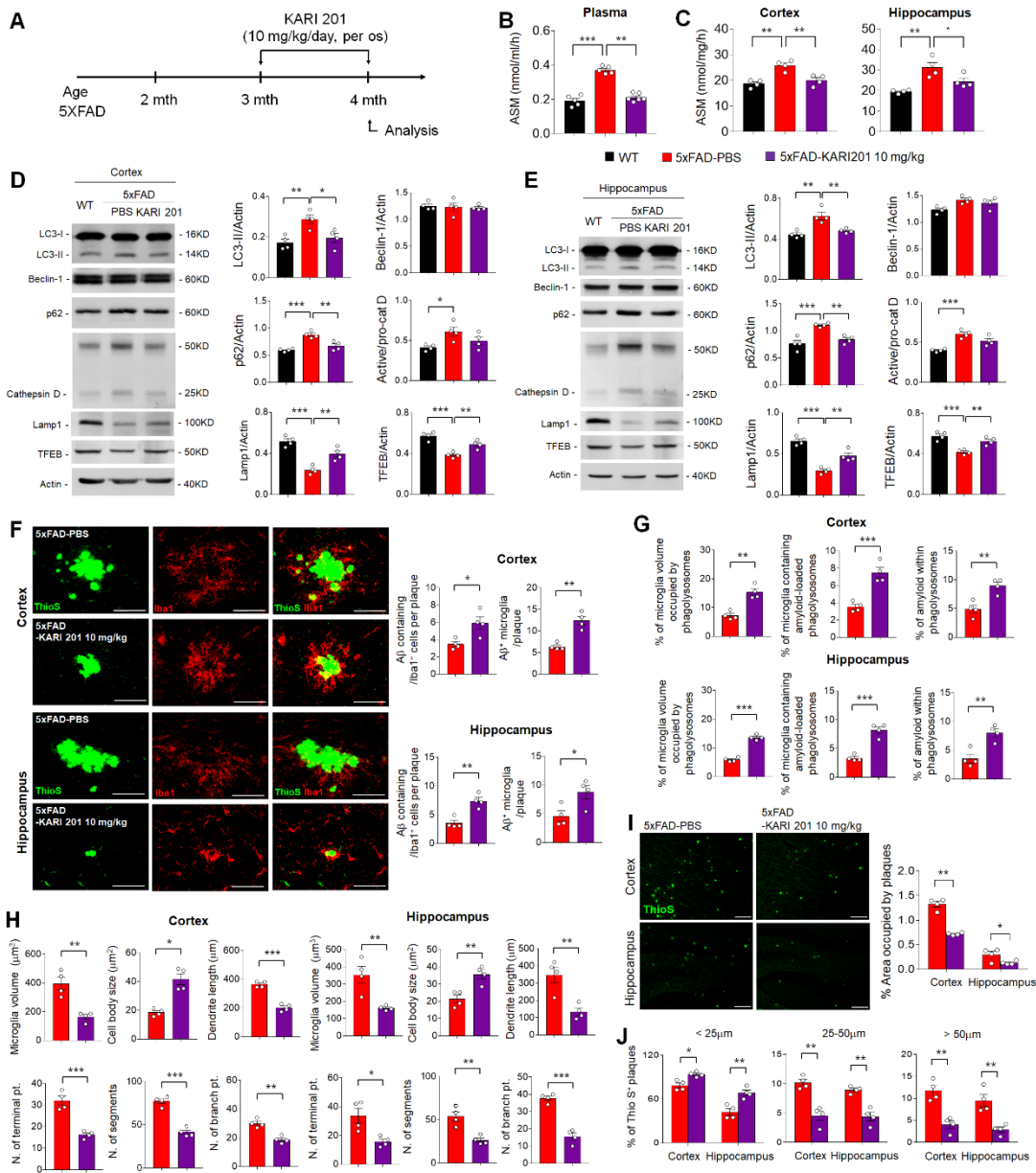
Fig. S21. KARI 201 treatment improves autophagy dysfunction, microglial phagocytosis, and Aβ accumulation in 5xFAD mice. (**A**) Scheme of experimental procedure. Daily administration of KARI 201 (10 mg kg^{-1}) or PBS orally to 3-mo-old 5xFAD mice for 4 weeks. (**B** and **C**) ASM activity in plasma (B; n = 5-6 mice per group), cortex, and hippocampus (C; n = 4 mice per group) of each group. (**D** and **E**) Western blot analyses and quantification for LC3, Beclin-1, p62, cathepsin D, Lamp1, and TFEB in the cortex (D) and hippocampus (E) of each group (n = 4 mice per group). (**F**) Immunostaining images of the colocalization of microglia (Iba1, red) with Aβ aggregates (ThioS, green)

and quantification of Aβ positive cells and microglia. (n = 4 mice per group). Scale bars = 10 μm. (**G**) Quantification of microglia volume occupied by Lamp1$^+$ phagolysosomes, percent of microglia containing Aβ-loaded phagolysosomes and Aβ encapsulated in phagolysosomes (n = 4 mice per group). (**H**) Imaris-based automated quantification of microglial morphology (n = 4 mice per group). (**I**) Left, representative immunofluorescence images of thioflavin S (ThioS, Aβ plaques) in cortex and hippocampus of each group. Scale bars, 100 μm. Right, quantification of area occupied by Aβ plaques (n = 4 mice per group). (**J**) Morphometric analysis of Aβ plaques in cortex and hippocampus of each group (n = 4 mice per group). B-E, One-way analysis of variance, Tukey's post hoc test. F-J, Student's t test. *P < 0.05, **P < 0.01, ***P <0.001. All error bars indicate s.e.m. All data analysis was done at 4-mo-old mice.
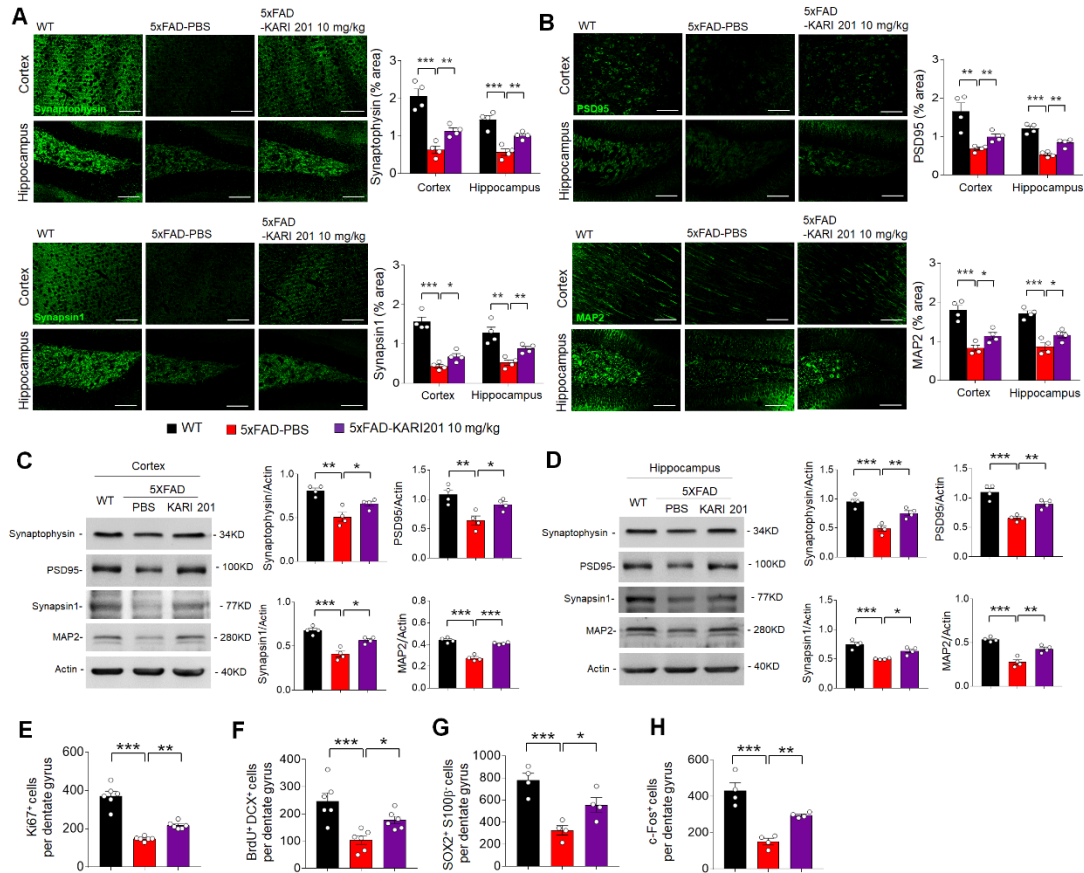
Fig. S22. KARI 201 treatment rescues synapse loss, hippocampal neurogenesis, and synapse plasticity in 5xFAD mice. (**A** and **B**) Representative immunofluorescence images and quantification of synaptophysin, PSD95, synapsin1, and MAP2 in cortex and hippocampus of WT and 5xFAD mice treated with PBS or KARI 201 (n = 4 mice per group). Scale bars, 100 μm. (**C** and **D**) Western blot analysis for synaptophysin, PSD95, synapsin1, and MAP2 in cortex and hippocampus of each group (n = 4 mice per group). (**E** to **G**) The number of Ki67$^+$ cell (E, proliferating cells, n = 6 mice per group), BrdU$^+$/DCX$^+$ cells (F, new neuroblasts, n = 6 mice per group) and SOX2$^+$/S100β$^-$ (G, neural stem cells, n = 4 mice per group) in dentate gyrus of each mice. (**H**) The number of c-Fos$^+$ neurons in dentate gyrus of each mice (n = 4 mice per group). A-H, One-way ANOVA, Tukey's post hoc test. *P < 0.05, **P < 0.01, ***P < 0.001. All error bars indicate s.e.m. All data analysis was done at 4-mo-old mice.
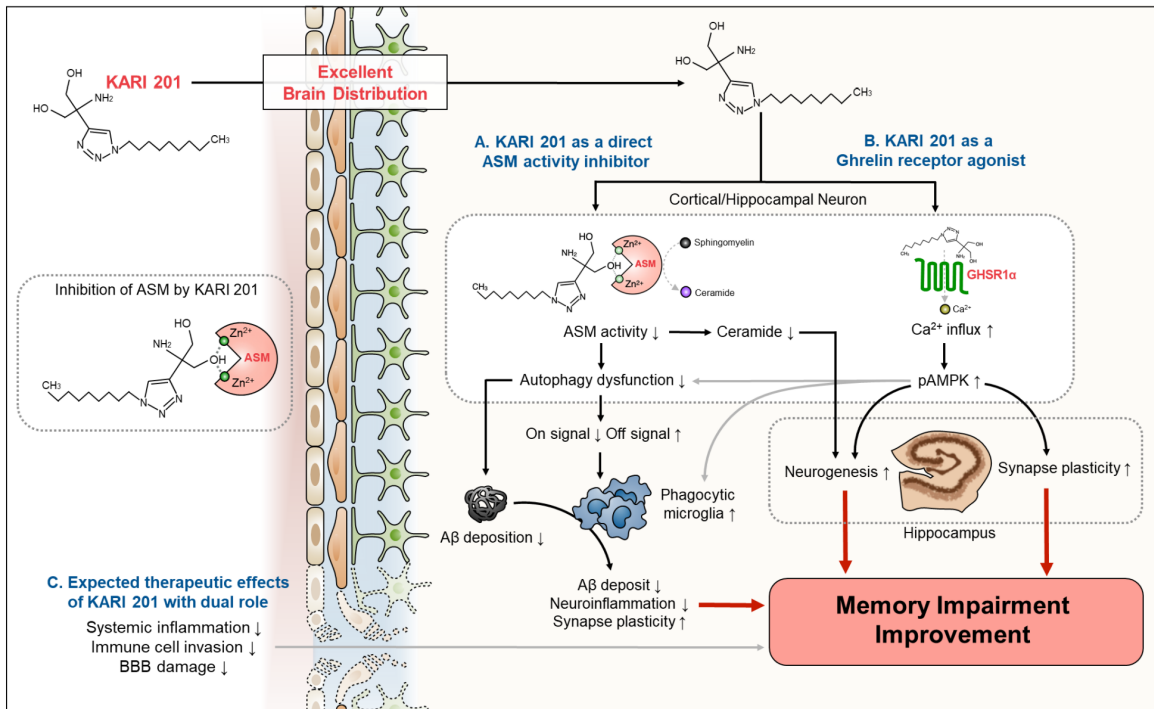
Fig. S23. The effects of KARI 201 on various neuropathological features in AD. (**A**) KARI 201 as a ASM direct inhibitor with excellent brain distribution restores autophagy dysfunction by improving lysosomal biogenesis in cortical and hippocampal neurons. The restoration of neuronal function by neuronal autophagic mitigation leads to enhancement of Aβ phagocytic function of microglia, resulting in synergistic effects on Aβ degradation, and mitigation of neuroinflammation and synapse loss. The ceramide reduction by ASM inhibition is contributed to improvement of hippocampal neurogenesis. (**B**) KARI 201 as a ghrelin receptor agonist induces Ca^{2+} release and phosphorylation of AMPK, resulting in enhancement of hippocampal neurogenesis and synaptic plasticity. The activation of AMPK is involved in improving the autophagy dysfunction and microglia phagocytosis. This dual role of KARI 201 consequentially leads to improvement of memory dysfunction in AD mice. (**C**) Moreover, the dual action of KARI 201 might be expected to effective in improving systemic inflammation, immune cell infiltration into the brain, and BBB damage by regulation peripheral immune cell activation, promoting attenuation of memory loss.

SI Appendix Tables

Table S1. Human plasma information for control subjects and subjects with AD.

Clinical diagnosis	Number	Age	Sex (Female %)	Amyloid PET
Normal	29	>60	31.0	1 (normal)
MCI due to AD	93	>60	54.8	1.5 (borderline- moderate)
AD, early stage	40	>60	57.5	2-3 (moderate-severe)
AD, advanced stage	21	>60	61.9	3 (severe)

MCI, mild cognitive impairment; Amyloid PET, amyloid positron emission tomography

Table S2. Sequences of Real-time PCR primer pairs

Gene	Forward	Reverse
hSMPD1	5'- ACCTACATCGGCCTTAATCC-3'	5'- TATGTTTGCCTGGGTCAGAT-3'
hARPP19	5'-AGAACTGCTCCTGTGGTTTG-3'	5'-AGAAGGCAGGTTGGCTTAAT-3'
hATG9A	5'-ACTGGGAGATCCACTCCTTC-3'	5'-CGGTGGTAGATGTCCAGTTC-3'
hATG10	5'-GCTACCCTTGGATGATTGTG-3'	5'-TCCTTCCCATATGTCCTTCA-3'
hMTX2	5'-ATGGATCTCCTTACCCTTGG-3'	5'-GGTTGTGTTCCCAGTCTTTG-3'
hARSA	5'-CCTCTCACCACACCCACTAC-3'	5'-ACATACGCATGGTCTCAGGT-3'
hARSB	5'-CTGTCCCGCCTACAGTTCTA-3'	5'-AGGTTTTCTAGCCTCCCTGA-3'
hATP6V0E1	5'-GCGGTCAGCTATTGACACTT-3'	5'-ACCCTTAGGGATGAACCAAG-3'
hATP6V1H	5'-GGAGAACTTGGAACAGCAGA-3'	5'-ATTTGTGCACAGGACTCCAT-3'
hCTSA	5'-GATTTGGGCAACATCTTCAC-3'	5'-ACGTACGGGTTGTTGAGGTA-3'
hCTSB	5'-CATTGCTGGTCAGGAACTCT-3'	5'-ACAGTGGAATGATTGCTGGT-3'
hCTSD	5'-CCGACTTGCTGTTTTGTTCT-3'	5'-TGCTCTGGATCAGCTCTACC-3'
hCLCN7	5'-TCAACGTCACTGAAACGAGA-3'	5'-AGATCCTCCAGGTCAGGAAC-3'
hGALNS	5'-GGCTACGTCAGCAAGATTGT-3'	5'-TGGCCTTGTTGTCATAAGGT-3'
hGNS	5'-TTTCTTGGCTCAAAAACCAG-3'	5'-ATCGCTTATTGCCTGAGTTG-3'
hHEXA	5'-ACAGGATGTGAAGGAGGTCA-3'	5'-GATTCACTGGTCCAAAGGTG-3'
hLAMP1	5'-AGTGTCTGCTGGACGAGAAC-3'	5'-GACCCTAAGCCCAGAGAAAG-3'
hPSAP	5'-GTGGACTCCTACCTCCCTGT-3'	5'-TTCAGCTCTGCTAGGTGCTT-3'
hSQSTM1	5'-GATGGGACTCCATAGCTCCT-3'	5'-CCTGACATGGAAGGTGAAAC-3'
hUVRAG	5'-TGTCCTGCATAACAGCTTCA-3'	5'-GGCTTCTGCAGATCCAGTTA-3'
hVPS11	5'-TCCACAGGTCAAAGAGAAGC-3'	5'-TAAAGGACACCATCCTGGAA-3'
hGAPDH	5'-TCACCCACAGGTGCCCATCT-3'	5'-GTGAGGATCTTCATGAGGTAGTCAGT-3'
mSmpd1	5'-GTT CCA GAC TGG GGA AAG TT-3'	5'-TAA TCC AGA TCC TGG GCA TA-3'
mTnf-α	5'-GATTATGGCTCAGGGTCCAA-3'	5'-GCTCCAGTGAATTCGGAAAG-3'
mIl-1β	5'-CCCAAGCAATACCCAAAGAA-3'	5'-GCTTGTGCTCTGCTTGTGAG-3'
mIl-6	5'-CCGGAGAGGAGACTTCACAG-3'	5'-TTGCCATTGCACAACTCTTT-3'
miNos	5'-CACCTGGAACAGCACTCTCT-3'	5'-CTTTGTGCGAAGTGTCAGTG-3'
mIl-10	5'-AAGGCCATGAATGAATTTGA-3'	5'-TTCGGAGAGAGGTACAAACG-3'
mIl-4	5'-ATCCATTTGCATGATGCTCT-3'	5'-GAGCTGCAGAGACTCTTTCG-3'
mTgf-β	5'-TTACCTGGATGGAAGTGGAA-3'	5'-TGTTATGAGGAAGGGGACAA-3'
mArg1	5'-AAGCCAAGGTTAAAGCCACT-3'	5'-CGATTCACCTGAGCTTTGAT-3'
mCxcl0	*5'-AAAAGGGCTCCTTAACTGGA-3'*	*5'-GCTGGTCACCTTTCAGAAGA-3'*

mCcl21	*5'-AGCTATGTGCAAACCCTGAG-3'*	*5'-CTCTTGAGGGCTGTGTCTGT-3'*
mMmp3	*5'-GGGTAGGATGAGCACACAAC-3'*	*5'-TAGAAGGAGGCAGCAGAGAA-3'*
mCd47	*5'-TGGTATCCAGCAAGCCTTAG-3'*	*5'-AAGACACCAGTGCCATCAAT-3'*
mCx3cl1	*5'-CCAGAGCTGGCAATAACCTA-3'*	*5'-GGCATACAGGGTACGATCTG-3'*
mBdnf	*5'-AATTTGGTAAACGGCACAAA-3'*	*5'-GCAAACAATCGCTTCATCTT-3'*
mArpp19	*5'-AGGCAAACTGGCTAAAACCT-3'*	*5'-CCACCAATCTATCCAAATGC-3'*
mAtg9a	*5'-AGCCTGTCAAGGTCACTCTG-3'*	*5'-GAAGGAGTGGATCTCCCAAT-3'*
mAtg10	*5'-GACATCTGCAGAAGCCTGTT-3'*	*5'-CTCCACAGCAGGAGAACTGT-3'*
mMtx2	*5'-AACCACATTTTGGCCTATCA-3'*	*5'-CAAAAACCAGAGCGTCAAGT-3'*
mArsa	*5'-TCCTGAGTCTGATCCGCTAC-3'*	*5'-TGGCACTCTAAGACCTCTGG-3'*
mArsb	*5'-CGTCTCAGTCCAACGTCTCT-3'*	*5'-GGAAGTGAGAAGGCACAGAA-3'*
mAtp6v0e1	*5'-GCACAGCTCAATCCTCTGTT-3'*	*5'-AGGTCTGATGTGCAGGTGAT-3'*
mAtp6v1h	*5'-AGGTCTGTGGGAAACATTCA-3'*	*5'-TGCCCCTGAAGATAAGACTG-3'*
mCtsa	*5'-ACTGCCCAGACTTCTCACAG-3'*	*5'-CCTCCTTGGGTTTCTCTAGC-3'*
mCtsb	*5'-TTTGTGTGGTCCTCAAACCT-3'*	*5'-ACCAAGTTGATCTGGCATGT-3'*
mCtsd	*5'-ACCTGAACGTCACTCGAAAG-3'*	*5'-GTCCCTGTGTCCACAATAGC-3'*
mClcn7	*5'-CCAAGGAGATTCCACACAAC-3'*	*5'-CAATGAGGGCACAGATAACC-3'*
mGalns	*5'-ATGGTCGGCAGATTTTATGA-3'*	*5'-GCATGTTGTGTCTGGATGAA-3'*
mGns	*5'-CGCACCAAGAAACAAGAACT-3'*	*5'-CTCCTGAAGGCGTCATCTAA-3'*
mHexa	*5'-TTCACTTTCCCAGAGCTCAC-3'*	*5'-TGAGACCCAGAGTAGCAAGG-3'*
mLamp1	*5'-TCTATGGCACTGCAACTGAA-3'*	*5'-GGCTCTGTTCTTGTTCTCCA-3'*
mPsap	*5'-AAGAATGGTGGGTTCTGTGA-3'*	*5'-TTCCACGAGGATCTCCAATA-3'*
mSqstm1	*5'-AGGAGCTGACAATGGCTATG-3'*	*5'-TTGCAACCATCACAGATCAC-3'*
mUvrag	*5'-TGGTTACACTGCACATTTGG-3'*	*5'-CTGTCAGCTTGTCGTTGATG-3'*
mVps11	*5'-TCCACAGGTCAAAGAGAAGC-3'*	*5'-TAAAGGACACCATCCTGGAA-3'*
mTuj1	*5'-AATGCACTGGTGTCCGAGTA-3'*	*5'-GGACGAATGCTGCTTGTCTT-3'*
mGap43	*5'-TACCACCATGCTGTGCTGTA-3'*	*5'-AATTTTGGTCGCAGGCTTAT-3'*
mMbp	*5'-GGAGTAGGGGTGAACTTGGA-3'*	*5'-CACCCCGACTGGTTAAAACT-3'*
mMap2	*5'- GGATGGGCTTGTGTCTGATT-3'*	*5'- CTGGACCCACTCCACTCCACAAACT-3'*
mGapdh	*5'-TGAATACGGCTACAGCAACA-3'*	*5'-AGGCCCCTCCTGTTATTATG-3'*

Tnf-α, tumor necrosis factor-alpha; *Il-1β*, interleukin 1 beta; Il6, interleukin 6; *iNos*, inducible nitric oxide synthase; *Il-10*, interleukin 10; *Il-4*, interleukin 4; *Tgf-β*, transforming growth factor beta; *Arg1*, arginase 1; *Cxcl10*, chemokine (C-X-C Motif)ligand 10; *Ccl21*, chemokine (C-C Motif) Ligand 21; *Mmp3*, matrix metallopeptidase 3; *CD47*, cluster of differentiation 47; *Cx₃cl1*, chemokine (C-X3-C Motif) ligand 1; *Bdnf*, brain-derived neurotrophic factor; *Arpp19*, cAMP regulated phosphoprotein 19; *Atg9a*, autophagy related 9A; *Atg10*, autophagy related 10; *Mtx2*, metaxin 2; *Arsa*, arylsulfatase A; *Arsb*, arylsulfatase B; *Atp6v0e1*, ATPase H+ transporting V0 subunit e1; *Atp6v1h*, ATPase H+ transporting V1 subunit H; *Clcn7*, chloride voltage-gated channel 7; *Ctsa*, cathepsin A; *Ctsb*, cathepsin B; *Ctsd*, cathepsin D; *Galns*, galactosamine (N-acetyl)-6-sulfatase; *Gns*, glucosamine (N-acetyl)-6-sulfatase; *Hexa*, hexosaminidase subunit alpha; *Lam*

p1, lysosomal associated membrane protein 1; *Psap*, prosaposin; *Sqstm1*, sequestosome 1; *Uvrag*, UV radiation resistance associated; *Vps11*, VPS11 core subunit of CORVET and HOPS complexes; *Tuj1*, class III beta-tubulin; *Gap43*, growth associated protein 43; *Mbp*, myelin basic protein; *Map2*, microtubule-associated protein 2; *Gapdh*, glyceraldehyde 3-phosphate dehydrogenase.

References

1. J. K. Lee, H. K. Jin, M. H. Park, B. R. Kim, P. H. Lee, H. Nakauchi, J. E. Carter, X. He, E. H. Schuchman, J. S. Bae, Acid sphingomyelinase modulates the autophagic process by controlling lysosomal biogenesis in Alzheimer's disease. *J. Exp. Med.* **211**, 1551-1570 (2014).

2. M. H. Park, J. Y. Lee, K. H. Park, I. K. Jung, K. T. Kim, Y. S. Lee, H. H. Ryu, Y. Jeong, M. Kang, M. Schwaninger, E. Gulbins, M. Reichel, J. Kornhuber, T. Yamaguchi, H. J. Kim, S. H. Kim, E. H. Schuchman, H. K. Jin, J. S. Bae, Vascular and neurogenic rejuvenation in aging mice by modulation of ASM. *Neuron* **100**, 167-182 (2018).

3. B. M. Cornali, F. W. Kimani, J. C. Jewett, Cu-click compatible triazabutadienes to expand the scope of aryl diazonium ion chemistry. *Org. Lett.* **18**, 4948-4950 (2016).

4. N. Naganna, N. Madhavan, Soluble and reusable poly(norbornene) supports with high loading capacities for peptide synthesis. *Org. Lett.* **15**, 5870-5873 (2013).

5. C. Chiappe, D. Pieraccini, P. Saullo, Nucleophilic displacement reactions in ionic liquids: substrate and solvent effect in the reaction of NaN3 and KCN with alkyl halides and tosylates. *J. Org. Chem.* **68**, 6710-6715 (2003).

6. S. G. Hansen, H. H. Jensen, Microwave irradiation as an effective means of synthesizing unsubstituted N-linked 1,2,3-triazoles from vinyl acetate and azides. *Synlett* **2009**, 3275-3276 (2009).

7. S. Kalhor-Monfared, C. Beauvineau, D. Scherman, C. Girard, Synthesis and cytotoxicity evaluation of aryl triazolic derivatives and their hydroxymethine homologues against B16 melanoma cell line. *Eur. J. Med. Chem.* **122**, 436-441 (2016).

8. H. Ooi, N. Ishibashi, Y. Iwabuchi, J. Ishihara, S. A. Hatakeyama, Concise route to (+)-lactacystin. *J. Org. Chem.* **69**, 7765-7768 (2004).

9. J. W. Lane, R. L. Halcomb, New design concepts for constraining glycosylated amino acids. *Tetrahedron* **57**, 6531-6538 (2001).

10. X. He, S. R. Miranda, X. Xiong, A. Dagan, S. Gatt, E. H. Schuchman, Characterization of human acid sphingomyelinase purified from the media of overexpressing Chinese hamster ovary cells. *Biochim. Biophys. Acta* **1432**, 251-264 (1999).

11. J. Y. Lee, S. H. Han, M. H. Park, B. Baek, I. S. Song, M. K. Chio, Y. Takuwa, H. Ryu, S. H. Kim, X. He, E. H. Schuchman, J. S. Bae, H. K. Jin, Neuronal SphK1 acetylates COX2 and contributes to pathogenesis in a model of Alzheimer's disease. *Nat. Commun.* **9**, 1479 (2018).

12. J. Y. Lee, S. H. Han, M. H. Park, I. S. Song, M. K. Chio, E. Yu, C. M. Park, S. H. Kim, E. H. Schuchman, H. K. Jin, J. S. Bae, N-AS-triggered SPMs are direct regulators of microglia in a model of Alzheimer's disease. *Nat. Commun.* **11**, 2358 (2020).

13. D. R. Howlett, J. C. Richardson, A. Austin, A. A. Parsons, S. T. Bate, D. C. Davies, M. I. Gonzalez, Cognitive correlates of Abeta deposition in male and female mice bearing amyloid precursor protein andpresenilin-1 mutant transgenes. *Brain Res.* **1017,** 130-136 (2004).

14. T. Goldmann, P. Wieghofer, P. F. Müller, Y. Wolf, D. Varol, S. Yona, S. M. Brendecke, K. Kierdorf, O. Staszewski, M. Datta, T. Luedde, M. Heikenwalder, S. Jung, M. Prinz, A new type of microglia gene targeting shows TAK1 to be pivotal in CNS autoimmune inflammation. *Nat. Neurosci.* **16,** 1618-1626 (2013).

15. J. K. Lee, H. K. Jin, J. S. Bae, Bone marrow-derived mesenchymal stem cells attenuate

amyloid β-induced memory impairment and apoptosis by inhibiting neuronal cell death. *Curr. Alzheimer Res.* **7,** 540-548 (2010).

16. M. H. Park, B. J. Choi, M. S. Jeong, J. Y. Lee, I K. Jung, K. H. Park, H. W. Lee, T. Yamaguchi, H. H. Marti, B. H. Lee, E. H. Schuchman, H. K. Jin, J. S. Bae, Characterization of the subventricular-thalamo-cortical circuit in the NP-C mouse brain, and new insights regarding treatment. *Mol. Ther.* **27,** 1507-1526 (2019).

17. J. Brewer, J. R. Torricelli, Isolation and culture of adult neurons and neurospheres. *Nat. Protoc.* **2**, 1490-1498 (2007).

Data S1. ^{1}H and ^{13}C NMR Spectra of chemical synthesis in materials and methods.

1a ^{1}H-NMR
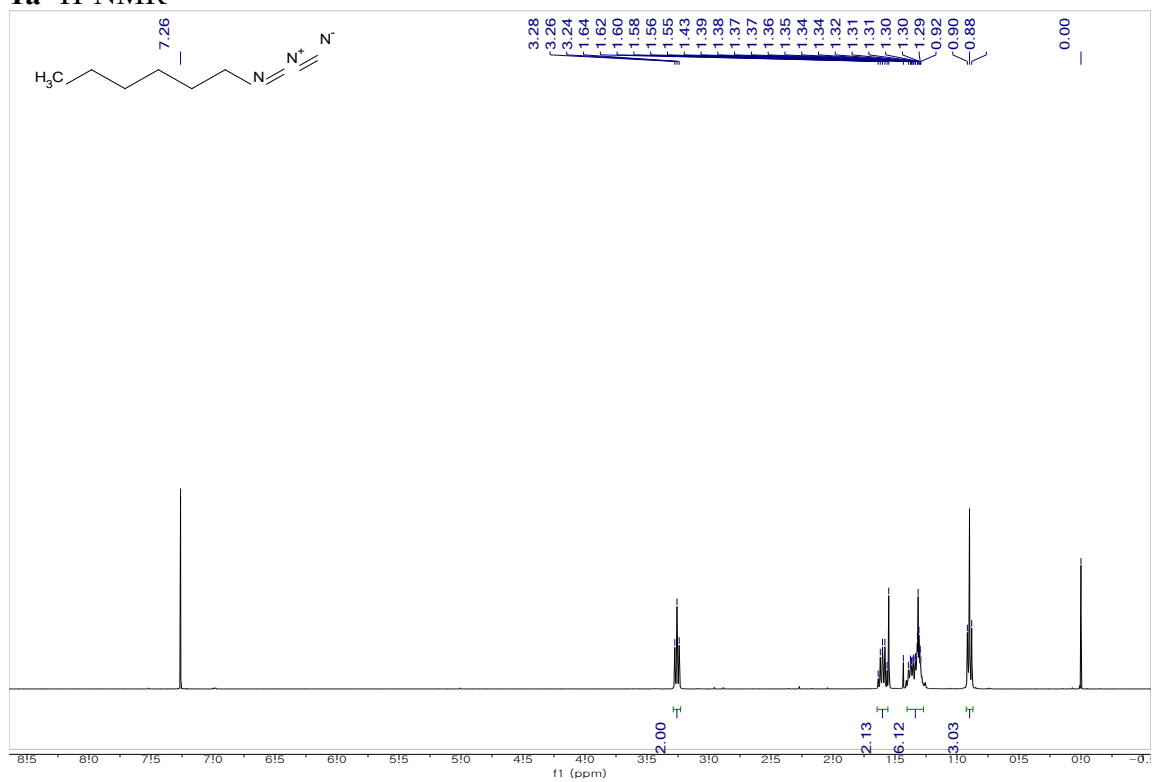
1b ^{1}H-NMR
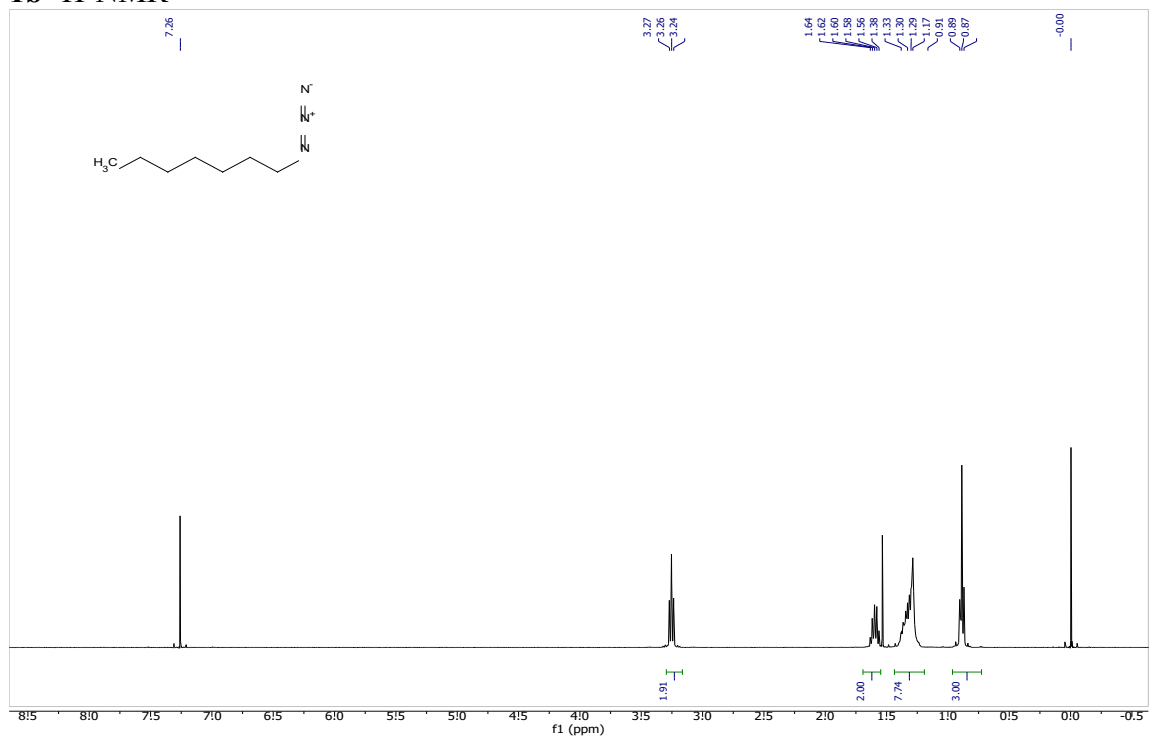
1c ¹H-NMR
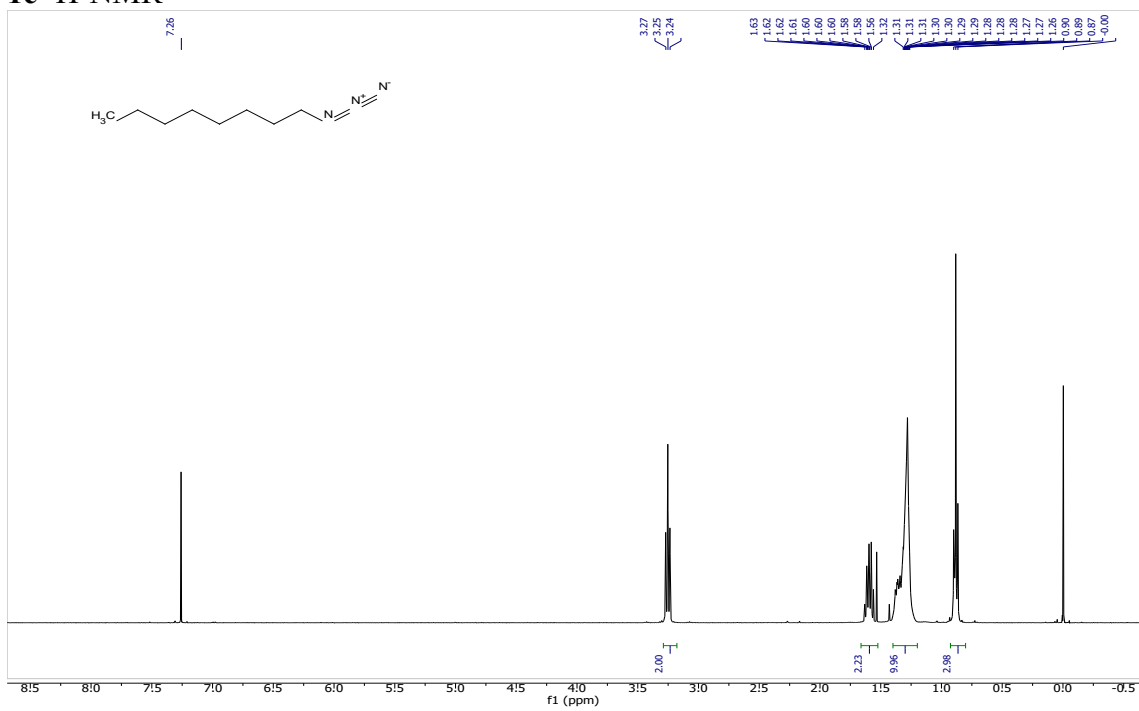
1d ¹H-NMR
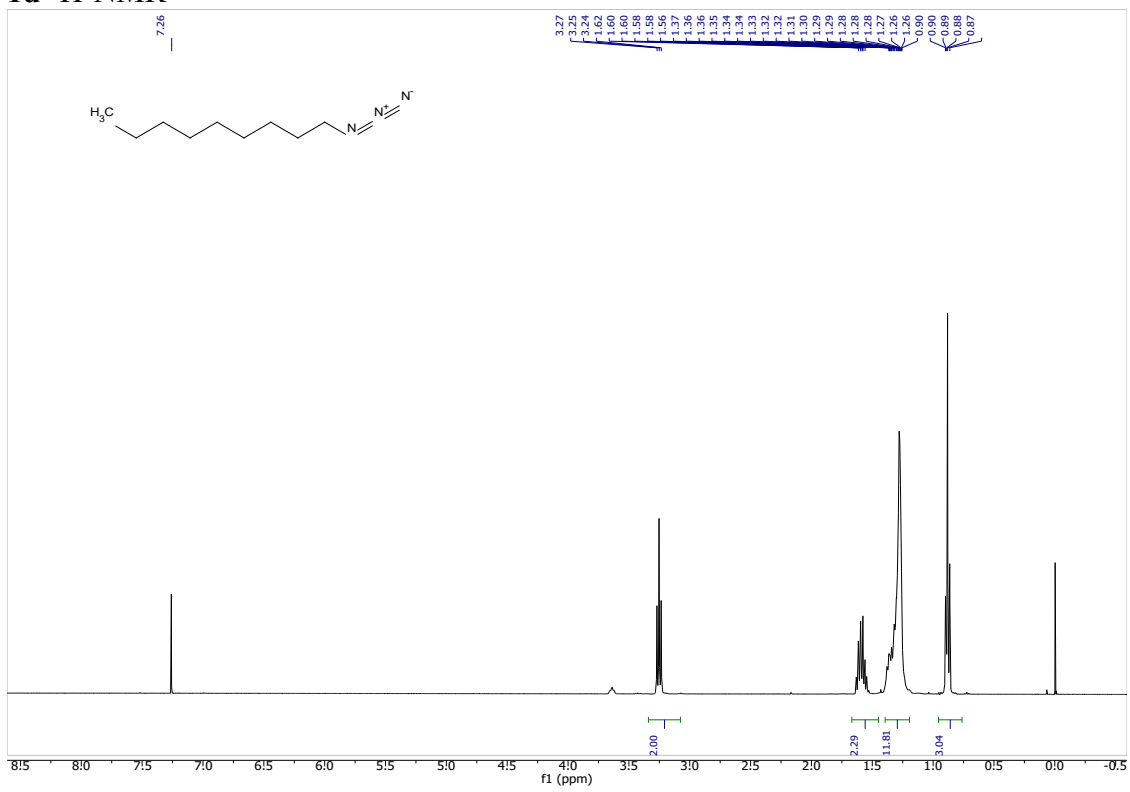
2a ^{1}H-NMR
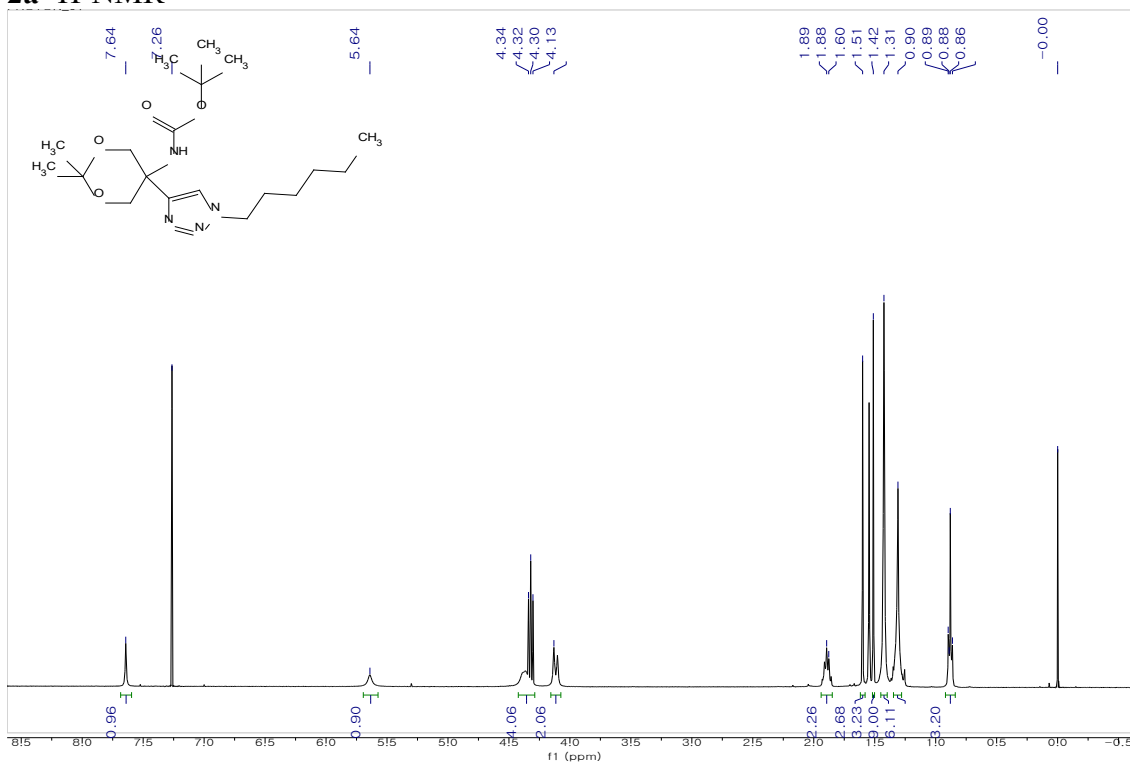
2a ^{13}C-NMR

2b ^{1}H-NMR

2b ^{13}C-NMR

65

2c ^{1}H-NMR

2c ^{13}C-NMR

66
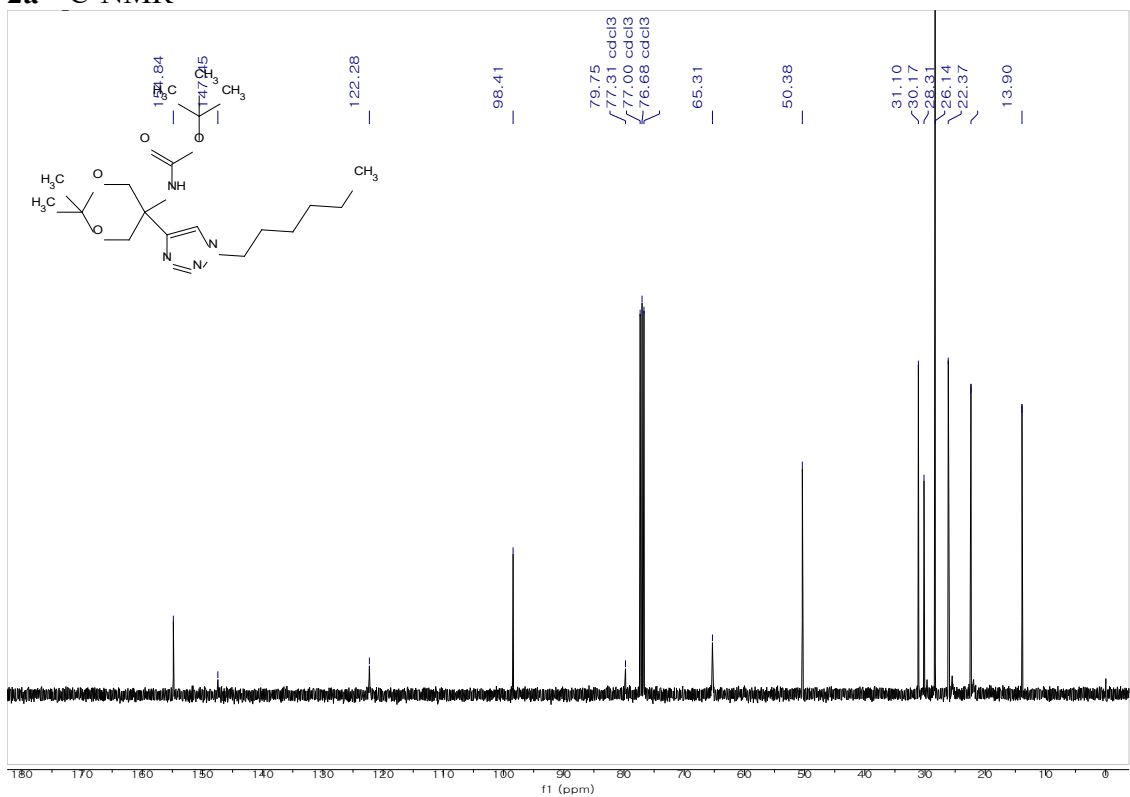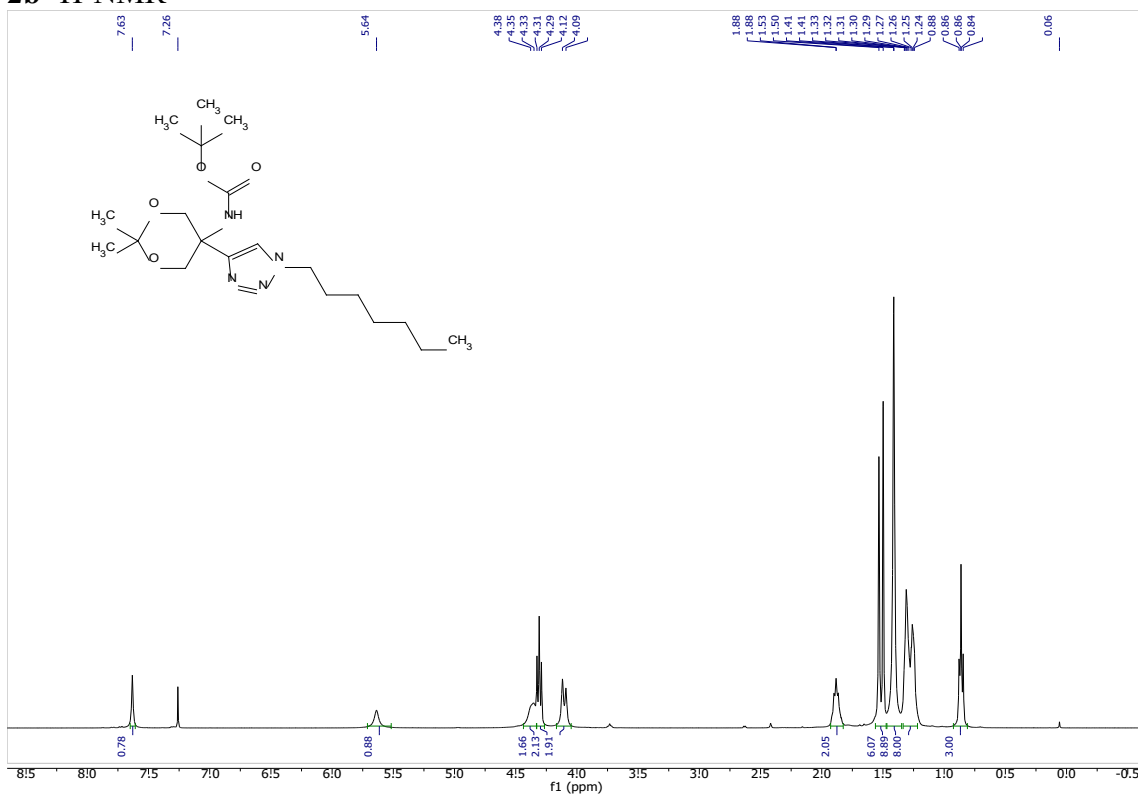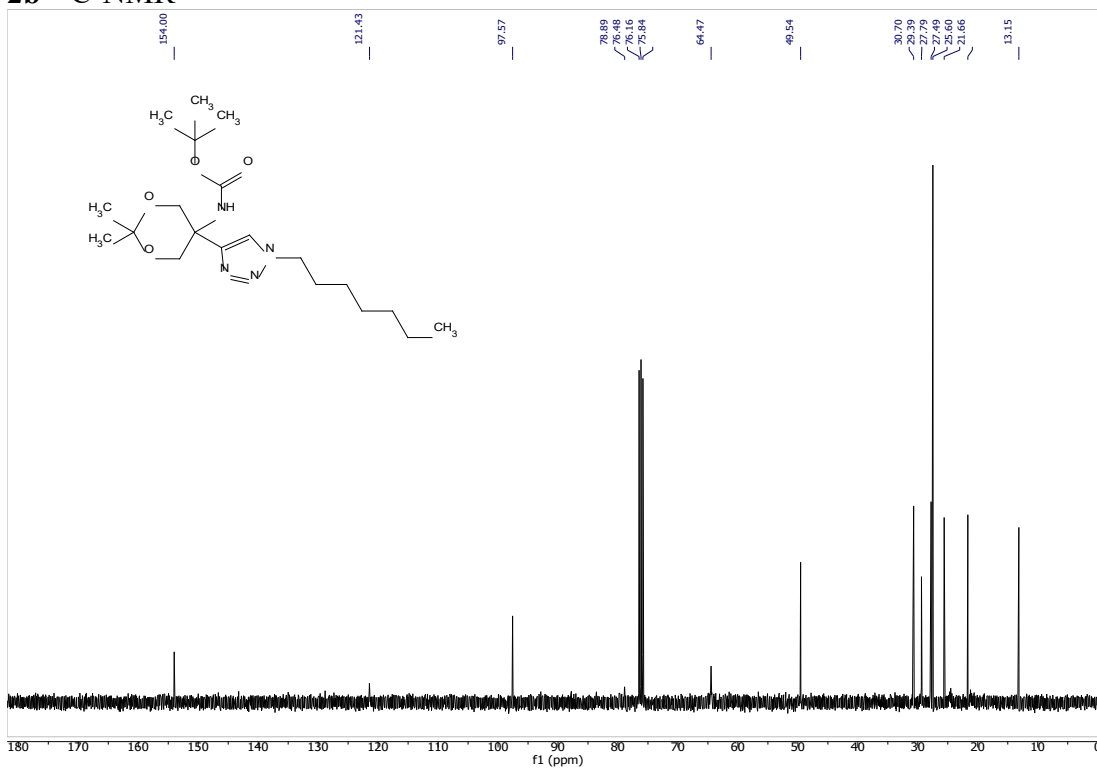
2d ¹H-NMR

2d ¹³C-NMR

3a ^{1}H-NMR

PROTON_01

3a ^{13}C-NMR

CARBON_01
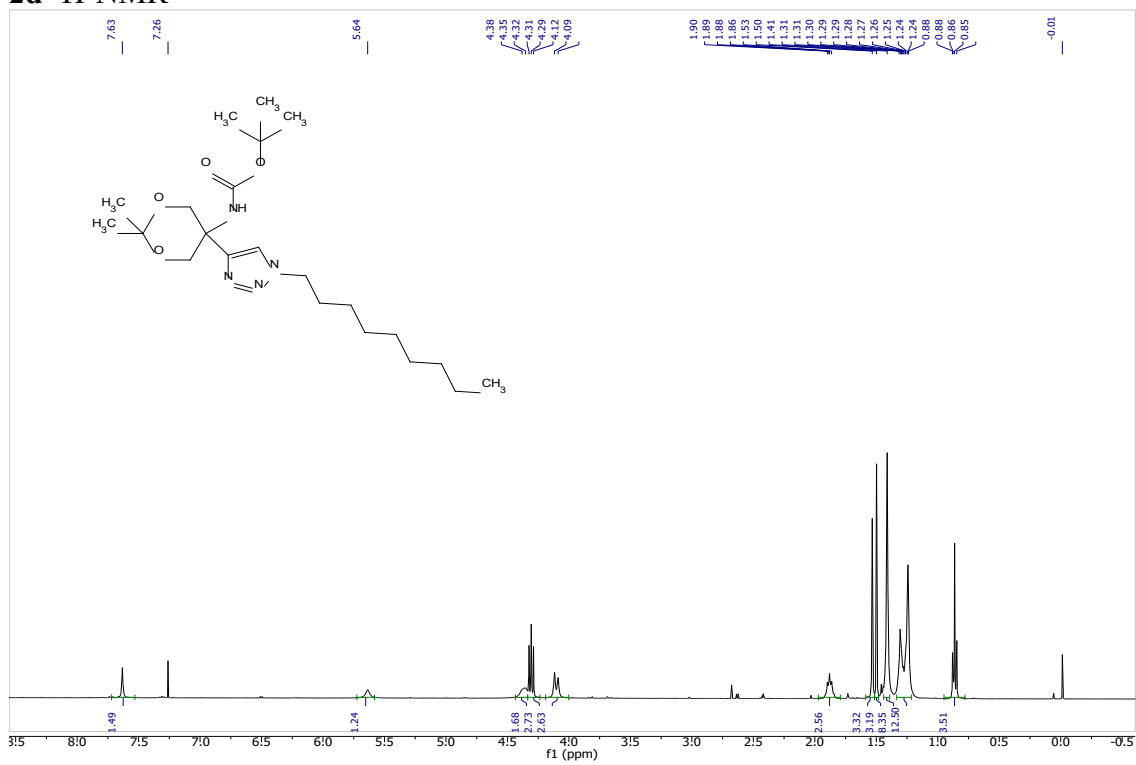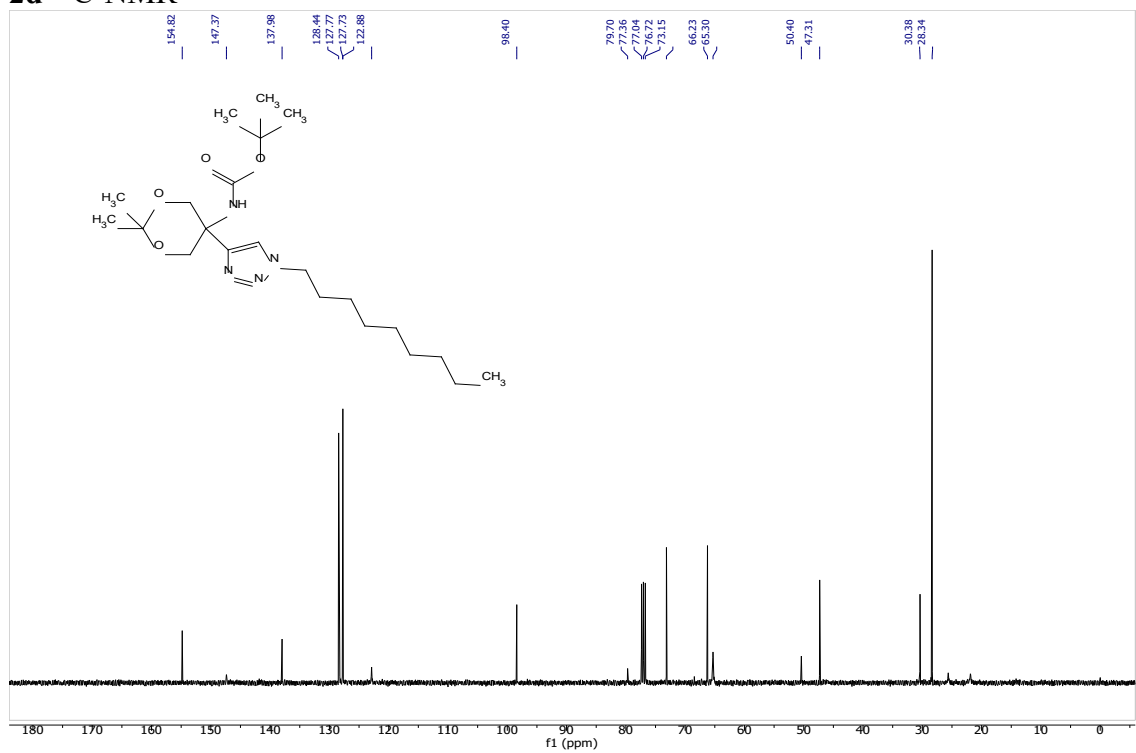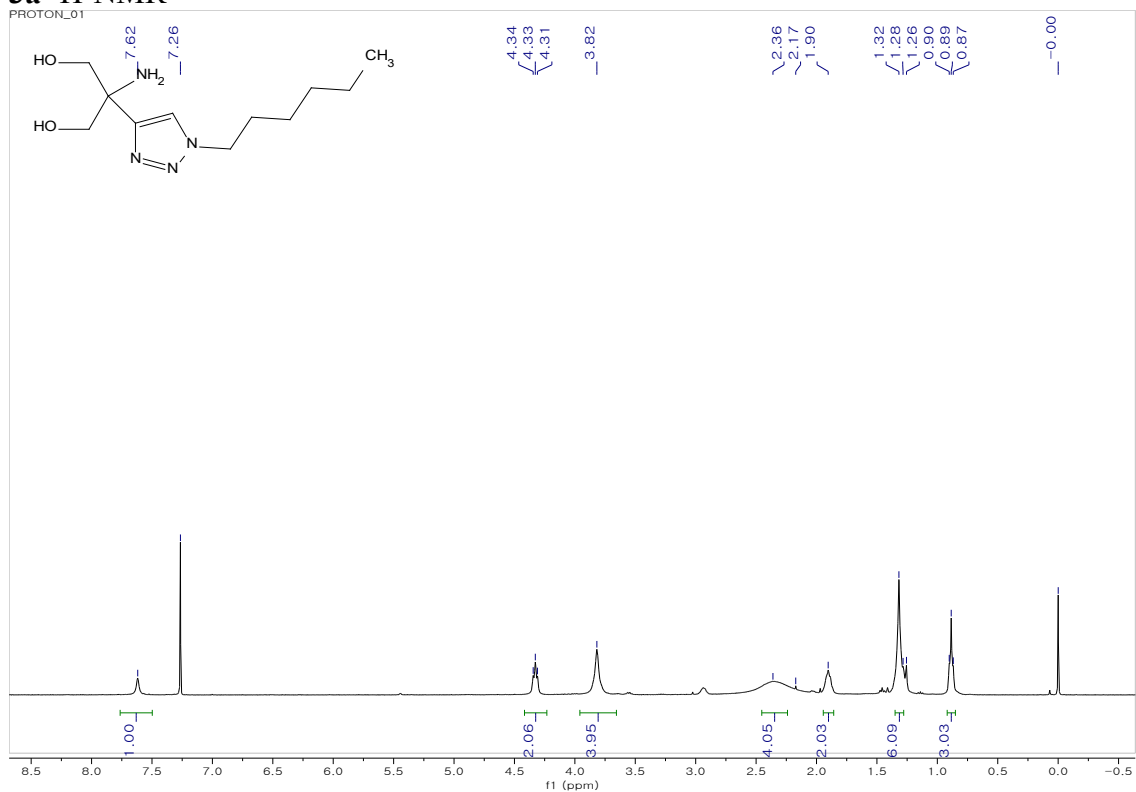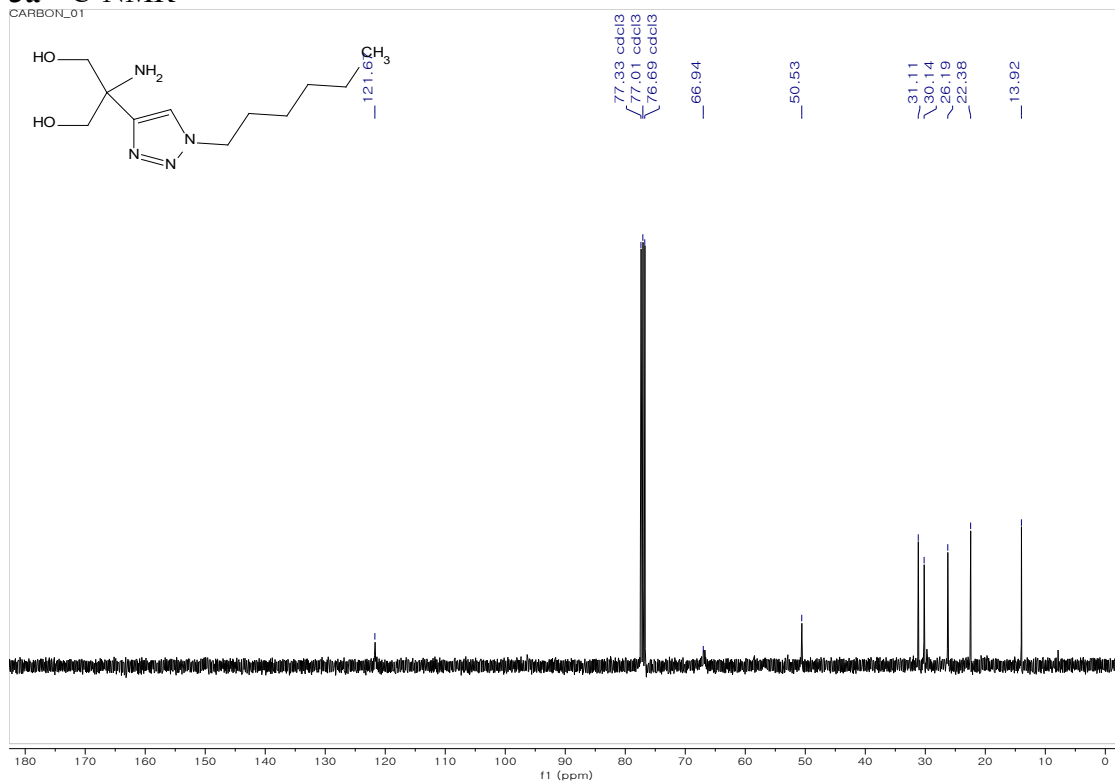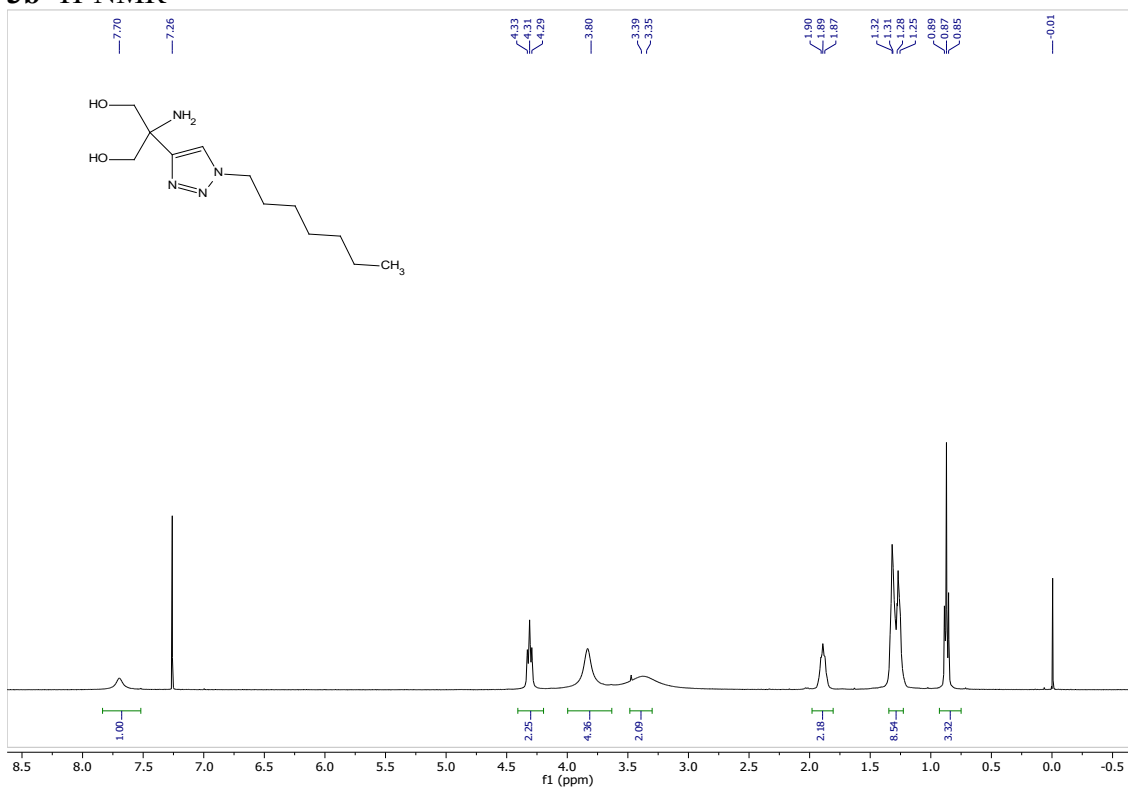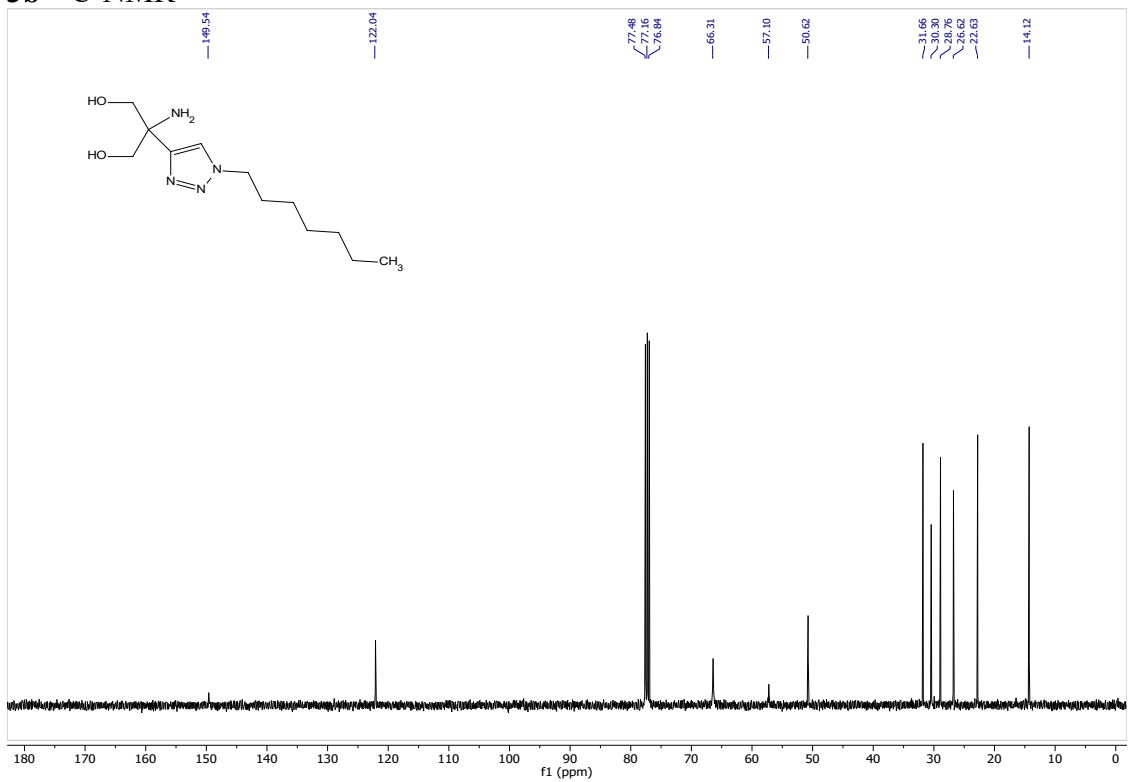
3b ^{1}H-NMR

3b ^{13}C-NMR

3c ^{1}H-NMR
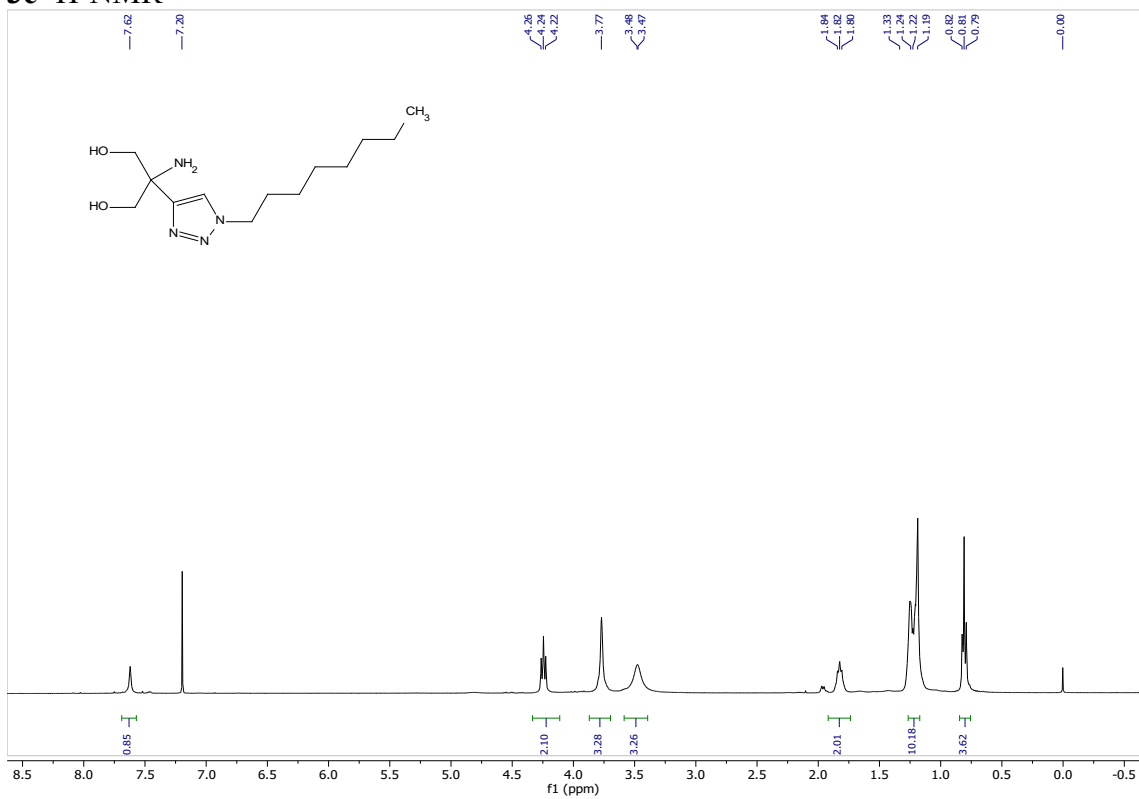
3c ^{13}C-NMR
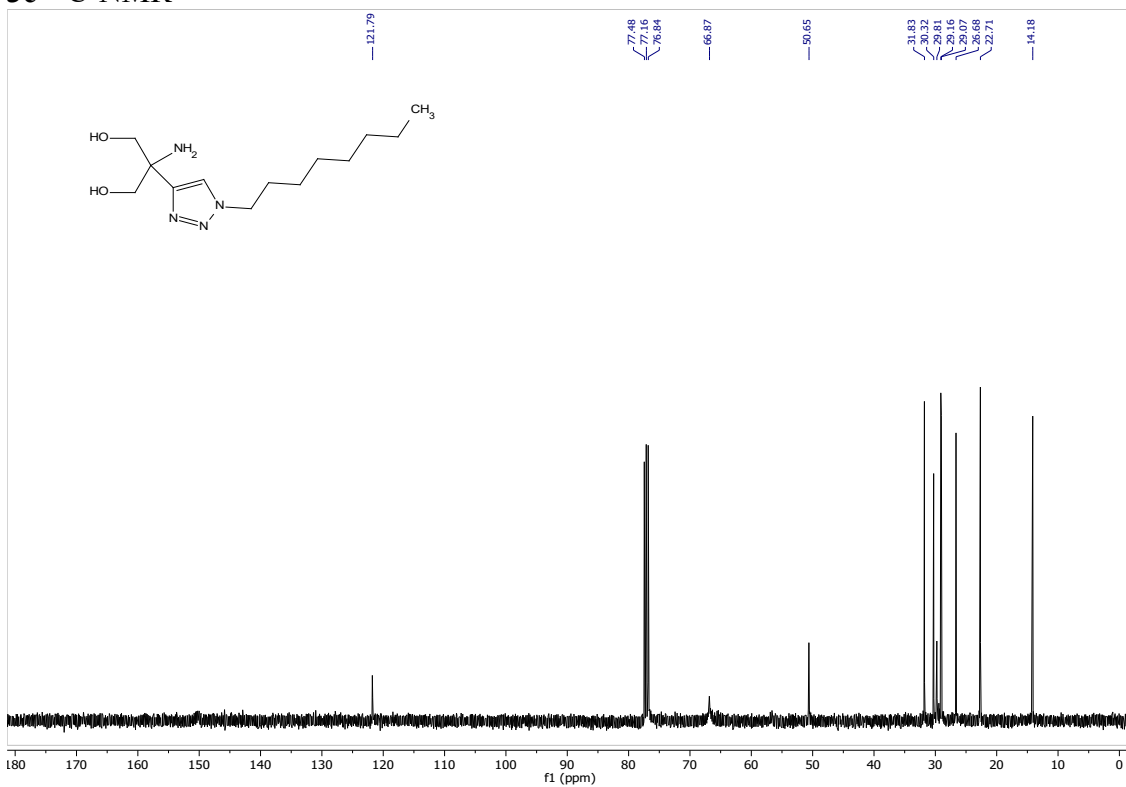
3d ^{1}H-NMR
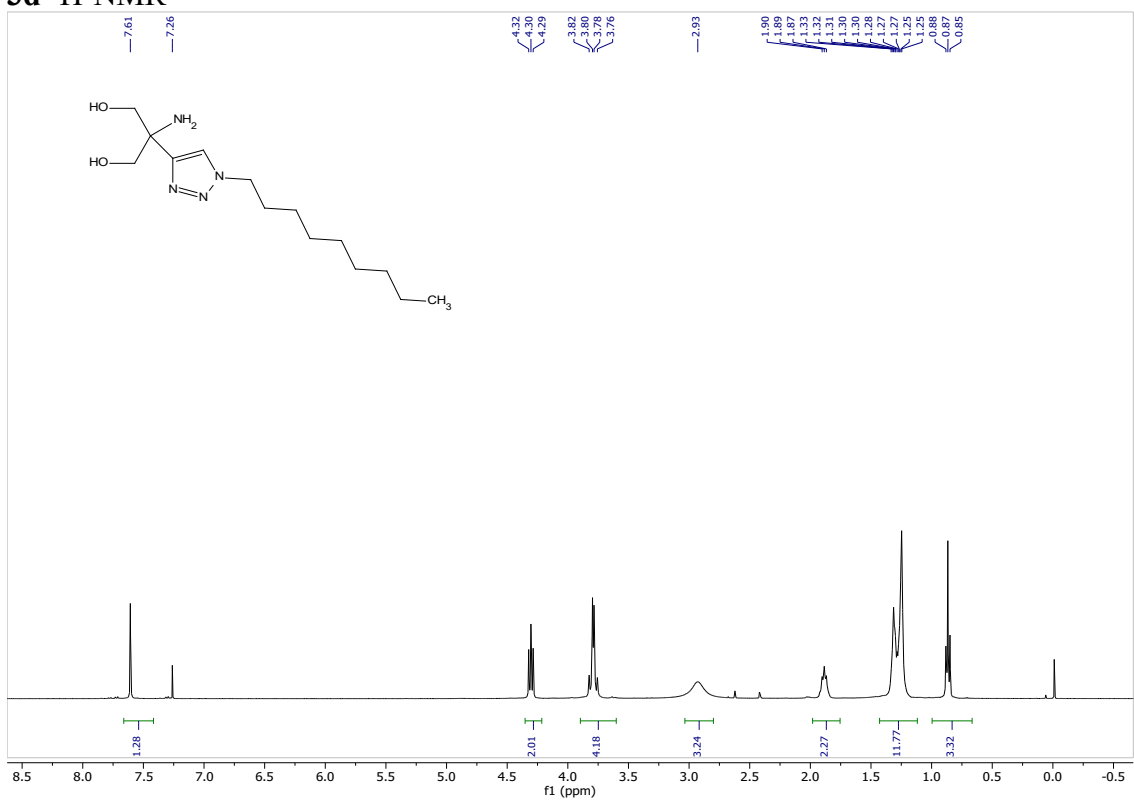
3d ^{13}C-NMR
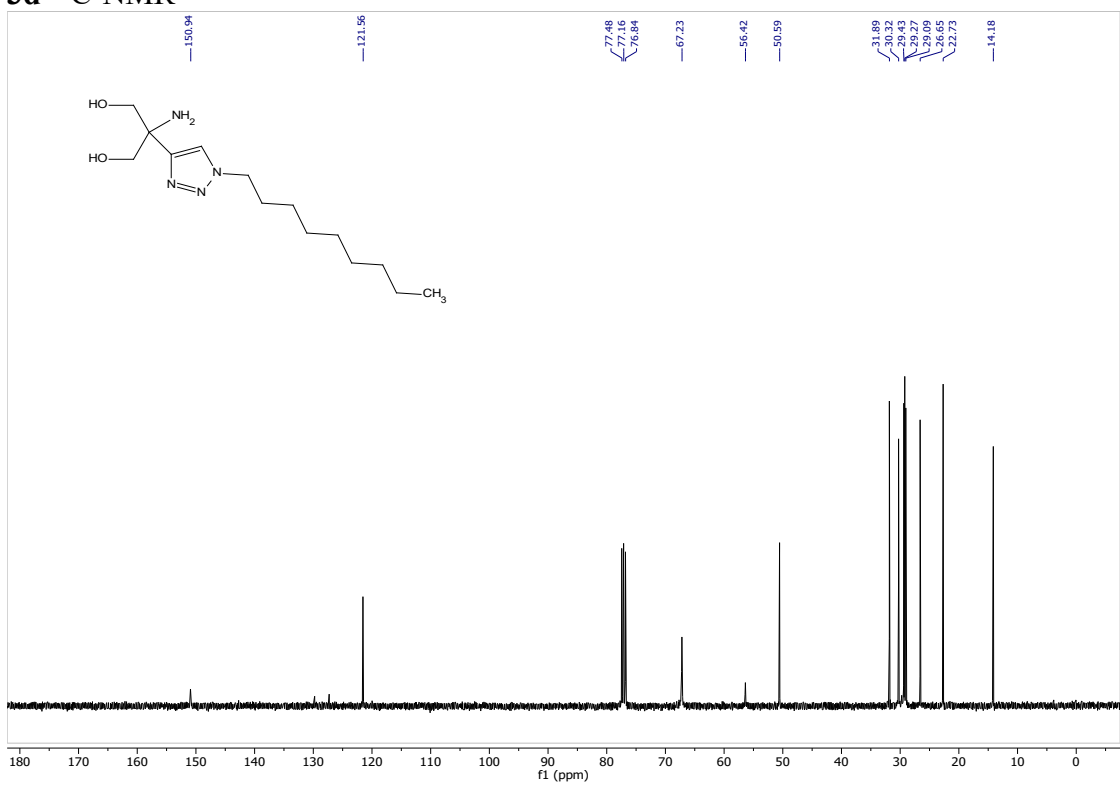
3e ^{1}H-NMR
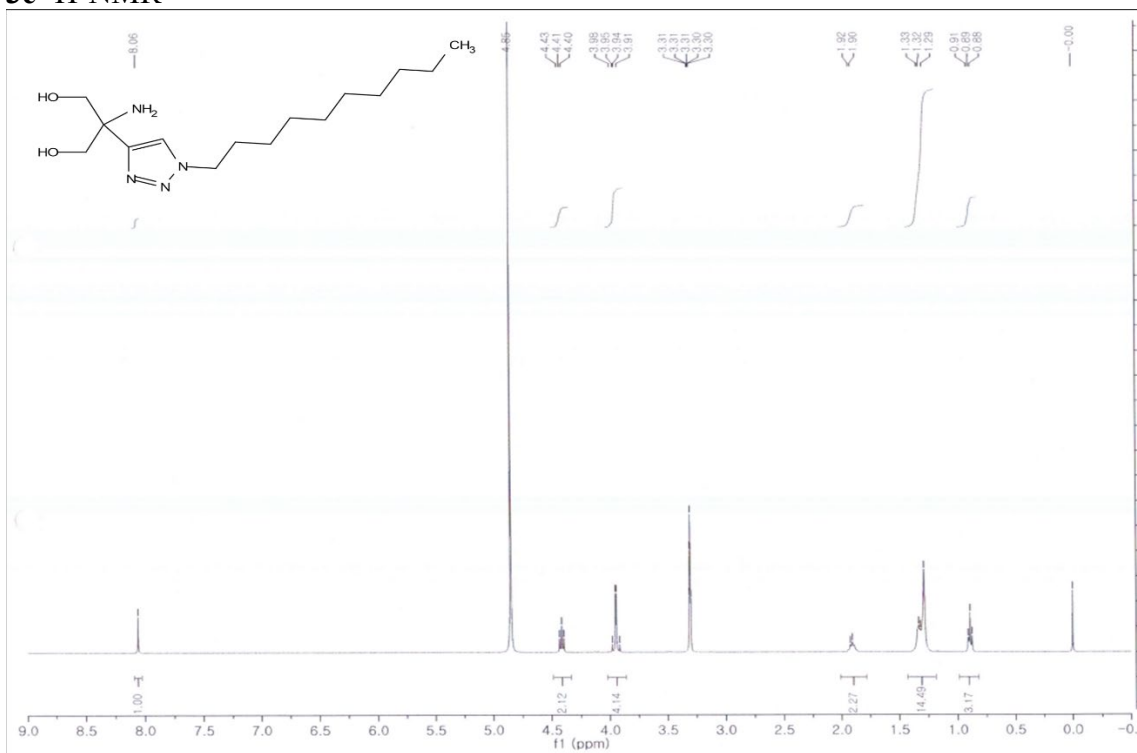
3e ^{13}C-NMR
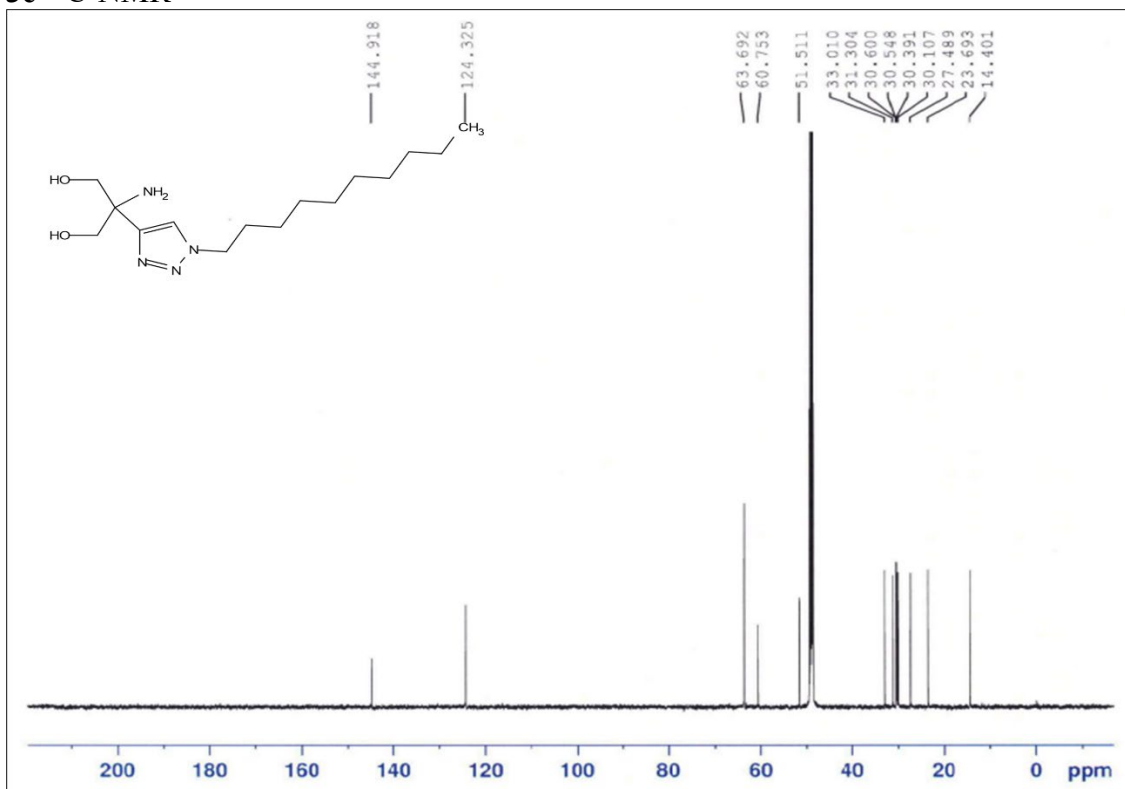
4a ^{1}H-NMR
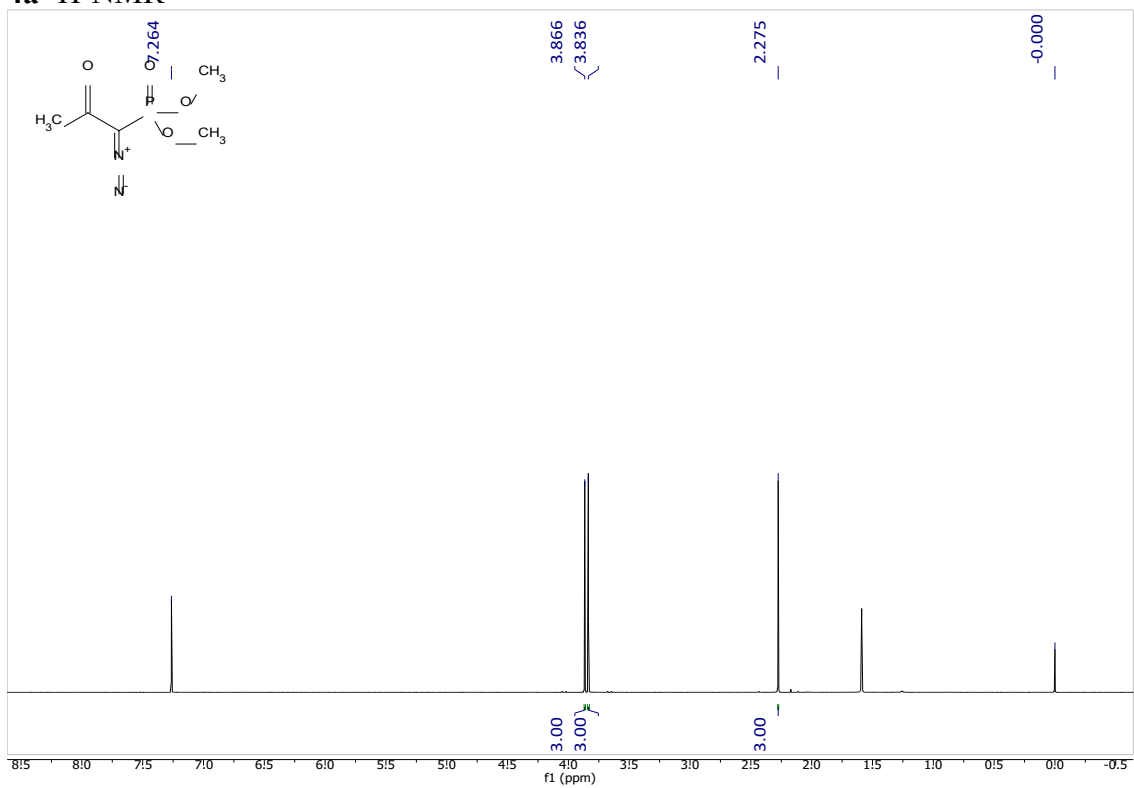
4b ^{1}H-NMR
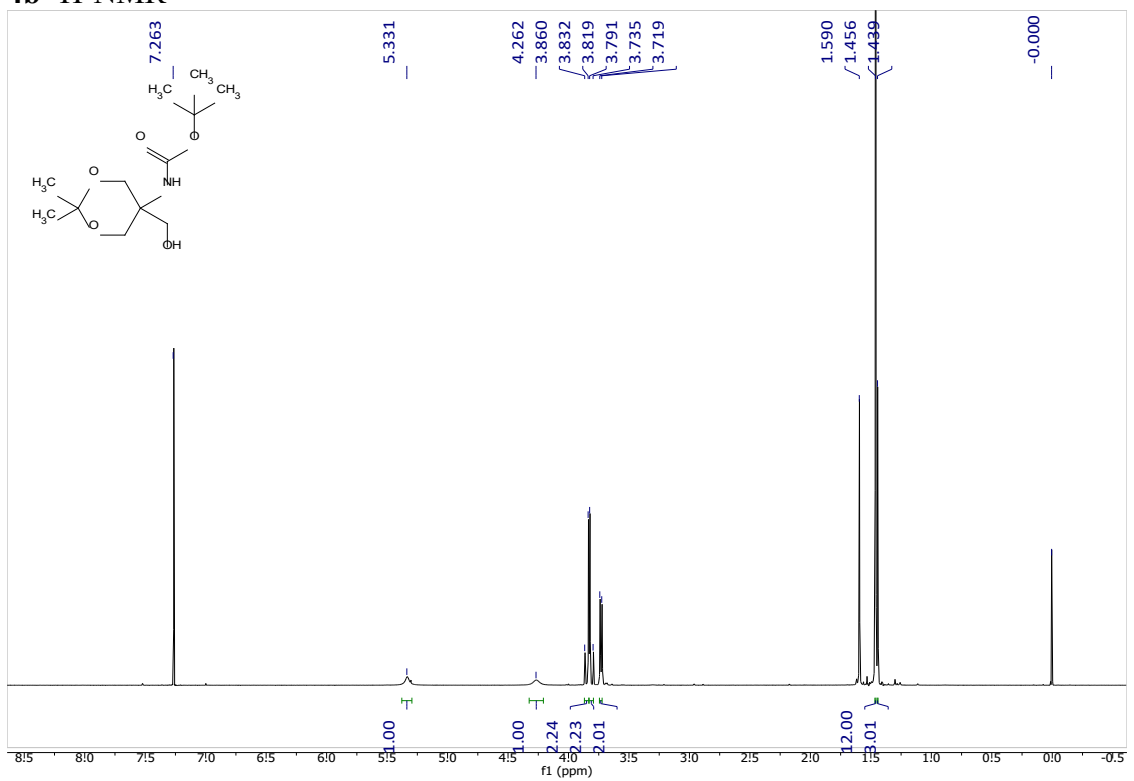
4c ^{1}H-NMR
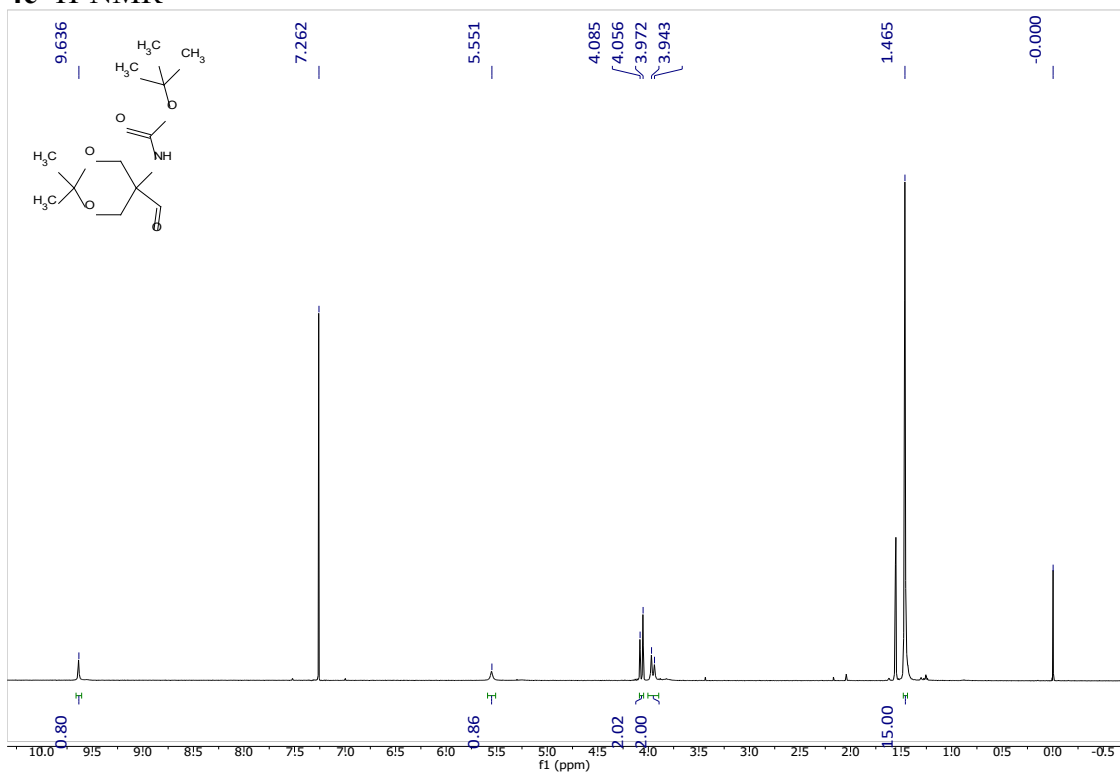
4d ^{1}H-NMR
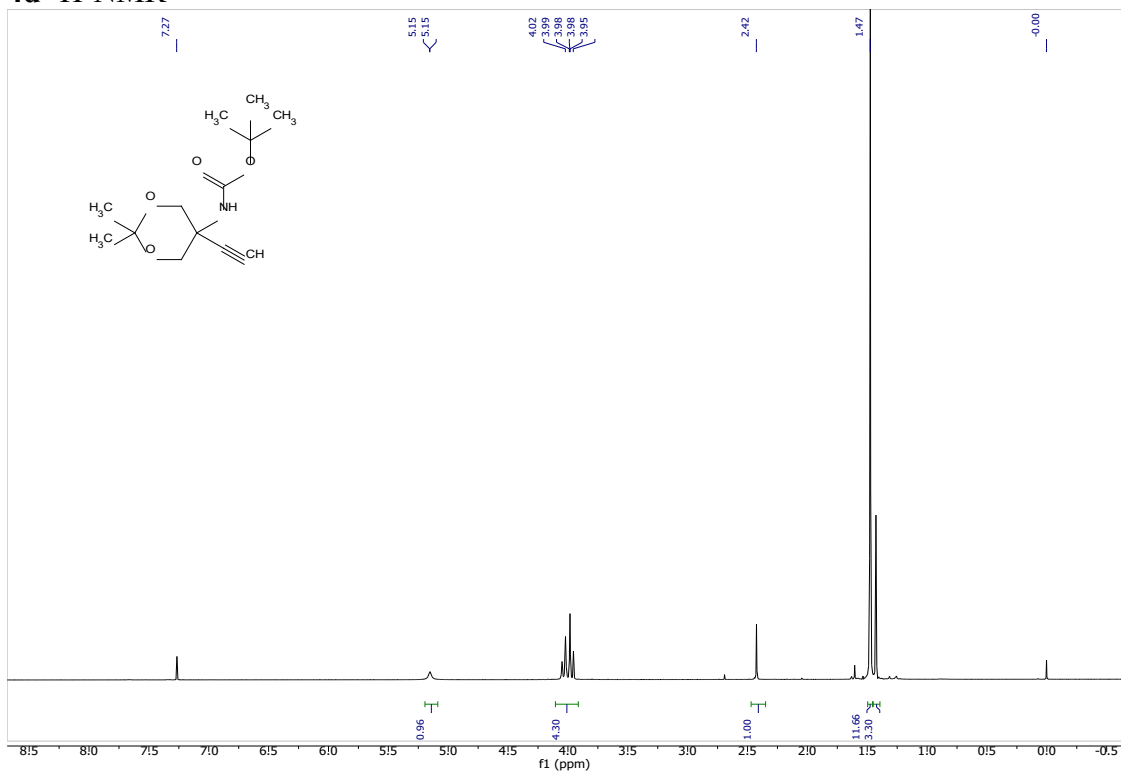
Data S2. Unprocessed western blots of SI Appendix Fig. S4E
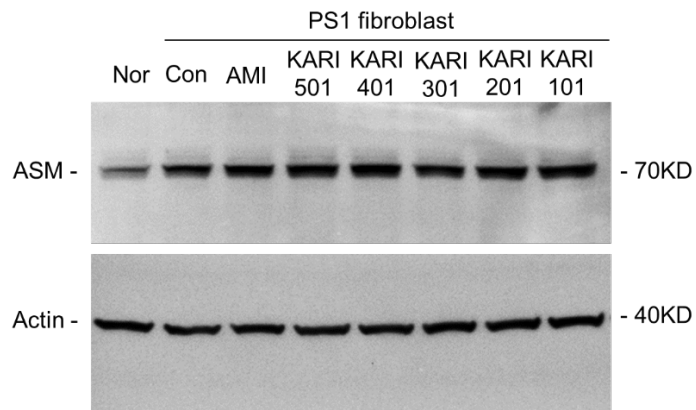
Data S3. Unprocessed western blots of SI Appendix Fig. S5F
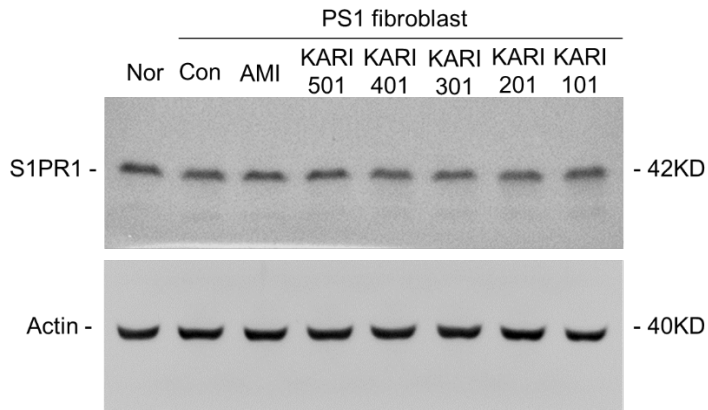
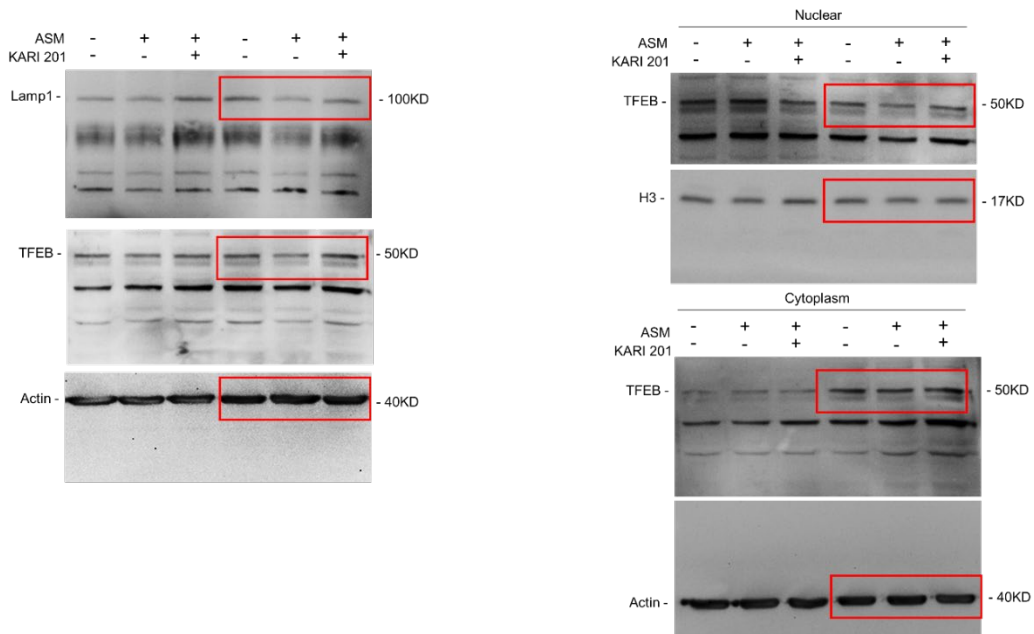**Data S4. Unprocessed western blots of SI Appendix Fig. S10D and S10E**
Unprocessed western blots of SI Appendix Fig. S10D
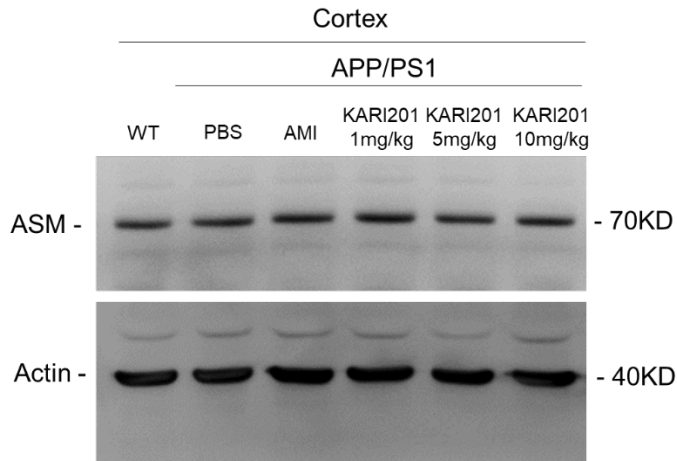
Unprocessed western blots of SI Appendix Fig. S10E
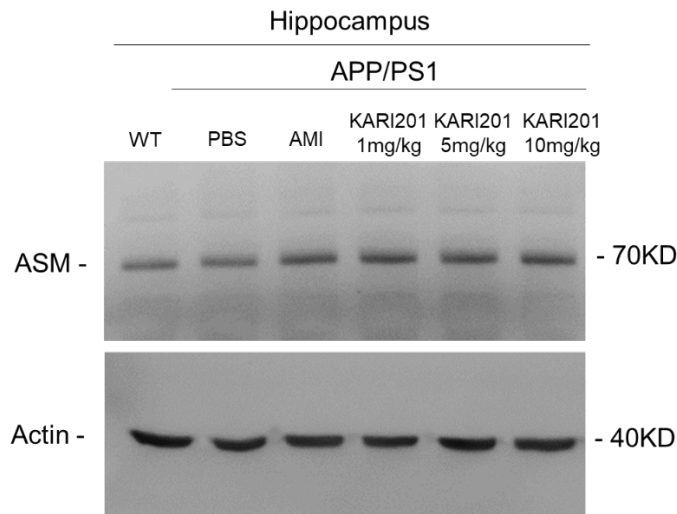
Data S5. Unprocessed western blots of SI Appendix Fig. S11A and S11B

Unprocessed western blots of SI Appendix Fig. S11A
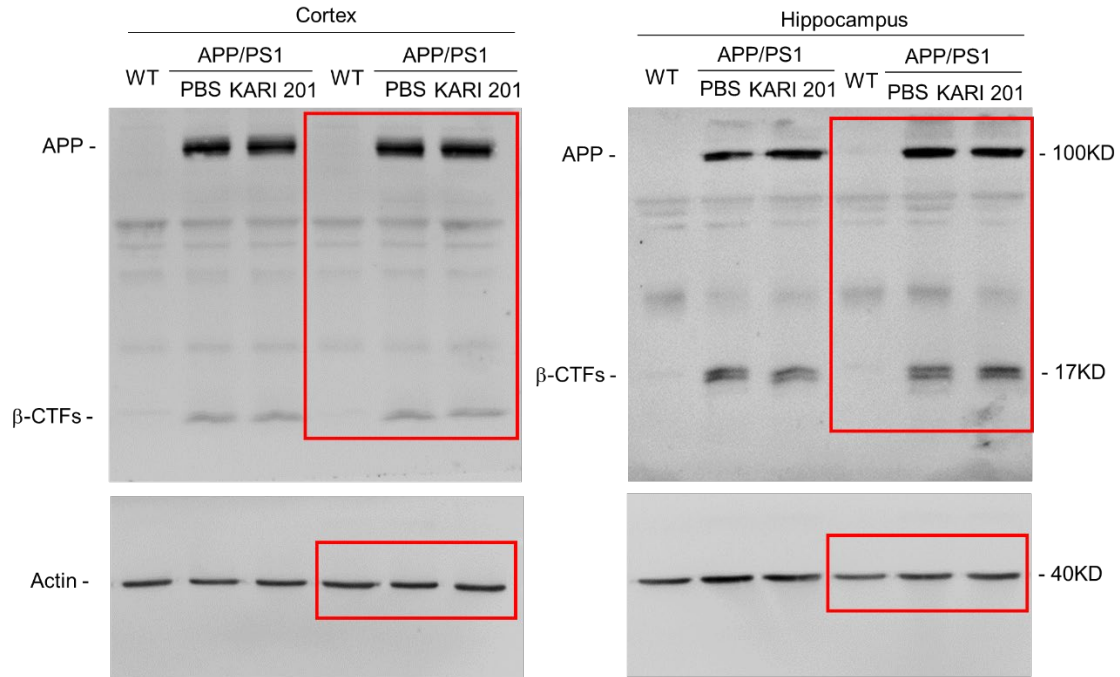
Unprocessed western blots of SI Appendix Fig. S11B
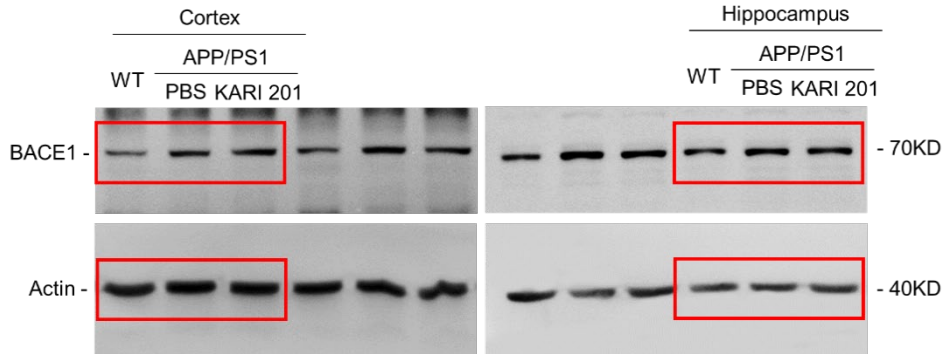
Data S6. Unprocessed western blots of SI Appendix Fig. S13C and S13D
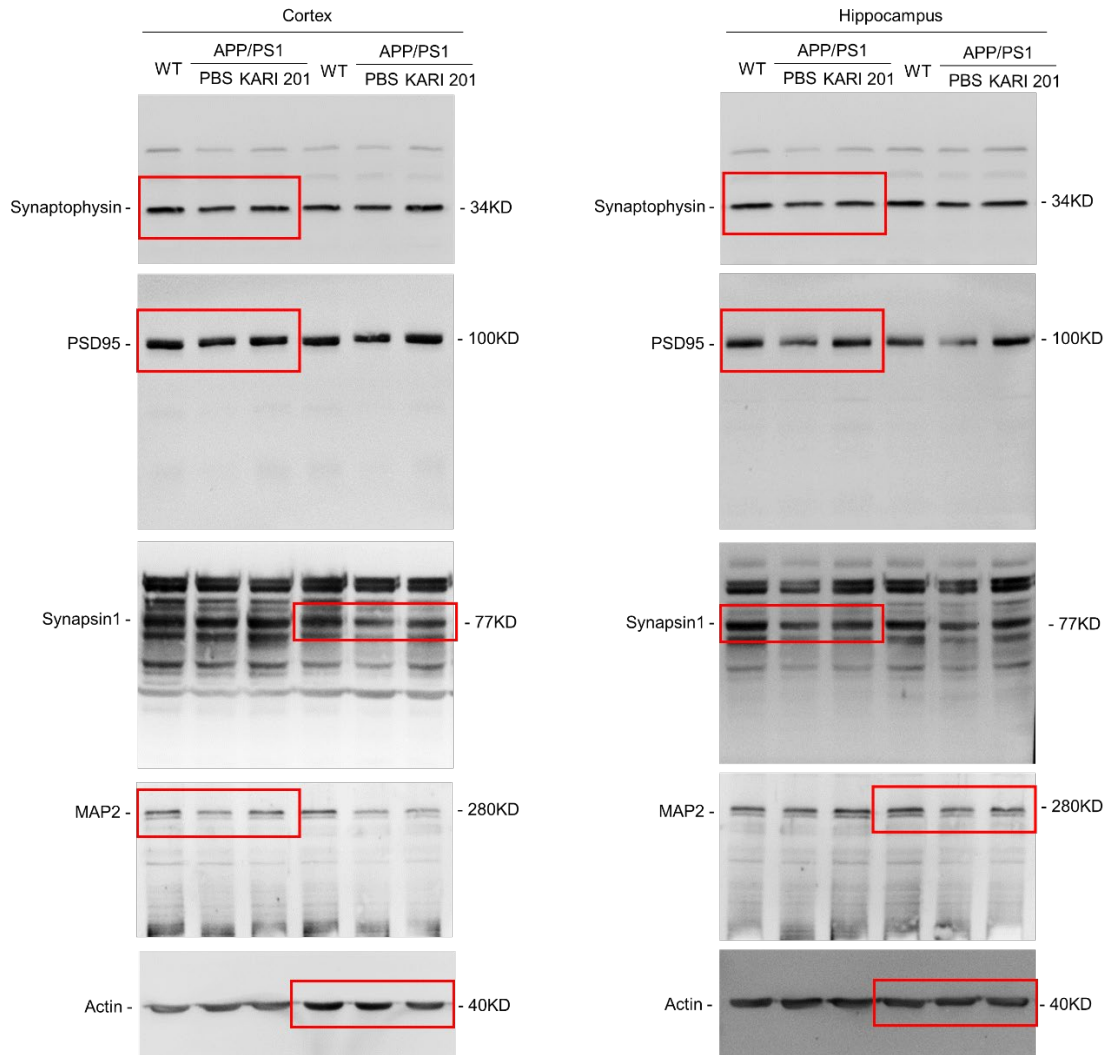
Data S7. Unprocessed western blots of Fig. 3A, 3B and 3D

Unprocessed western blots of Fig. 3A
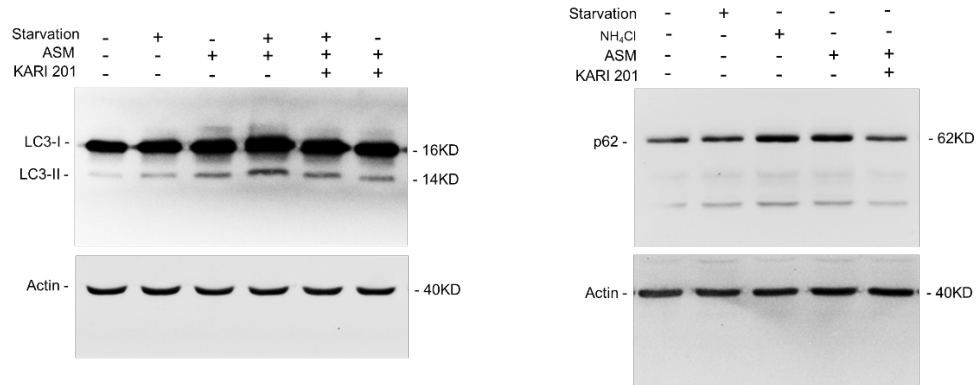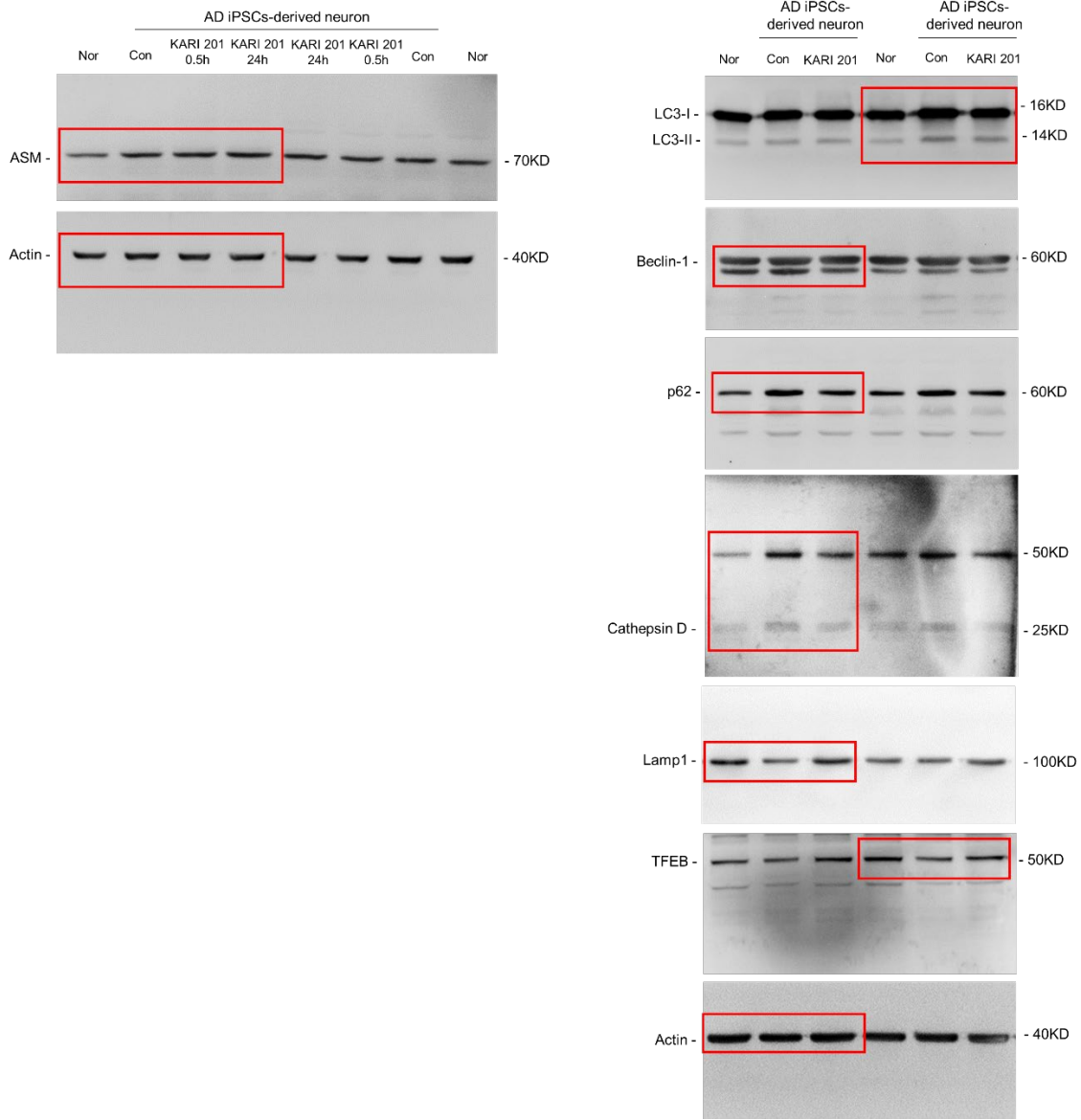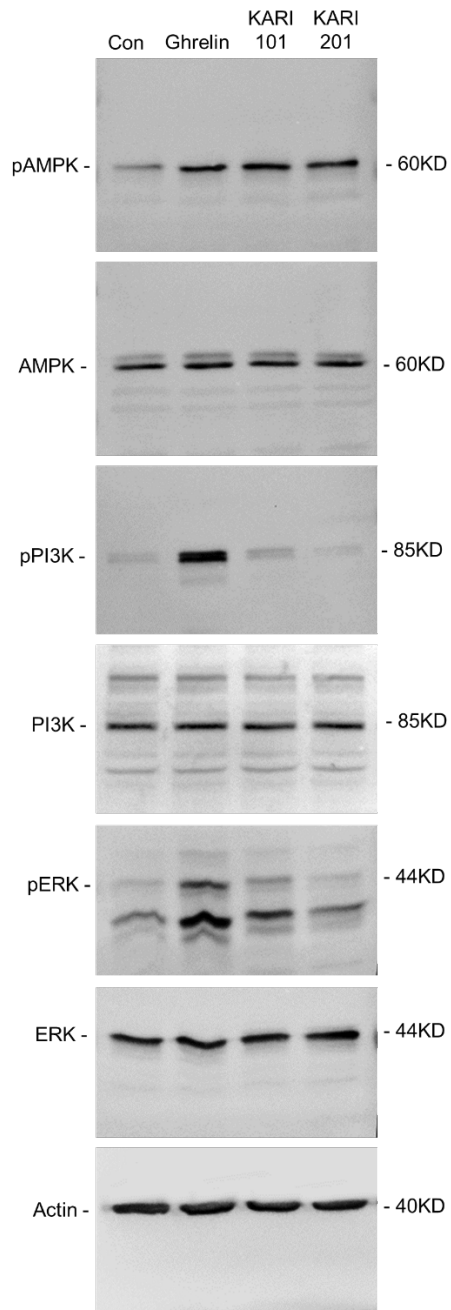

Unprocessed western blots of Fig. 3B and 3D

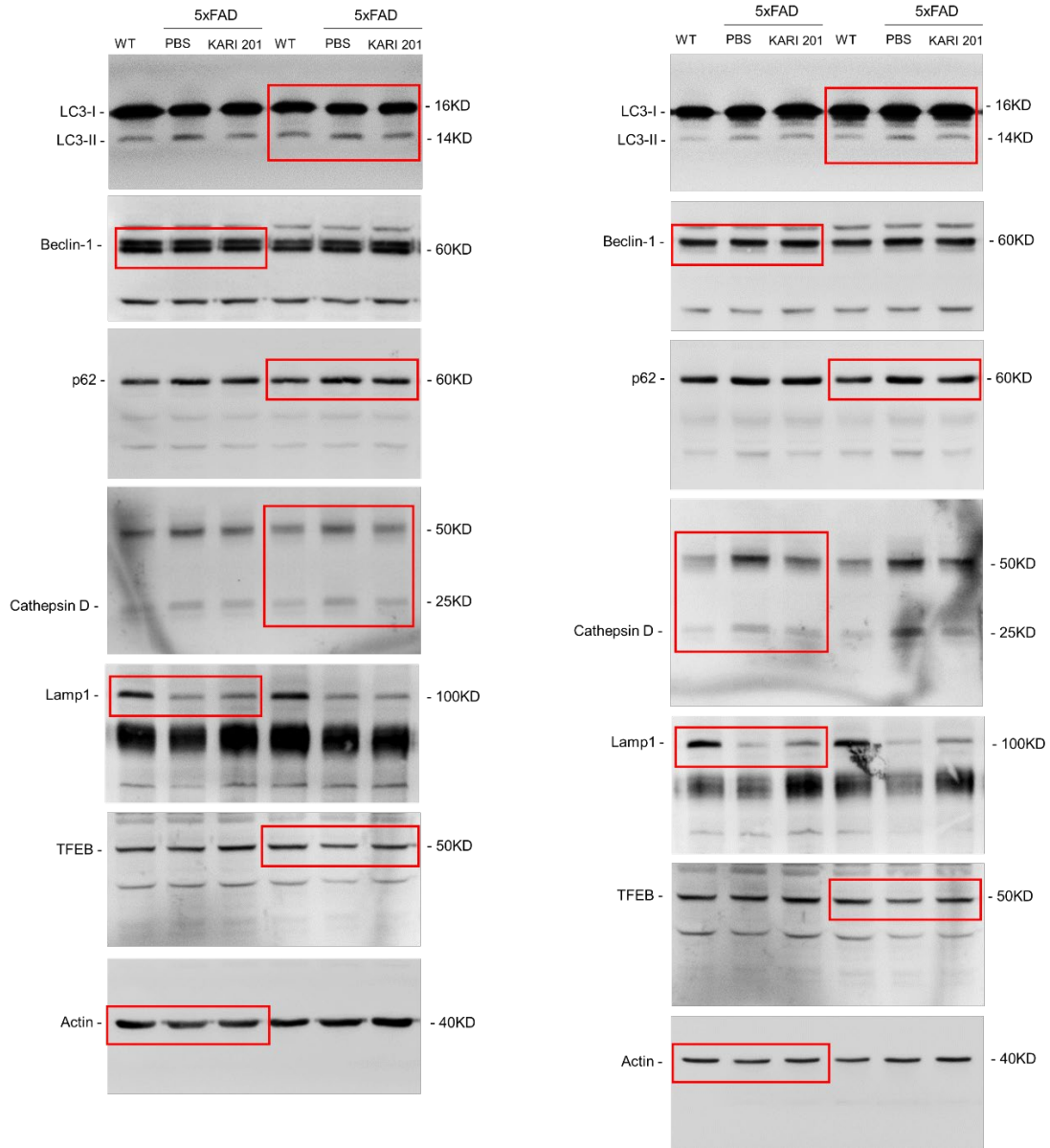## Data S8. Unprocessed western blots of Fig. 3F and 3G
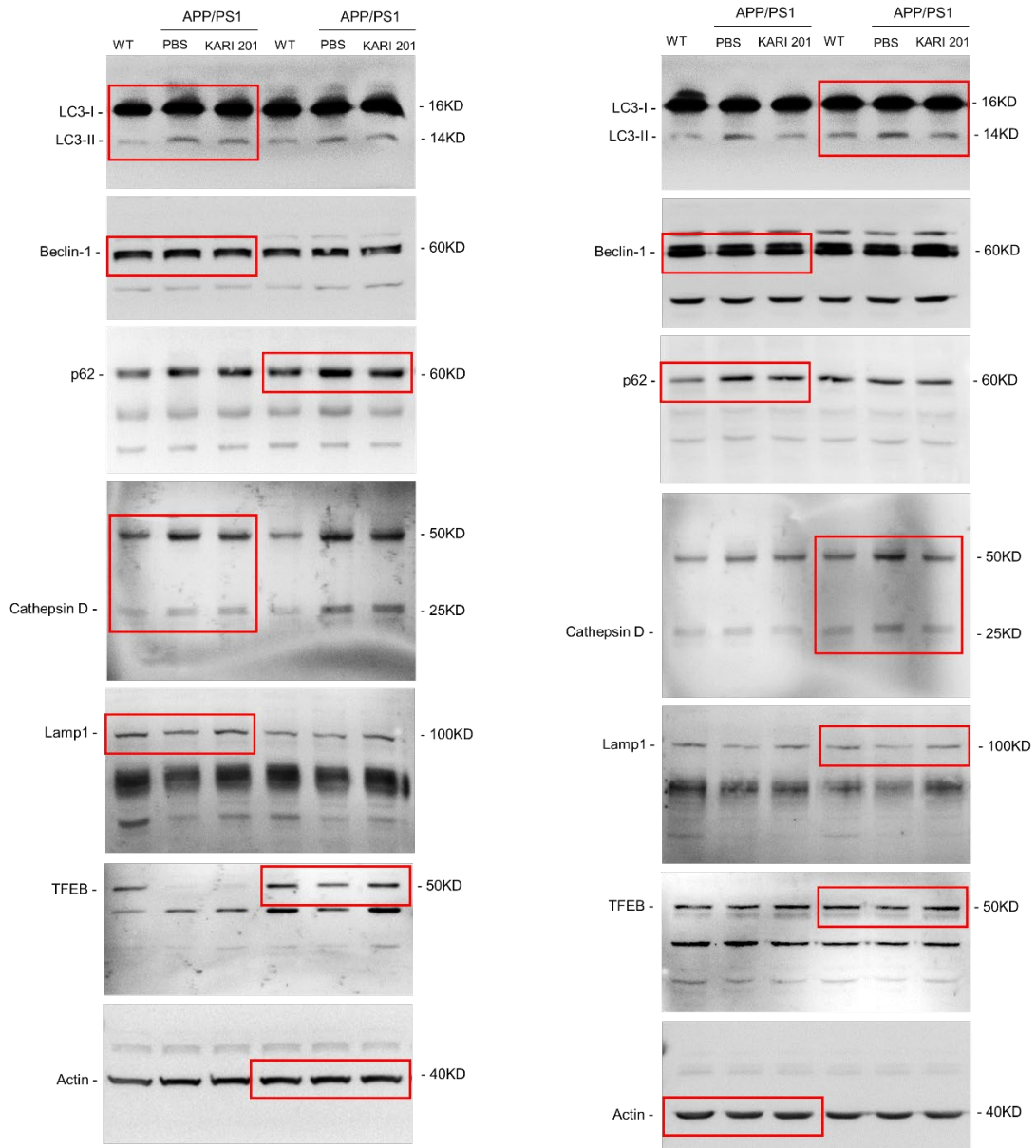
Data S9. Unprocessed western blots of SI Appendix Fig. S16E and S16H

Data S10. Unprocessed western blots of Fig. 5B

Data S11. Unprocessed western blots of SI Appendix Fig. S21D and S21E

Data S12. Unprocessed western blots of SI Appendix Fig. S22C and S22D